Investigation of Stokes' second problem for non-Newtonian fluids

Deals Shaun Rikhotso
Student no: 0610426R

School of Computational and Applied Mathematics,
University of the Witwatersrand,
Johannesburg, South Africa.

A dissertation submitted to the Faculty of Science, University of the Witwatersrand, in fulfillment of the requirements for the degree of Master of Science.

February 27, 2014

Declaration

I, Deals Shaun Rikhotso, student at the University of the Witwatersrand, Johannesburg, South Africa, hereby declare that the contents of this dissertation titled

"Investigation of Stokes' second problem for non-Newtonian fluids"

to be my own work and that

1. This dissertation is submitted for the degree of Master of Science at the University of the Witwatersrand, Johannesburg, South Africa.

2. The work I am submitting for the degree of Master of Science has not been submitted to any other university, or for any other degree.

3. The use of all material from other sources has been properly and fully acknowledged.

D.S Rikhotso | *27 February 2014*

Signature of candidate | **Date**

Abstract

The motion of an incompressible fluid caused by the oscillation of a plane flat plate of infinite length is termed Stokes' second problem. We assume zero velocity normal to the plate and thus simplified Navier-Stokes equations. For the unsteady Stokes' second problem, solutions may be obtained by using Laplace transforms, perturbation techniques, homotopy, differential transform method or Adomian decomposition method. Stokes' second problem is discussed for second-grade and Oldroyd-B non-Newtonian fluids. This dissertation summarizes previously published work.

Acknowledgments

This dissertation would not have been possible without the supervision of Professor Shirley Abelman, whose support, enthusiasm and never ending patience have been invaluable. I believe she deserves a lot more than a line in my dissertation acknowledgements. Many thanks should also go to all my fellow MSc students for the sharing of sweets and laughs throughout the many hours spent in the computer room. I would also like to acknowledge the financial support provided by the National Research Foundation (NRF), Pretoria which has been very important in the completion of this study.

Lastly I would like to thank my parents, who allowed me to dream, and with hopes for the dreams my children will have one day. *" Eka wena Ntlholameri Christinah N'wa jekejeke ra milomu wa nkuwa rale ndleleni raku miyeta N'wana ni vusiku, N'wa rhaku rikulu Shipalana vaka Dzungeni na wena Ndzhwamba David Rivisi, Barhula, Munyamatsi, makula kondzo laha u kandziyaka kona ku baleka hlangasi, Rikhotso. Ndzi khensa rirhandzu leri mindzi nyikeke rona"*, not forgetting my entire lovely family (*Showman, Alleta, Kanelani, Dollar*), and friends for their encouragement and support over the years.

Above all I would like to thank the Lord, Jesus Christ for the blessings He has bestowed on my life. He has provided me with more than I could ever have

imagined. He has surrounded me with people who always look out for me. He has provided me with family and friends who bless me every day. Thank you Lord for provision. In you name, Amen.

Contents

List of Figures

List of Tables

Chapter 1

Introduction

1.1 Background Knowledge

Fluid mechanics deals with the study of all fluids under static and dynamic situations. Fluid mechanics is a branch of continuum mechanics which deals with a relationship between forces, motions, and statical conditions in a continuous material. This study area deals with many and diversified problems such as surface tension, fluid statics, flow in enclosed bodies, or flow round bodies (solid or otherwise), flow stability, etc.

Fluid mechanics started with the need to obtain water supply. For example, people realized that wells needed to be dug and crude pumping devices needed to be constructed. Later, a large population created a solution to solve waste (sewage) problems and some basic understanding was created. At some point, people realized that water can be used to move things and provide power. When cities increased to a larger size, aquaducts were constructed. These aquaducts reached their greatest size and grandeur in the cities of Rome and

China.

The fundamental principles of hydrostatics were given by Archimedes in his work on floating bodies, around 250 B.C. Yet, almost all can be summarized as applications of instincts, with Archimedes (250 B.C.) working on the principles of buoyancy; for example, larger tunnels built for a larger water supply, etc. There were no calculations even with the great need for water supply and transportation. The first progress in fluid mechanics was made by Leonardo Da Vinci (1452-1519) who built the first chambered canal lock near Milan. He also made several attempts to study the flight (birds) and developed some concepts on the origin of the forces. After his initial work, the knowledge of fluid mechanics (hydraulic) increasingly gained impetus by the contributions of Galileo, Torricelli, Euler, Newton, Bernoulli family, and D'Alembert. At that stage theory and experiments had some discrepancy. This fact was acknowledged by D'Alembert who stated that, "The theory of fluids must necessarily be based upon experiment".

Fluid mechanics is concerned with the behaviour of materials which deform without limit under the influence of shearing forces. Even a very small shearing force will deform a fluid body, but the velocity of the deformation will be correspondingly small. The study on the flow of a viscous fluid over an oscillating plate is not only of fundamental theoretical interest but also occurs in many applied problems. In the literature this motion is termed as Stokes' second problem [1]. The first problem of Stokes (1851) is also known as Rayleigh's problem. Stokes' first and second problems have received much attention due to their practicle applications. Stokes' first problem refers to the shear flow of a viscous fluid near a flat plate which is suddenly accelerated from the rest and moves in its own plane with a constant velocity [2]. If the plate executes linear harmonic oscillations, parallel to itself, the problem is referred to as Stokes' second problem [3]. Rayleigh's problem is one of the first problems in which Navier-Stokes equations were solved. It admits an analytical solution and the complete result of the problem is the sum of steady-state and transient solutions. Numerical and analytical solutions for the steady-state solutions due to the sinusoidal oscillation of the plate were studied in depth by Sin and Wong [4]. Ali and Vafai [3] investigated Stokes' second problem for non-Newtonian fluids. Devakar and Iyengar [5] solved Stokes' problem for an incompressible couple stress fluid under isothermal conditions.

1.2 Preliminary

1.2.1 Constitutive Equations

The rheological properties of materials are generally specified by their so called constitutive equations. Generally constitutive equations describe a mathematical relationship model between two physical quantities (especially how kinetic quantities are related) that are specific to a material or substance, and approximate the response of that material to external forces. These are combined with other equations governing physical laws to solve physical problems, like the flow of a fluid in a pipe, or the response of a crystal to an electric field.

The constitutive equations corresponding to different materials must satisfy some general principle e.g. the symmetry principle, the objectivity principle etc. The simplest constitutive equation in three dimensional form is a Newtonian one

$$\mathbf{T} = -p\mathbf{I} + \mathbf{S}, \ \ \mathbf{S} = \mu\mathbf{A},$$

where p is the hydrostatic pressure, $\mathbf{T}$ is the Cauchy stress tensor, $\mathbf{I}$ is the unit tensor, $\mathbf{S}$ is the extra-stress tensor, μ is the dynamic viscosity and

$$\mathbf{A} = \mathbf{L} + \mathbf{L}^T$$

is the first Rivlin-Ericksen tensor [6, 7, 8, 9, 10], the superscript T indicates the transpose operation and $\mathbf{L}$ is the velocity gradient. In the following we state the constitutive equations of some different fluids of rate type.

Maxwell fluids:

$$\mathbf{T} = -p\mathbf{I} + \mathbf{S}, \ \ \mathbf{S} + \lambda\frac{\delta\mathbf{S}}{\delta t} = \mu\mathbf{A},$$

where λ is relaxation time,

$$\frac{\delta\mathbf{S}}{\delta t}$$

is the upper convective derivative defined by

$$\frac{\delta\mathbf{S}}{\delta t} = \dot{\mathbf{S}} - \mathbf{L}\mathbf{S} - \mathbf{S}\mathbf{L}^T$$

and the superposed dot denotes the material time derivative.

Oldroyd-B fluids:

$$\mathbf{T} = -p\mathbf{I} + \mathbf{S}, \ \ \mathbf{S} + \lambda\frac{\delta\mathbf{S}}{\delta t} = \mu(\mathbf{A} + \lambda_r\frac{\delta\mathbf{S}}{\delta t})$$

where λ and $\lambda_r(\leq \lambda)$ are relaxation and retardation times and $\frac{\delta}{\delta t}$ indicates the material time derivative [10]

Now the constitutive equation of a second grade fluid

$$\mathbf{T} = -p\mathbf{I} + \mathbf{S}, \quad \mathbf{S} = \mu\mathbf{A}_1 + \alpha_1\mathbf{A}_2 + \alpha_2\mathbf{A}_2,$$

where α_1 and α_2 are measured material constants also called stress moduli. They denote elasticity and cross viscosity respectively. $\mathbf{A_1}$ and $\mathbf{A_2}$ are the first and second Rivlin-Ericksen tensors, $\mathbf{A_2}$ being defined by

$$\mathbf{A}_2 = \frac{d\mathbf{A}_1}{dt} + \mathbf{A}_1(\text{grad } \mathbf{v}) + (\text{grad } \mathbf{v})^T\mathbf{A}_1,$$

where $\mathbf{v}$ is the velocity field and:

$$\mathbf{A}_1 = (\text{grad } \mathbf{v}) + (\text{grad } \mathbf{v})^T, \quad \mathbf{L} = \text{grad } \mathbf{v}.$$

Johnson-Segalman fluids:

Johnson-Segalman [11] proposed an integral model which can also be written in the rate type form. With an appropriate choice of the kernel function and the time constants the Cauchy stress σ in such a Johnson-Segalman fluid is related to the fluid motion through:

$$\sigma = -p\mathbf{I} + \mathbf{T},$$

where [12, 13]

$$\mathbf{T} = 2\mu\mathbf{D} + \mathbf{S},$$

$$\mathbf{S} + \lambda(\frac{d\mathbf{S}}{dt} + \mathbf{S}(\mathbf{W} - a\mathbf{D}) + (\mathbf{W} - a\mathbf{D})^T\mathbf{S}) = 2\eta\mathbf{D}.$$

$\mathbf{D}$ is the symmetric part of the velocity gradient, $\mathbf{W}$ is the skew symmetric part of the velocity gradient

$$\mathbf{D} = \frac{1}{2}(\mathbf{L} + \mathbf{L}^T), \quad \mathbf{W} = \frac{1}{2}(\mathbf{L} - \mathbf{L}^T), \quad \mathbf{L} = \text{grad } \mathbf{v}.$$

η and μ are the viscosities, λ is the relaxation time and "a" is called the slip parameter. A Johnson-Segalman fluid reduces to a Maxwell fluid when $a = 1$ and $\mu = 0$. The model also reduces to classical Navier-Stokes fluid when $\lambda = 0$.

1.2.2 Equations of Motion

We use mathematical equations based on how an object moves to predict its future motion. Mathematical models of the behaviour of moving objects, such as fluids, stars and planets, allow predictions to be made about their position and speed at certain times.

Equations of motion are equations that describe the behaviour of a physical system in terms of its motion as a function of time [14]. More specifically, the equations of motion describe the behaviour of a physical system as a set of mathematical functions in terms of dynamic variables: normally spatial coordinates and time are used, but others are also possible, such as momentum components and time. The most general choice are generalized coordinates which can be any convenient variables characteristic of the physical system [15].

The **Navier-Stokes equations** (general)

$$\rho \left(\frac{\partial \mathbf{v}}{\partial t} + \mathbf{v} \cdot \nabla \mathbf{v} \right) = -\nabla p + \nabla \cdot \mathbb{T} + \mathbf{f}$$

where $\mathbf{v}$ is the flow velocity, ρ is the fluid density, p is the pressure, $\mathbb{T}$ is the (deviatoric) stress tensor, and $\mathbf{f}$ represents body forces (per unit volume) acting on the fluid and ∇ is the del operator. This is a statement of the conservation of momentum in a fluid and it is an application of Newton's second law to a continuum; in fact this equation is applicable to any non-relativistic continuum and is known as the Cauchy momentum equation.

Cartesian coordinates

Writing the vector equation explicitly,

$$\rho\left(\frac{\partial u}{\partial t}+u\frac{\partial u}{\partial x}+v\frac{\partial u}{\partial y}+w\frac{\partial u}{\partial z}\right)=-\frac{\partial p}{\partial x}+\mu\left(\frac{\partial^2 u}{\partial x^2}+\frac{\partial^2 u}{\partial y^2}+\frac{\partial^2 u}{\partial z^2}\right)+\rho g_x,$$

$$\rho\left(\frac{\partial v}{\partial t}+u\frac{\partial v}{\partial x}+v\frac{\partial v}{\partial y}+w\frac{\partial v}{\partial z}\right)=-\frac{\partial p}{\partial y}+\mu\left(\frac{\partial^2 v}{\partial x^2}+\frac{\partial^2 v}{\partial y^2}+\frac{\partial^2 v}{\partial z^2}\right)+\rho g_y,$$

$$\rho\left(\frac{\partial w}{\partial t}+u\frac{\partial w}{\partial x}+v\frac{\partial w}{\partial y}+w\frac{\partial w}{\partial z}\right)=-\frac{\partial p}{\partial z}+\mu\left(\frac{\partial^2 w}{\partial x^2}+\frac{\partial^2 w}{\partial y^2}+\frac{\partial^2 w}{\partial z^2}\right)+\rho g_z.$$

1.2.3 Some Integral Transforms

Laplace Transform

The Laplace transform is perhaps the mathematical signature of the electrical engineer, having a long history of application to problems of electrical engineering. Despite its Gallic name, the transform originates with the Swiss mathematician, Leonhard Euler (1707-1783), who in 1744 wrote integrals that look much like the modern version [16].

Given f, a function of time, with value $f(t)$ at time t, the Laplace transform of f is denoted $\tilde{f}$ and it gives an average value of f taken over all positive values of t such that the value $\tilde{f}(s)$ represents an average of f taken over all possible time intervals of length s.

$$\mathfrak{L}[f(t)] = \tilde{f}(s) = \int_a^b e^{-st} f(t)\, dt, \text{ for } s > 0.$$

Inverse Laplace Transform

Given a function f, of t, we denote its Laplace transform by $\mathfrak{L}[f] = \tilde{f}$; the inverse process is written:

$$\mathfrak{L}^{-1}[\tilde{f}] = f.$$

A common situation occurs when $\tilde{f}(s)$ is a polynomial in s, or more generally, a combination of polynomials; then if possible we use partial fractions to simplify the expressions. An expression for a Laplace transform of the form N/D where numerator N and denominator D are both polynomials of s, possibly in the form of factors, may be constant if we use partial fractions.

The Convolution Integral

If we identify a Laplace transform $H(s)$ as the product of two other transforms of two known functions $F(s)$ and $G(s)$ that are the transforms of two known functions $f(t)$ and $g(t)$, then the "generalized product" of $f(t)$ and $g(t)$ is called convolution and $H(s)$ would be the transform of the convolution of f and g.

Definition: Let $f(t)$ and $g(t)$ be two piecewise continuous functions on $[0, b]$ and of order exponential with constant a. Convolution of the functions f and g denoted by $f * g$ is defined by the integral

$$f * g = \int_0^t f(\tau)g(t-\tau)d\tau,$$

and the integral is known as the convolution integral.

1.2.4 Power Law Fluid

A power law gives a relationship in which a relative change in one quantity is directly proportional to other quantity, independent of the initial size of those quantities. A power law fluid, or the Ostwald-de Waele relationship, is a type of fluid generalized by Newtonian fluid for which the shear stress, τ, is given by [17, 18, 19]

$$\tau = k\frac{\partial u}{\partial y}^n$$

where n is the flow behaviour index, k is a flow consistency index and $\frac{\partial u}{\partial y}$ is the shear rate or velocity gradient. The index n plays an import rule when differentiating a Newtonian fluid from a non-Newtonian fluid. When $n = 1$ the shear stress is proportional to the shear rate and the behaviour is a Newtonian fluid

$$\tau = k\frac{\partial u}{\partial y}^1.$$

The index n plays an important rule in different power law fluids. When $n = 1$ the the fluid behaviour is Newtonian, when $n > 1$ the fluid is dilitant, or shear thickening. When $n < 1$ the fluid is pseudoplastic or shear thinning. Examples of shear thickening fluids are cornstarch, water and those of shear thinning fluids are glycerine, corn syrup.

1.3 Dissertation Organisation

The contents of this dissertation are as follows:

In **chapter 2**, we investigate a power law fluid occupying the domain $y > 0$. An infinitely extended flat plate located at $y = 0$ is suddenly accelerated from rest. The fluid is disturbed at time $t = 0^+$ and the flat plate begins to oscillate in its plane with angular velocity Ω. The velocity disturbance induced in the fluid at $t > 0$ and shear stress distributions are to be determined. This problem is also known as the second problem of Stokes.

In **chapter 3**, we illustrate a model overview of numerical solutions to the momentum equation using finite difference approximations. The forward finite difference, the backward finite difference, the central finite difference and Crank-Nicolson schemes are developed and applied to the governing momentum equation for fluid flow. The numerical results are obtained using MATLAB.

In **chapter 4**, we show the application of He's homotopy perturbation method (HPM) on solving the momentum equation. HPM reduces a complex problem domain into a simple problem examination and depends on the choice of initial condition, having a good guess for the initial condition, a few iterations are enough to give a good approximate solution. The method generates a convergent series solution.

In **chapter 5**, the differential transform method (DTM) is applied to the momentum equation for fluid flow. Differential transform method is a numerical method based on Taylor series expansions and is capable of reducing the challenge arising in the calculation of Adomian polynomials. The method can be applied for solving linear and nonlinear partial differential equations. The approximate solutions of the momentum equation are obtained in the form of a polynomial series solution based on an iterative procedure.

In **chapter 6**, Adomain decomposition method (ADM) is applied to the momentum equation to approximate analytical solutions. The ADM focuses on avoiding simplifications and restrictions which change the nonlinear problem to a mathematically tractable one, whose solution differs with the physical solution. The approximate solutions are expressed in a series form with easily computable components of the decomposition series. The ADM is an efficient and powerful technique for determining approximate solutions of the momentum equation. This method is directly applied to the momentum equation and avoids linearisation or any assumptions.

In **chapter 7**, a summary of each chapter is presented.

Finally, **Appendix A** gives an overview of Laplace transform of compound functions, whilst **Appendix B** provides and proves differential transform method theorems.

Chapter 2

Second Problems of Stokes for non-Newtonian fluids

2.1 Introduction

In this chapter we investigate a power law fluid occupying the domain $y > 0$. An infinitely extended flat plate located at $y = 0$ is suddenly accelerated from rest. The fluid is disturbed at time $t = 0^+$ and the flat plate begins to oscillate in its plane with angular velocity Ω. The velocity disturbance induced in the fluid at $t > 0$ and shear stress distributions are to be determined. This problem is also known as the second problem of Stokes shown in Figure 2.1.

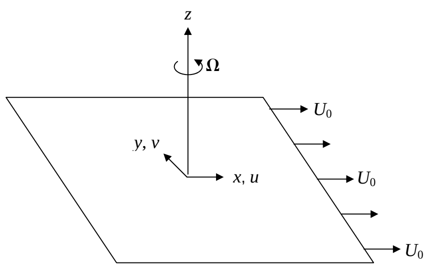

Figure 2.1: Schematic diagram of the problem.

The exact solutions for the velocity field corresponding to the second problem of Stokes describing the flow for small and large times, are established by the Laplace transform method. These solutions, presented as a sum of the steady-state and transient solutions, are in accordance with previous solutions obtained by a different technique. The required time to reach the steady-state is determined by graphical illustrations. This time decreases if the frequency of the velocity increases. The effects of the material parameters on the decay of the transients are also investigated by graphs.

The time required to reach the steady-state for cosine oscillations of the wall is smaller than that for sine oscillations of the wall. Numerically computations show that the steady-state solutions can be reduced to the classical forms [20, 21], while the diagrams of the transient solutions, as illustrated graphically, are in close proximity to those obtained in [22] by a different technique. This steady-state for cosine oscillations decreases if the frequency of the velocity of the boundary increases.

2.2 Governing Equations

Consider a Newtonian fluid at rest over an infinitely extended flat plate perpendicular to the y-axis of a Cartesian coordinate system x, y and z. At time $t = 0^+$ the flat plate begins to oscillate in its plane with angular velocity Ω. Due to the shear, the fluid above the plate is gradually moved, and transmits the motion into the fluid. The fluid velocity is of the form [1, 3]

$$\mathbf{V} = \mathbf{V}(y, t) = u(y, t)\mathbf{i}, \tag{2.1}$$

where **i** is the unit vector along the x-direction. For such flows the constraint of incompressibility is automatically satisfied. In the absence of body forces and a pressure gradient in the flow direction, the governing equation is [23, 24]

$$\frac{\partial u}{\partial t} = \nu \frac{\partial^2 u}{\partial y^2}; \quad y,\, t > 0, \tag{2.2}$$

This governing equation is also referred to as the momentum equation [3]. $u(y,t)$ is the velocity, ν is the kinematic viscosity of the fluid and t is the time.

The boundary and initial conditions corresponding to cosine oscillations of the boundary are given by [7, 21, 24].

$$u(0,t) = U\cos(\omega t) \text{ for all } t > 0, \tag{2.3}$$

where ω is the frequency of the velocity of the wall

and

$$u(y,0) = 0 \text{ for all } y > 0. \tag{2.4}$$

Moreover, the natural condition must also satisfied. It ensures that the fluid is quiescent far away from the plate [25].

$$u(y,t) \to 0 \text{ as } y \to \infty.$$

The boundary and initial conditions for sine oscillations are

$$u(0,t) = U\sin(\omega t) \text{ for all } t > 0,$$
$$u(y,0) = 0 \text{ for all } y \geq 0,$$
$$u(y,t) \to 0 \text{ as } y \to \infty. \tag{2.5}$$

2.3 Solution of the Problem

In order to solve the partial differential equation (2.2), with the boundary and initial conditions (2.3) - (2.5) describing the flow at small and large times after the start of the boundary plane, we use the Laplace transform method. The boundary condition given by Eq. (2.3) shows a discontinuity at $y = 0,\ t = 0$. The plate velocity is indeed initially at zero (rest). It is suddenly accelerated from rest due to the oscillation of the plane wall. The boundary condition given by Eq. (2.5) is continuous at $y = 0,\ t = 0$ and is therefore more realistic, however the boundary condition given by Eq. (2.3) is frequently used in the literature.

The Laplace transform of u is defined by the relation

$$\bar{u} = \int_0^\infty ue^{-st}\,dt.$$

Then Eq. (2.2) takes the form

$$\bar{u}'' - \frac{s}{\nu}\bar{u} = 0, \tag{2.6}$$

where the prime denotes differentiation with respect to y. The conditions (2.3)

- (2.4) become

$$\bar{u} = U\frac{s}{s^2 + w^2} \ \text{ at } \ y = 0, \tag{2.7}$$

$$\bar{u} = 0, \ \text{ at } \ y \to \infty, \tag{2.8}$$

and the boundary conditions (2.5) have the form

$$\bar{u} = U\frac{s}{s^2 + w^2} \ \text{ at } \ y = 0, \tag{2.9}$$

$$\bar{u} = 0, \ \text{ at } \ y \to \infty. \tag{2.10}$$

The development will be made for both the cosine oscillations and the sine oscillations, where the solutions of Eq. (2.6) subject to the boundary conditions (2.7) - (2.8) and (2.9) - (2.10) will be considered. In the first case, the plate at $y = 0$ oscillates as $u = U\cos(\omega t)$ and in the second case the plate at $y = 0$ oscillates as $u = U\sin(\omega t)$.

The analytical solution of the differential equation Eq. (2.6) subject to the boundary condition of (2.7) is found to be

$$\frac{\bar{u}}{U} = \frac{1}{2}\left[\frac{\exp(-\sqrt{(\frac{s}{\nu})}y}{s + iw} + \frac{\exp(-\sqrt{(\frac{s}{\nu})}y}{s - iw}\right], \text{ where the complex number}$$

$$i = \sqrt{-1} \quad \text{i.e } i^2 = -1. \tag{2.11}$$

Multiplying both sides by U, Eq. (2.11) reduces to

$$\bar{u} = \frac{Us}{s^2 + w^2} \exp\left(-\sqrt{(\frac{s}{\nu})} y \right), \ y > 0. \tag{2.12}$$

$\bar{u}$ denotes the Laplace transform of u, thus $\bar{u} = u(y, s)$ and $u = u(y, t)$ results in $u(y, s) \to u(y, t)$.

Regard the right hand side of Eq. (2.12) as a product of two functions, $\bar{u}_1(s)$ and $\bar{u}_2(y, s)$

where

$$\bar{u}_1(s) = \frac{Us}{s^2 + w^2} \tag{2.13}$$

$$\bar{u}_2(y, s) = \exp\left(-\sqrt{\left(\frac{s}{\nu}\right)} y \right). \tag{2.14}$$

Then using the well known result from inverse Laplace transforms [26] we obtain,

$$\mathfrak{L}^{-1}\left[\frac{s}{s^2 + w^2}; \frac{w}{s^2 + w^2} \right] = \{\cos(\omega t); \sin(\omega t)\}, \tag{2.15}$$

$$\mathfrak{L}^{-1}\left[\exp\left(-\sqrt{\left(\frac{s}{\nu}\right)} y \right) \right] = \frac{y}{2t\sqrt{\pi \nu t}} \exp\left(-\frac{y^2}{4st} \right). \tag{2.16}$$

Taking the inverse Laplace transforms of Eq. (2.11), we can write the velocity $u = u(y, t)$ as a convolution product,

$$\begin{aligned}
\mathfrak{L}^{-1}[\bar{u}_1.\bar{u}_2(y,s)] &= u(y,t) \\
&= u_1(t) * u_2(y,t) \\
&= \int_0^t u_1(t-s)u_2(y,s)\,ds \\
&= \int_0^t u_1(s)u_2(y,t-s)\,ds. \qquad (2.17)
\end{aligned}$$

The convolution product of two functions is denoted by $*$; $u_1(.)$ and $u_2(y,.)$ are given by the inverse Laplace transforms. Thus,

$$\begin{aligned}
u_1(t) = L^{-1}\left\{\bar{u}_1(s)\right\} &= \left\{u_c, u_s\right\} \\
&= \left\{U\cos(\omega t), U\sin(\omega t)\right\}. \qquad (2.18)
\end{aligned}$$

In order to determine the function $u_2(y,t)$, we use the inversion formula of (A1) compound functions choosing $F(y,q)$ and $w(q)$ given by

$$F(y,q) = \exp(-\sqrt{(\frac{s}{\nu})}y \text{ and } w(s) = \frac{s}{s+\beta}.$$

Thus

$$u_2(y,t) = \frac{y}{2t\sqrt{\pi\nu t}}\exp\left(-\frac{y^2}{4\nu t}\right), \qquad (2.19)$$

which is the inverse Laplace equation of $\bar{u}_2(y,s)$,

$$L^{-1}\left\{\bar{u}_2(y,s)\right\} = u_2(y,t),$$

given by Eq. (2.16).

Finally, using Eqs. (2.15), (2.17), (2.19) and appendix (A3) simplify to the velocity field $u(y,t)$

$$u(y,t) = \frac{Uy}{2\sqrt{\pi\nu}} \int_0^t \frac{\cos\left[\omega(t-s)\right]}{s\sqrt{s}} \exp\left(-\frac{y^2}{4\nu s}\right) ds. \tag{2.20}$$

Similarly the velocity generated by the sine oscillation, is

$$u(y,t) = \frac{Uy}{2\sqrt{\pi\nu}} \int_0^t \frac{\sin\left[\omega(t-s)\right]}{s\sqrt{s}} \exp\left(-\frac{y^2}{4\nu s}\right) ds. \tag{2.21}$$

When decomposed, the integral form of Eqs. (2.20) and (2.21) under the form

$$\int_{cy}^{t} f(y,t,s)ds = \int_{cy}^{\infty} f(y,t,s)ds - \int_{t}^{\infty} f(y,t,s)ds, \tag{2.22}$$

the solution Eqs. (2.20) and (2.21) can written into an equivalent but more suitable form

$$\begin{aligned} u_c(y,t) =& \frac{Uy}{2\sqrt{\pi\nu}} \int_0^\infty \frac{\cos\left[\omega(t-s)\right]}{s\sqrt{s}} \exp\left(-\frac{y^2}{4\nu s}\right) ds \\ &- \frac{Uy}{2\sqrt{\pi\nu}} \int_t^\infty \frac{\cos\left[\omega(t-s)\right]}{s\sqrt{s}} \exp\left(-\frac{y^2}{4\nu s}\right) ds. \end{aligned} \tag{2.23}$$

Similarly

$$\begin{aligned} u_s(y,t) =& \frac{Uy}{2\sqrt{\pi\nu}} \int_0^\infty \frac{\sin\left[\omega(t-s)\right]}{s\sqrt{s}} \exp\left(-\frac{y^2}{4\nu s}\right) ds \\ &- \frac{Uy}{2\sqrt{\pi\nu}} \int_t^\infty \frac{\sin\left[\omega(t-s)\right]}{s\sqrt{s}} \exp\left(-\frac{y^2}{4\nu s}\right) ds. \end{aligned} \tag{2.24}$$

The velocity field solutions $u_c(y,t)$ and $u_s(y,t)$ given in Eqs. (2.23) and (2.24) describe fluid flow for small and large times.

For the start time $t = 0$, Eqs. (2.23) and (2.24) reduce to,

$$\left.\begin{array}{l} u_c(y,t) \\ u_s(y,t) \end{array}\right\} \to 0$$

which satisfy the initial condition $u(y, 0) = 0$.

For large times $t \to \infty$, the second term of Eqs. (2.23) and (2.24) is respectively

$$\frac{Uy}{2\sqrt{\pi\nu}} \int_t^\infty \frac{\cos\left[\omega(t-s)\right]}{s\sqrt{s}} \exp\left(-\frac{y^2}{4\nu s}\right) ds \to 0$$

and

$$\frac{Uy}{2\sqrt{\pi\nu}} \int_t^\infty \frac{\sin\left[\omega(t-s)\right]}{s\sqrt{s}} \exp\left(-\frac{y^2}{4\nu s}\right) ds \to 0$$

and shows that for large values of time (t), the velocity field solution tends to the steady-state solution, which is periodic in time for both sine and cosine oscillations and does not depend on the initial conditions.

2.3.1 Non-Dimensionalisation

The equivalent forms of cosine and sine oscillations Eqs. (**??**) and (**??**) under the boundary conditions $u = U\cos(\omega t)$ for all $t > 0$ on Eq. (2.3) and $u = U\sin(\omega t)$ for all $t > 0$ on Eq. (2.3) appear not to be satisfied. In order to obtain this in a more suitable form, we introduce the non-dimensional quantity defined by s

$$s = \frac{1}{\sigma}. \tag{2.25}$$

In one-dimensional calculus we often use a change of variable to simplify an integral. Making the change of variable in the first integrals from Eqs. (**??**) and (**??**) and using the fact that

$$\cos(x) = \cosh(ix) \text{ and } \sin(x) = -i\sinh(ix), \tag{2.26}$$

and

$$\int_0^\infty \frac{\exp\left(-a^2 s - \frac{b^2}{4s}\right)}{2s} e^{-x}\, ds = \frac{\sqrt{\pi}}{2a} e^{-ab}, \tag{2.27}$$

we find that

$$\begin{aligned} u(y,t) =& U\mathrm{e}^{-y\sqrt{\omega/2\nu}} \cos\left(\omega t - y\sqrt{\frac{\omega}{2\nu}}\right) \\ & - \frac{Uy}{2\sqrt{\pi\nu}} \int_t^\infty \frac{\cos\left[\omega(t-s)\right]}{s\sqrt{s}} \exp\left(-\frac{y^2}{4\nu s}\right) ds \end{aligned} \tag{2.28}$$

and

$$\begin{aligned} u(y,t) =& U\mathrm{e}^{-y\sqrt{\omega/2\nu}} \sin\left(\omega t - y\sqrt{\frac{\omega}{2\nu}}\right) \\ & - \frac{Uy}{2\sqrt{\pi\nu}} \int_t^\infty \frac{\sin\left[\omega(t-s)\right]}{s\sqrt{s}} \exp\left(-\frac{y^2}{4\nu s}\right) ds. \end{aligned} \tag{2.29}$$

2.3.2 Shear Stress and Velocity Profile at the Plate Boundary

Since any real fluid (liquids and gases included) moving along a solid boundary will incur a shear stress on that boundary, the corresponding shear stress is

$$\tau(y,t) = \mu \left(\frac{\partial u(y,t)}{\partial y} \right)^n. \tag{2.30}$$

However, introducing Eqs. (2.28) and (2.29) into Eq. (2.30), we find that

$$\tau(y,t) = \mu \left[\frac{\partial \left(U\mathrm{e}^{-y\sqrt{\omega/2\nu}} \sin\left(\omega t - y\sqrt{\frac{\omega}{2\nu}}\right)\right)}{\partial y} - \frac{\partial \left(\frac{Uy}{2\sqrt{\pi\nu}} \int_t^\infty \frac{\sin\left[\omega(t-s)\right]}{s\sqrt{s}} \exp\left(-\frac{y^2}{4\nu s}\right) ds \right)}{\partial y} \right]^n, \tag{2.31}$$

using the difference derivative rule which states that, the derivative of a difference of functions is the difference of the derivative of these functions. If we let two function to be $f(x)$ and $g(x)$ and both differentiable at a point x then,

$$\frac{d}{dx}[f(x) - g(x)] = \frac{d}{dx}[f(x)] - \frac{d}{dx}[g(x)]. \tag{2.32}$$

Treating μ as a constant we have that

$$\tau(y,t) = \mu \left(\frac{\partial \left[U\mathrm{e}^{-y\sqrt{\omega 2\nu}} \sin\left(\omega t - y\sqrt{\frac{\omega}{2\nu}}\right)\right]}{\partial y} - \mu \frac{\partial \left[\frac{Uy}{2\sqrt{\pi\nu}} \int_t^\infty \frac{\sin[\omega(t-s)]}{s\sqrt{s}} \exp\left(-\frac{y^2}{4\nu s}\right) ds \right]}{\partial y} \right)^n, \tag{2.33}$$

and using the product rule Eq. (2.33) simplifies to,

$$\begin{aligned}\tau(y,t) =&\mu U\left[-\sqrt{\frac{\omega}{2\nu}}e^{-y\sqrt{\omega/2\nu}}\cos\left(\omega t - y\sqrt{\frac{\omega}{2\nu}}\right)\right.\\&+ \left. e^{-y\sqrt{\omega/2\nu}}\sin\left(\omega t - y\sqrt{\frac{\omega}{2\nu}}\right)\left(-\sqrt{\frac{\omega}{2\nu}}\right)\right]\\&-\mu U\left[\frac{y}{2\sqrt{\pi\nu}}\int_t^\infty \frac{\cos\left[\omega(t-s)\right]}{s\sqrt{s}}\exp\left(-\frac{y^2}{4\nu s}\right)\, ds\right.\\&+ \left.\left.\frac{y^2}{4\sqrt{\pi\nu}}\int_t^\infty \frac{\cos\left[\omega(t-s)\right]}{s\sqrt{s}}\exp\left(-\frac{y^2}{4\nu s}\right)\, ds\right]\right)^n. \qquad (2.34)\end{aligned}$$

After algebraic manipulation Eq. (2.34) simplifies to

$$\begin{aligned}\tau(y,t) = \mu&\left(U\sqrt{\frac{\omega}{\nu}}e^{-y\sqrt{\omega/2\nu}}\sin\left(\omega t - y\sqrt{\frac{\omega}{2\nu}}-\frac{\pi}{4}\right)\right.\\&-\frac{\mu U}{2\sqrt{\pi\nu}}\int_t^\infty \frac{\cos\left[\omega(t-s)\right]}{s\sqrt{s}}\exp\left(\frac{y^2}{4\nu s}\right)\, ds\\&+\left.\frac{\mu U y}{2\sqrt{\pi\nu}}\int_t^\infty \frac{\cos\left[\omega(t-s)\right]}{s\sqrt{s}}\exp\left(\frac{y^2}{4\nu s}\right)\, ds\right)^n. \qquad (2.35)\end{aligned}$$

Similarly,

$$\begin{aligned}\tau(y,t) = -\mu&\left(U\sqrt{\frac{\omega}{\nu}}e^{-y\sqrt{\omega/2\nu}}\cos\left(wt - y\sqrt{\frac{\omega}{2\nu}}-\frac{\pi}{4}\right)\right.\\&-\frac{\mu U}{2\sqrt{\pi\nu}}\int_t^\infty \frac{\sin\left[\omega(t-s)\right]}{s\sqrt{s}}\exp\left(\frac{y^2}{4\nu s}\right)\, ds\\&+\left.\frac{\mu U y}{2\sqrt{\pi\nu}}\int_t^\infty \frac{\sin\left[\omega(t-s)\right]}{s\sqrt{s}}\exp\left(\frac{y^2}{4\nu s}\right)\, ds\right)^n. \qquad (2.36)\end{aligned}$$

Now letting $t \to \infty$ in Eqs (2.35) - (2.36), we obtain the classical steady-state solutions

$$\tau(y,t) = \mu\left(U\sqrt{\frac{\omega}{\nu}}e^{-y\sqrt{\omega/2\nu}}\sin\left(wt - y\sqrt{\frac{\omega}{2\nu}}-\frac{\pi}{4}\right)\right)^n, \qquad (2.37)$$

$$\tau(y,t) = -\mu\left(U\sqrt{\frac{\omega}{\nu}}e^{-y\sqrt{\omega/2\nu}}\cos\left(wt - y\sqrt{\frac{\omega}{2\nu}} - \frac{\pi}{4}\right)\right)^n. \tag{2.38}$$

Eqs. (2.28) and (2.29) reach the steady-state solutions:

$$u(y,t) = Ue^{-y\sqrt{\omega/2\nu}}\cos\left(wt - y\sqrt{\frac{\omega}{2\nu}}\right), \tag{2.39}$$

$$u(y,t) = Ue^{-y\sqrt{\omega/2\nu}}\sin\left(wt - y\sqrt{\frac{\omega}{2\nu}}\right). \tag{2.40}$$

The shear stresses are periodic in time and independent of the initial conditions.

2.3.3 Shear Stress and Velocity Profile at the Plate Wall

We determine the shear stress at the wall from Eqs. (2.35) and (2.36)

$$\tau(0,t) = \mu\left(U\sqrt{\frac{\omega}{\nu}}\sin\left(wt - \frac{\pi}{4}\right) - \frac{\mu U}{2\sqrt{\pi\nu}}\int_t^\infty \frac{\cos\left[\omega(t-s)\right]}{s\sqrt{s}}\,ds\right)^n \tag{2.41}$$

for the cosine oscillations of the boundary, and

$$\tau(0,t) = \mu U\left(\sqrt{\frac{\omega}{\nu}}\cos\left(wt - \frac{\pi}{4}\right) - \frac{\mu U}{2\sqrt{\pi\nu}}\int_t^\infty \frac{\sin\left[\omega(t-s)\right]}{s\sqrt{s}}\,ds\right)^n \tag{2.42}$$

for the sine oscillations of the boundary.

The oscillations occur when a system is disturbed from a position of stable equilibrium and are given in terms of the graphs of the wall shear stresses, corresponding to the cosine and sine oscillations of the boundary. These are presented in section 2.4. For a better comparison the plots are presented together as well as separately. The two oscillations have similar magnitude of change in the oscillating variable with each oscillation and a phase shift that persists for all times.

By now letting $\omega \to 0$ into Eqs. (2.28) and (2.29) we obtain the velocity field to be the classical solution

$$
\begin{aligned}
u(y,t) &= U - \frac{Uy}{2\sqrt{\pi\nu}} \int_t^\infty \frac{1}{s\sqrt{s}} \exp\left(-\frac{y^2}{4\nu s}\right) ds \\
&= U[1 - \frac{y}{2\sqrt{\pi\nu}} \int_t^\infty \frac{1}{s\sqrt{s}} \exp\left(-\frac{y^2}{4\nu s}\right) ds] \\
&= U[1 - \operatorname{erf}\left(-\frac{y^2}{4\nu s}\right)] \\
&= U \operatorname{erfc}\left(-\frac{y^2}{4\nu s}\right).
\end{aligned}
\tag{2.43}
$$

By letting $\omega \to 0$ in Eq. (2.34) we obtain the classical solution of the shear stress

$$
\tau(y,t) = -\frac{\mu U}{\sqrt{\pi\nu s}} \exp\left(-\frac{y^2}{4\nu s}\right). \tag{2.44}
$$

2.4 Numerical Results and Conclusion

In this chapter we have studied the solutions corresponding to the second problem of Stokes for Newtonian fluids. The solutions differ from those obtained in [27]. We have introduced the Laplace transform method and applied it directly. The solutions are presented as a sum of steady-state and transient solutions. The solutions obtained in Eqs. (2.37) and (2.38) when $t \to \infty$ as the limiting case, are similar to the solution obtained in [28, 29] using a different technique if we consider the index $n = 1$. The solution is the same as those obtained in [1, 30, 31] using Laplace transforms. The velocity fields correspond to the motions of non-Newtonian fluids due to the cosine and sine oscillation are shown to agree with the solution obtained in [3]. Graphical illustration of the transient solutions, as depicted in Figures 2.4, 2.5, 2.6 and 2.7 describe the motion of the fluid for small and large times. This graphical solution for $n = 2$, 2.1 and 2.2 for sine wave oscillations are similar to the solution obtain by Ali and Vafai [3]. It is observed that for large time the fluid flow decays and the magnitude of oscillation is a minimum as shown in Figures 2.2 and 2.3. The time is indirectly proportional to the frequency of the velocity. Figures 2.8 and 2.9 show a smooth sine and cosine oscillation at different time as the fluid flow oscillation approaches zero.

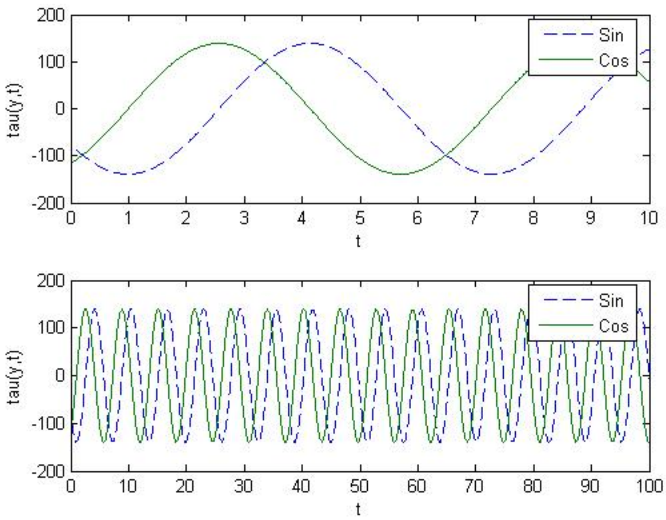

Figure 2.2: Wall shear stresses corresponding to the cosine, and sine wave oscillation, for a relatively short time $\omega = 1$, $U = 5$, for time t; $t \epsilon [0, 10]$ and $t \epsilon [0, 100]$ and $\nu = 0.0011746$.

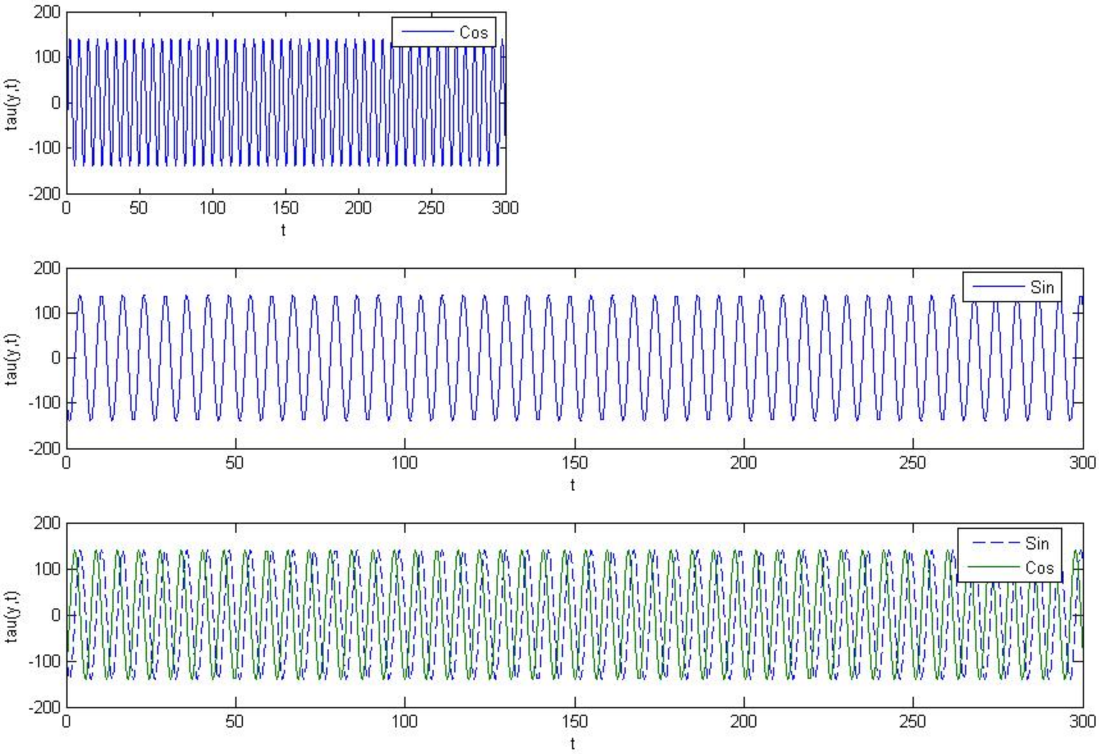

Figure 2.3: Long time profile wall shear stresses corresponding to the cosine, and sine wave oscillation, for a relatively short time $\omega = 1$, $U = 5$, and $\nu = 0.0011746$ for $t \, \epsilon \, [0, 300]$.

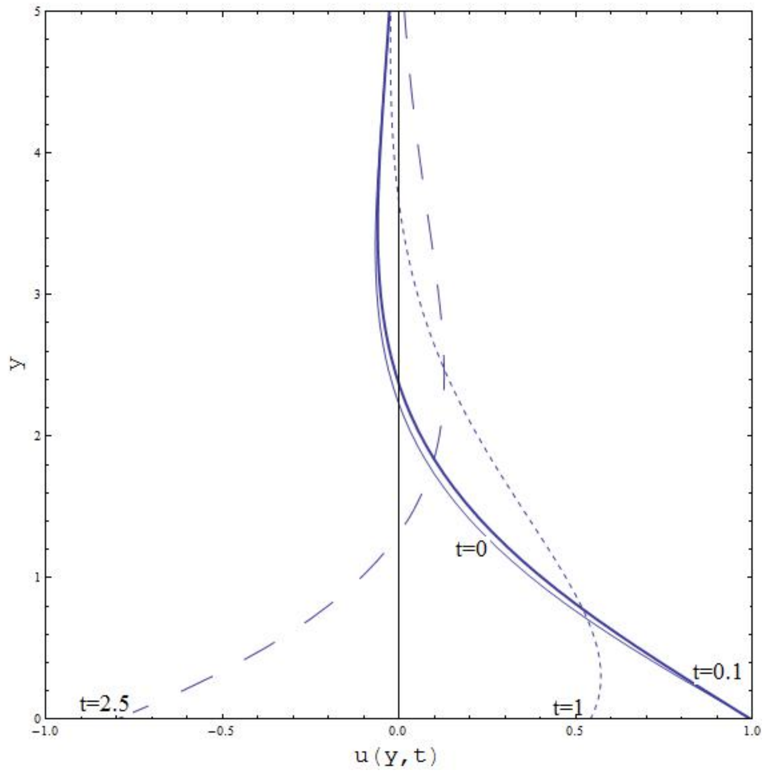

Figure 2.4: Profile velocity $u(y,t)$ corresponding to the cosine wave oscillation, for different values of times t. $\omega = 1$, $U = 1$, and $\nu = 1$.

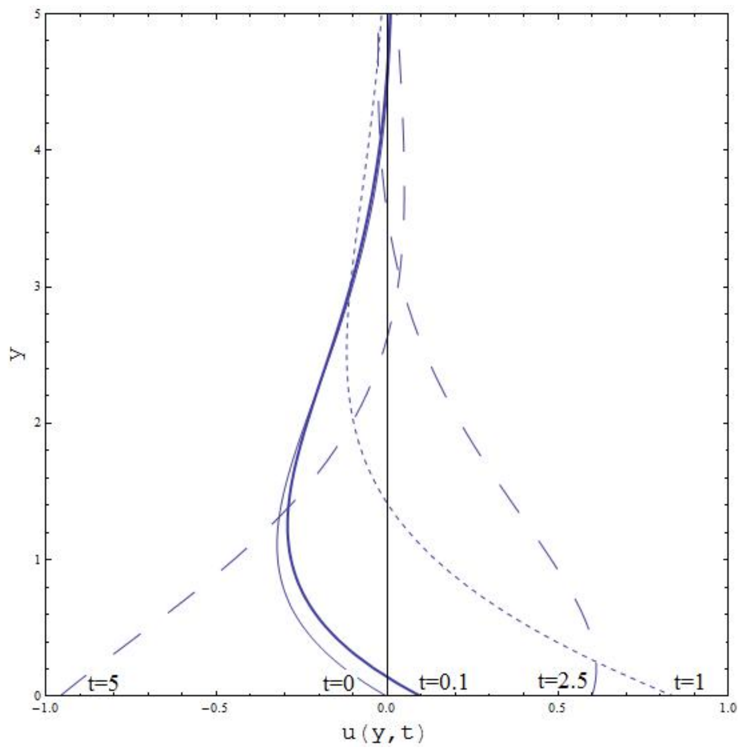

Figure 2.5: Profile velocity $u(y,t)$ corresponding to the sine wave oscillation, for different values of times t. $\omega = 1$, $U = 1$, and $\nu = 1$.

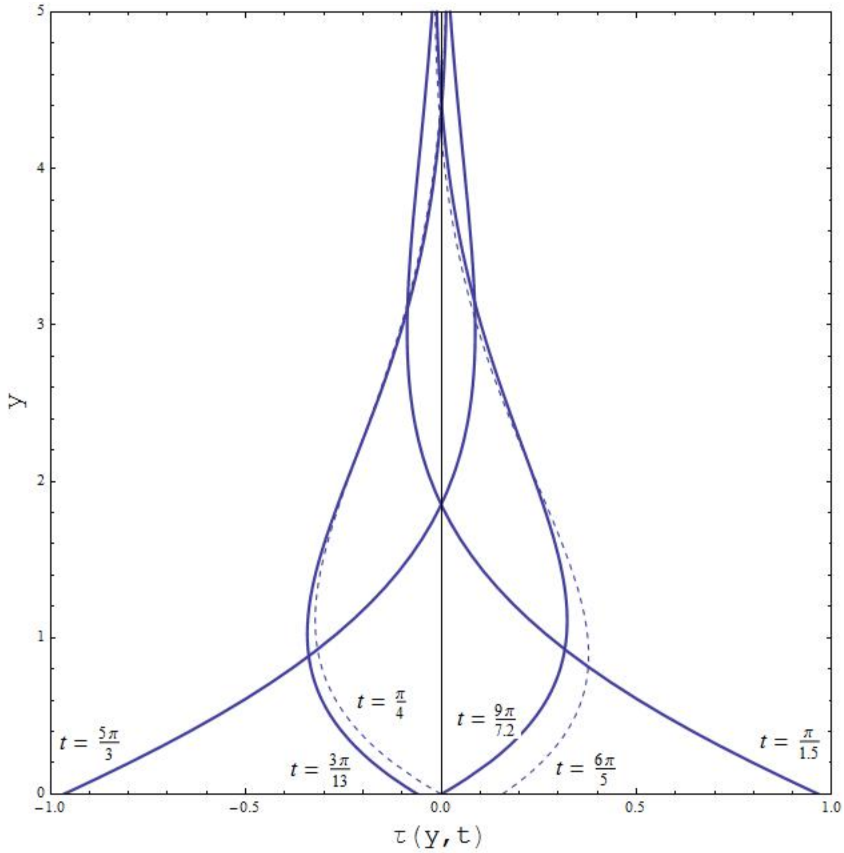

Figure 2.6: Profile of the transient shear stresses for corresponding to the cosine oscillation, $\tau(y,t)$ at different times t, $\omega = 1$, $U = 5$, for index $n = 2,\ 2.1$, $n = 2.2$ and $\nu = 0.0011746$.

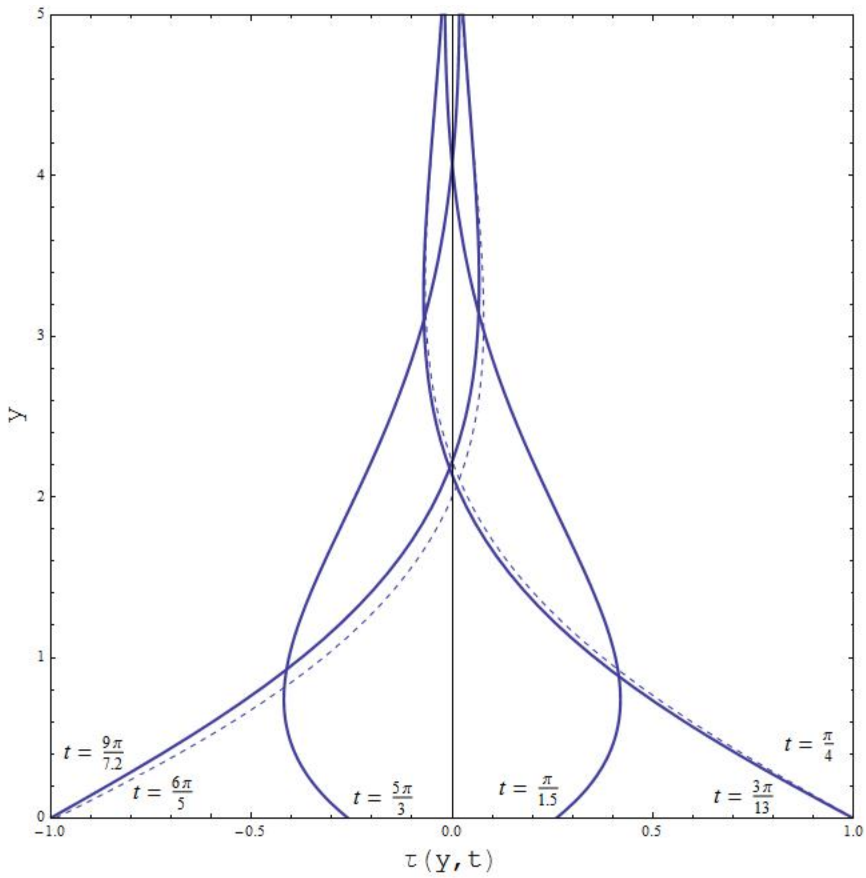

Figure 2.7: Profile of the transient shear stresses for corresponding to the cosine oscillation, $\tau(y,t)$ at different times t, $\omega = 1$, $U = 5$, for index $n = 2,\ 2.1$, $n = 2.2$ and $\nu = 0.0011746$.

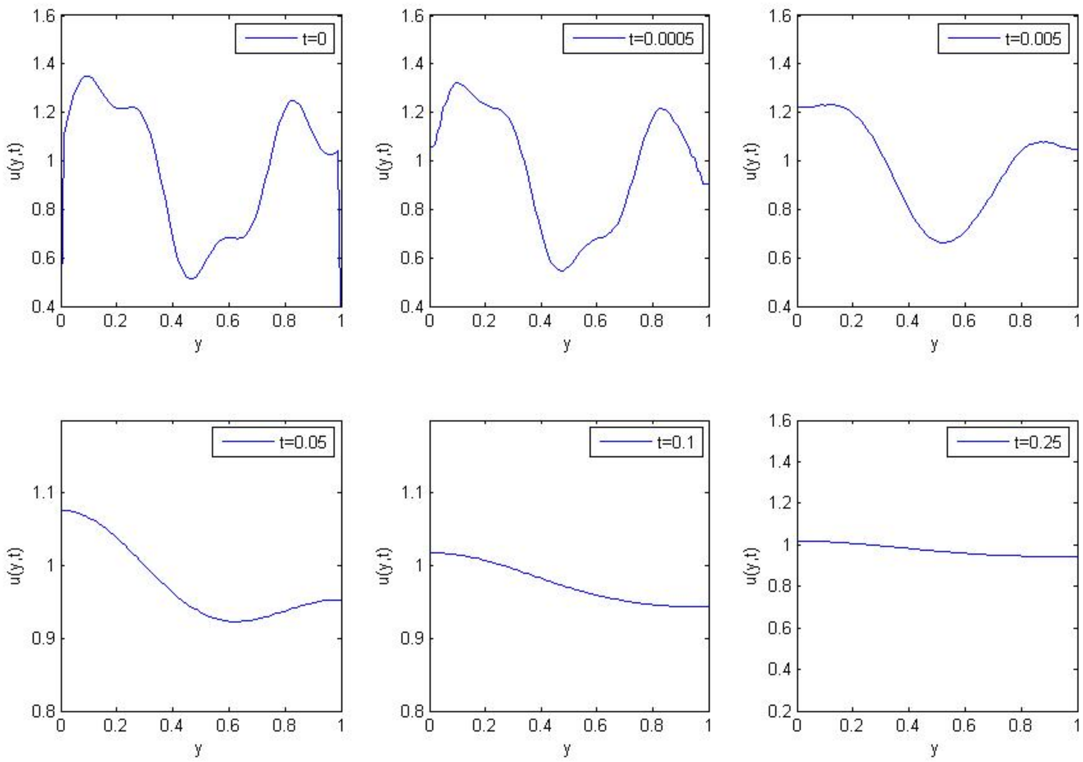

Figure 2.8: Smooth sine oscillation.

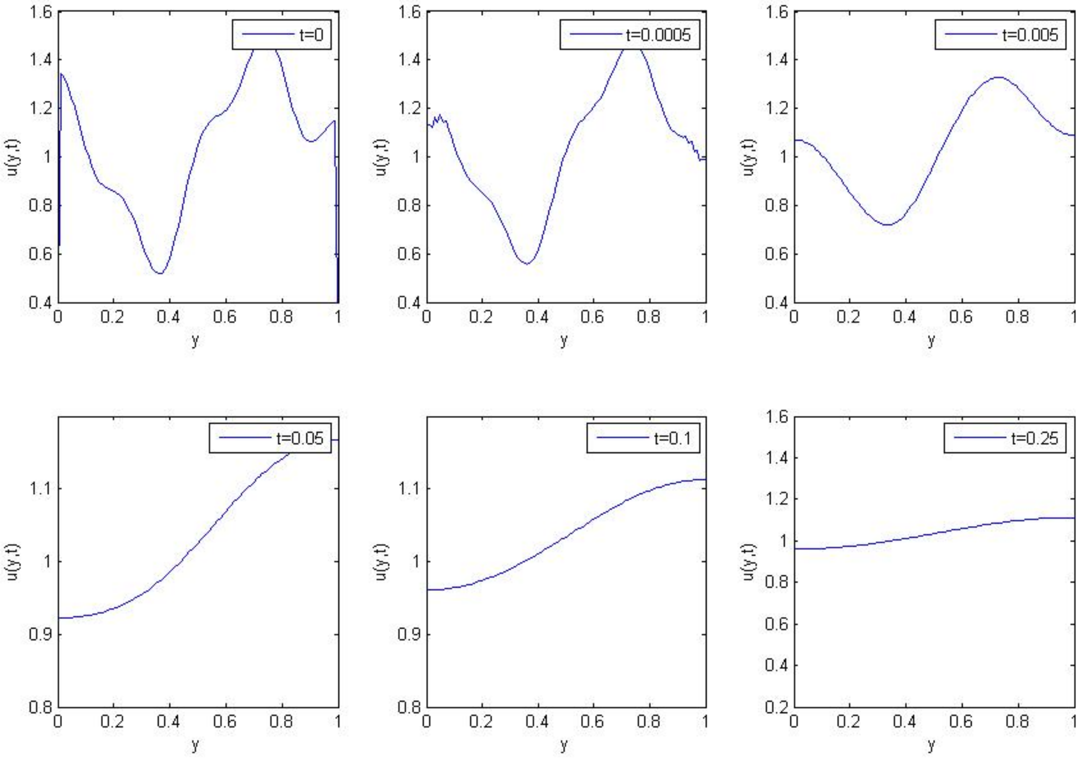

Figure 2.9: Smooth cosine oscilllation.

Chapter 3

Finite Different Approximations of the Momentum Equation

3.1 Introduction

This chapter provides a model overview of numerical solutions to the momentum equation [3] using finite difference approximations. The forward finite difference, the backward finite difference, the central finite difference and Crank-Nicolson schemes are developed and applied to the governing momentum equation for fluid flow.

The numerical results are obtained using MATLAB. The results of running the code on one dimensional meshes, and with smaller time steps are illustrated graphically. The numerical approximation shows that the schemes realize theoretical predictions of how their truncation errors depend on the spatial mesh spacing and time step.

3.2 Numerical differentiation

A finite difference is a mathematical expression of the form $f(x+b)-f(x+a)$ where f is either some explicitly known function or is given as a set of function values at distinct ordinate values [32]. Linear approximation is crucial to many known numerical techniques such as Euler's method to approximate solutions to ordinary differential equations. The idea of linear approximations rests in the closeness of the tangent line to the graph of the function around a point. Let x_0 be in the domain of the function $f(x)$. The equation of the tangent line to the graph of $f(x)$ at the point (x_0, y_0), where $y_0 = f(x_0)$, is

$$y - y_0 = f'(x_0)(x - x_0)\cdot$$

If x_1 is close to x_0, we will write $x_1 = x_0 + \Delta x$, and we will approximate $(x_0 + \Delta x)$, $y(x_0 + \Delta x)$ by the point (x_1, y_1) on the tangent line given by:

$$y_1 = y_0 + \Delta x f'(x_0)\cdot$$

If we write $\Delta y = y_1 - y_0$, we have

$$\Delta y = \Delta x f'(x_0)\cdot$$

When x is close to x_0, we have

$$f(x) \approx f(x_0) + f'(x_0)(x - x_0)\ \cdot$$

3.2.1 Taylor's Theorem

Taylor's theorem

Let $k \geq 1$ be an integer and let the function $f : R \to R$ be k times differentiable at the point $a \in R$. Then there exists a function $h_k : R \to R$ such that

$$f(x) = f(a)+f'(a)(x-a)+\frac{f''(a)}{2!}(x-a)^2+\cdots+\frac{f^{(k)}(a)}{k!}(x-a)^k+h_k(x)(x-a)^{k+1}+\cdots$$

$$\text{and} \quad \lim_{x\to a} h_k(x) = 0.$$

The polynomial appearing in Taylor's theorem is the *k-th* order Taylor polynomial

$$P_k(x) = f(a) + f'(a)(x-a) + \frac{f''(a)}{2!}(x-a)^2 + \cdots + \frac{f^{(k)}(a)}{k!}(x-a)^k$$

of the function f at the point a. The Taylor polynomial is the unique "asymptotic best fit" polynomial in the sense that if there exists a function h_k : $R \to R$ and a *k-th* order polynomial p such that

$$f(x) = p(x) + h_k(x)(x-a)^{k+1}, \quad \lim_{x\to a} h_k(x) = 0$$

then $p(x) = P_k$. Taylor's theorem describes the asymptotic behaviour of the remainder term

$$R_k(x) = f(x) - P_k(x)$$

which is the approximation error when approximating f with its Taylor polynomial. Using the little-o notation the statement in Taylor's theorem reads as

$$R_k(x) = o(|x-a|^{k+1}), \quad x \to a.$$

Assuming the function whose derivatives are to be approximated is properly-behaved, then by Taylor's theorem,

$$f(x_0+h) = f(x_0) + \frac{f'(x_0)}{1!}h + \frac{f^{(2)}(x_0)}{2!}h^2 + \cdots + \frac{f^{(n)}(x_0)}{n!}h^n + R_n(x),$$

where $n!$ denotes the factorial of n. $R_n(x)$ is a remainder term denoting the difference between the Taylor polynomial of degree n and the original function. Using the first derivative of the function f as an example, by Taylor's theorem,

$$f(x_0+h) = f(x_0) + f'(x_0)h + R_1(x).$$

Setting, $x_0 = a$ and $(x-a) = h$ we have,

$$f(a+h) = f(a) + f'(a)h + R_1(x).$$

Dividing through by h gives:

$$\frac{f(a+h)}{h} = \frac{f(a)}{h} + f'(a) + \frac{R_1(x)}{h}.$$

Solving for $f'(a)$:

$$f'(a) = \frac{f(a+h) - f(a)}{h} - \frac{R_1(x)}{h},$$

so that for $R_1(x)$ sufficiently small,

$$f'(a) \approx \frac{f(a+h) - f(a)}{h}.$$

Indeed, if f is differentiable at a, then $f'(a)$ is

$$f'(a) = \lim_{h \to 0} \frac{f(a+h) - f(a)}{h}.$$

To determine how close an approximation is to the true derivative, assume $f(x)$ is given by the Taylor expansion

$$f(x) = f(a) + f'(a)(x-a) + \frac{f''(a)}{2!}(x-a)^2 + \cdots + \frac{f^{(k)}(a)}{k!}(x-a)^k + h_k(x)(x-a)^k.$$

Assume $f(x)$ is twice differentiable at the point a and examine its first order Taylor expansion given by

$$f(a+h) = f(a) + f'(a)h + \frac{1}{2}f''(\xi)h^2$$

using Lagrange's formula for the remaining terms [33] . We choose ξ such that it is a point that lies between the point a and $a+h$ and depends on both a and h. We find

$$\frac{f(a+h) - f(a)}{h} - f'(a) = \frac{1}{2}f''(\xi)h.$$

The absolute error in a method's solution is defined as the difference between its approximation and the exact analytical solution. The two sources of error in finite difference methods are round-off error, the loss of precision due to computer rounding of decimal quantities, and truncation error or discretization error, the difference between the exact solution of the finite difference equation and the exact quantity assuming perfect arithmetic (that is, assuming no round-off) [33].

Thus the truncation error is bounded by

$$\left|\frac{f(a+h)-f(a)}{h} - f'(a)\right| \leq E|h|,$$

where $E = \text{Max}\frac{1}{2}|f''(\xi)|$ depends on the second derivative of the function f.

The big $\mathcal{O}$ notation also written as $\mathcal{O}(h)$ is used to describe the limiting behaviour of a particular function according to its growth. More precisely it refers to a term that is proportional to h whose absolute value is bounded by a constant multiple of $|h|$ as $h \to 0$. Thus since the truncation error is proportional to the first power of h, we conclude that the finite different quotient is a first order approximation of $f'(x)$. We write

$$f'(a) = \frac{f(a+h)-f(a)}{h} + \mathcal{O}(h).$$

Only three forms of finite difference are commonly considered namely forward, backward, and central differences.

3.2.2 Forward Difference Formula

Geometrically, the derivative of f at a measures the slope of the secant line through the point f at $(a, f(a))$ and f at $(a + h, f(a + h))$. A good approximation to the slope of the tangent line, $f'(a)$ is given when h is chosen to be small enough, as illustrated in the Figure (3.1). Throughout this chapter, the step length h which may be either any real number, is assumed to be small $|h| << 1$.

$$f'(a) = \frac{f(a+h) - f(a)}{h} + \mathcal{O}(h).$$

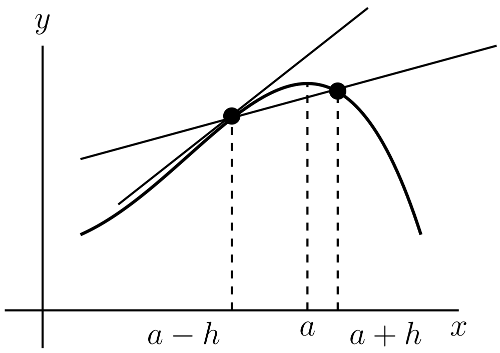

Figure 3.1: Forward difference.

A **forward difference** is an expression of the form

$$\Delta_h[f](a) = f(a+h) - f(a).$$

Depending on the application, the spacing h may be variable or constant.

3.2.3 Backward Difference Formula

From the Taylor series approximation in Section 3.2.1 we have

$$f'(a) = \frac{f(a+h) - f(a)}{h} + \mathcal{O}(h).$$

A backward difference uses the function values at a and $a-h$, instead of the function values at $a+h$ and a. Figure (3.2) shows a graphical illustration.

$$\nabla_h[f](a) = f(a) - f(a-h).$$

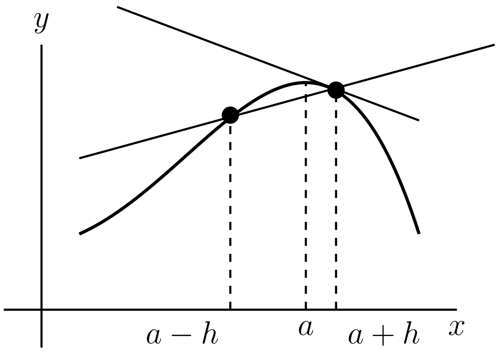

Figure 3.2: Backward difference.

3.2.4 Central Difference

Finally, the central difference is given by

$$\Delta_h[f](a) = f(a+h) - f(a-h).$$

Figure (3.3), shows a geometrical illustration of central difference.

To use a finite difference method to attempt to solve (or, more generally, approximate the solution to) a problem, one must first discretize the problem domain. This is usually done by dividing the domain into a uniform grid see Section 3.4.1 where forward differences, backward differences and central differences are used to approximate the derivatives in ordinary or partial differential equation(s). Note that this means that finite difference methods produce sets of discrete numerical approximations to the derivative, often in a "time-stepping" manner. i.e specifically, instead of solving for $c(x,t)$ with x and t continuous, we solve for $c_{i,j} \equiv c(x_i, t_j)$, where

$$y_i \equiv i\delta y, \quad i = 0, 1, 2, 3, \cdots$$

$$t_j \equiv j\delta t \quad j = 0, 1, 2, 3, \cdots$$

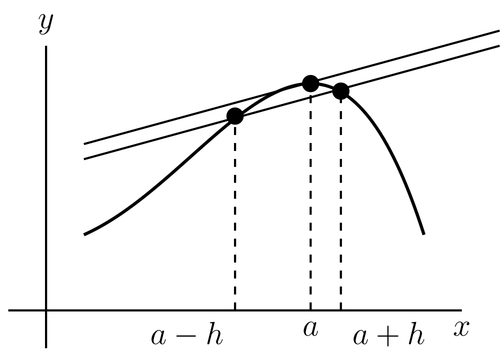

Figure 3.3: Central difference.

3.3 Momentum Equation Approximation using Finite Difference Method

Consider a non-Newtonian fluid at rest over an infinitely extended flat plate perpendicular to the y-axis of a Cartesian coordinate system x, y and z. At time $t = 0^+$ the flat plate begins to oscillate in its plane with angular velocity Ω.

Due to the shear, the fluid above the plate is gradually moved, and transmits the motion into the fluid. The fluid velocity is of the form [1, 3]

The one dimensional momentum equation is defined as

$$\rho \frac{\partial u}{\partial t} = \frac{\partial}{\partial y}(\nu \frac{\partial u}{\partial y}) \quad y > 0 \tag{3.1}$$

where $u = u(y, t)$ is the dependent variable, u, t and ν are the velocity in the x direction, time and the dynamic viscosity of the fluid, respectively and $y > 0$ is the space occupied by the fluid.

In practical computation, the solution is obtained only for a finite time, say t_{max}. Solution to Eq. (3.1) requires specification of boundary conditions at $y = 0$ and $y = L$, and the initial conditions at $t = 0$. Simple boundary and initial conditions are

$$u(0, t) = u_0, u(L, t) = u_L, u(y, 0) = f_0(y). \tag{3.2}$$

Other boundary conditions can be specified. To keep the presentation as simple as possible, only the conditions in Eq. (3.2) are considered. The idea is to replace the derivatives in the momentum equation by different quotients. We consider the relationships between u at (y, t) and its neighbours a distance Δy apart at a time Δt later.

3.4 Finite Difference Method

The finite difference method is one of several techniques for obtaining a numerical approximation of Eq. (3.1). The partial differential equation is replaced with a discrete approximation.

3.4.1 The Discrete Mesh

The finite difference method obtains approximate solutions for $u(y,t)$ at a finite set of y and t. The grid points for this situation are (y_i, t_m) where the discrete y are uniformly spaced in the interval $0 \leq y \leq L$ such that

$$y_i = (i)\Delta y, \quad i = 1, 2, 3, \cdots N$$

N is the total number of spatial nodes, which include also the points on the boundary.

Given L and N, the spacing between the grid points y is computed with

$$\Delta y = \frac{L}{N}.$$

Time is discretized in a similar manner on the mesh, the discrete t are uniformly spaced in $0 \leq t \leq t_{max}$.

$$t_m = (m)\Delta t, \quad m = 1, 2, 3, \cdots M.$$

M is the maximum number of time steps and Δt is the change in the time step.

$$\Delta t = \frac{t_{max}}{M}.$$

In order to affect the numerical approximation to the solution of the momentum equation, we maintain a uniform rectangular mesh spacing in both directions of nodes given by $(y_i, t_m) \in \mathbb{R}^2$ with

$$0 = t_0 < t_1 < t_2 < \cdots < t_{max}; \quad 0 = y_0 < y_1 < y_2 < \cdots < y_N = L.$$

We use the notation

$$u_{i,m} \approx u(y_i, t_m) \quad \text{where} \quad t_m = (m)\Delta t,\ y_i = (i)\Delta y$$

to define the numerical approximation.

The mesh points are shown in Figure (3.4)

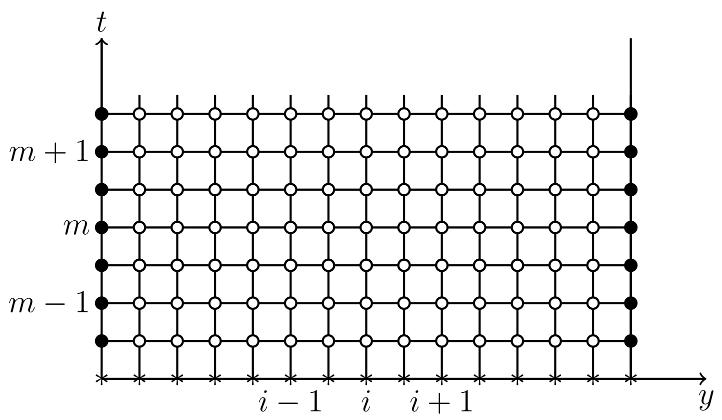

Figure 3.4: Mesh points.

In Figure (3.4) the $*$ indicates a vector location of known initial values. The solid circles show the location of the known boundary domain solution values, for $y = 0$ and $y = L$ and the open circles show the location of the finite difference approximations that are computed.

3.4.2 Numerical Finite Difference Approach

Finite differences can be considered in more than one variable, using discrete approximations such as

$$\frac{\partial u}{\partial y} \approx \frac{u_{i+1} - u_i}{\Delta y}, \tag{3.3}$$
$$\frac{\partial u^2}{\partial y^2} \approx \frac{u_{i+1} - 2u_i + u_{i-1}}{\Delta y^2}. \tag{3.4}$$

The right hand side quantities are defined on the finite difference mesh. The differential equation approximations are obtained by replacing all continuous derivatives by their discrete approximations. The numerical solution to the PDE is an approximation to the exact solution and is obtained using a discrete representation to the PDE at the grid points y_i in the discrete spatial mesh at every time level t_m . Let us denote this approximate as

$$u_i^m \approx u(y_i, t_m).$$

Thus, the numerical solution is a collection of finite values,

$$U^m = [U_1^m, U_2^m, ..., U_{N-1}^m]$$

at each time level t_m. The boundary conditions determine the values of u_0^m and u_N^m for all m. The initial conditions determine the values of U_0 at each spatial grid point.

The relationship between the continuous (exact) solution and the discrete approximation is shown in Figure (3.5). Numerical computation of u_i^m from the finite different model is a very distinct step used on translating the continuous

$$\begin{array}{c} \text{Continuous PDE} \\ u(y,t) \end{array} \longrightarrow \begin{array}{c} \text{Discrete} \\ \text{Equation} \end{array} \longrightarrow \begin{array}{c} \text{Approximate solution} \\ u_i^m \text{ to } u(y,t) \end{array}$$

Figure 3.5: Relationship between continuous and discrete problem.

problem domain to the discrete problem domain. Finite difference formulas are first being modeled with the dependent variable u as a function of only one independent variable, y, thus $u = u(y)$. The resulting formulas are then used to approximate derivatives with respect to either space or time. By initially working with one independent variable $u = u(y)$, the notation is simplified without any loss of generality in the result.

3.4.3 Partial Derivative Approximations

This subsection aims to determine a numerical solution for the momentum equation, with the idea of replacing the derivatives in the momentum equation Eq. (3.1) by their finite difference approximations.

First Order Forward Difference Method

Considering a Taylor series of $u(y)$ expanded around the point y_i

$$u(y_i + \delta y) = u(y_i) + \delta y \left.\frac{\partial u}{\partial y}\right|_{y_i} + \frac{\delta y^2}{2!} \left.\frac{\partial^2 u}{\partial y^2}\right|_{y_i} + \frac{\delta y^3}{3!} \left.\frac{\partial^3 u}{\partial y^3}\right|_{y_i} + ... \tag{3.5}$$

If we consider the value of u at the next point after y_i, i.e y_{i+1} on the mesh line

$$u(y_i+\Delta y) = u(y_{i+1}) = u(y_i) + \Delta y \frac{\partial u}{\partial y}\bigg|_{y_i} + \frac{\Delta y^2}{2!}\frac{\partial^2 u}{\partial y^2}\bigg|_{y_i} + \frac{\Delta y^3}{3!}\frac{\Delta^3 u}{\partial y^3}\bigg|_{y_i} + ... \quad (3.6)$$

Rearrange the equation and solving for $\frac{\partial u}{\partial y}$ at y_i

$$\frac{\partial u}{\partial y}\bigg|_{y_i} = \frac{u(y_i+\Delta y) - u(y_i)}{\Delta y} - \frac{\Delta y^1}{2!}\frac{\partial^2 u}{\partial y^2}\bigg|_{y_i} - \frac{\Delta y^2}{3!}\frac{\Delta^3 u}{\partial y^3}\bigg|_{y_i} + ... \quad (3.7)$$

Using the approximate solution $u_i \approx u(y_i)$ and $u_{i+1} \approx u(y_i + \Delta y)$

$$\frac{\partial u}{\partial y}\bigg|_{y_i} = \frac{u_{i+1} - u_i}{\Delta y} - \frac{\Delta y^1}{2!}\frac{\partial^2 u}{\partial y^2}\bigg|_{y_i} - \frac{\Delta y^2}{3!}\frac{\Delta^3 u}{\partial y^3}\bigg|_{y_i} + ... \quad (3.8)$$

Using the big $\mathcal{O}$ notation, the equation can be written as

$$\frac{\partial u}{\partial y}\bigg|_{y_i} = \frac{u_{i+1} - u_i}{\Delta y} + \mathcal{O}(\Delta y). \quad (3.9)$$

First Order Backward Difference Method

Expanding $u(y_i - \Delta y)$ in a Taylor series we obtain

$$u_{i+1} = u_i - \Delta y\,\frac{\partial u}{\partial y}\bigg|_{y_i} + \frac{\Delta y}{2!}\frac{\partial^2 u}{\partial y^2}\bigg|_{y_i} - \frac{(\Delta y)^3}{3!}\frac{\partial^3}{\partial y^3}\bigg|_{y_i} + ... \quad (3.10)$$

Solve for $\frac{\partial u}{\partial y}$ at y_i

$$\frac{\partial u}{\partial y}\bigg|_{y_i} = \frac{u_{i+1} - u_i}{\Delta y} + \frac{\Delta y}{2!}\frac{\partial^2 u}{\partial y^2}\bigg|_{y_i} - \frac{\Delta y^2}{3!}\frac{\Delta^3 u}{\partial y^3}\bigg|_{y_i} + ... \quad (3.11)$$

Using the big $\mathcal{O}$ notation, the equation can be written as

$$\left.\frac{\partial u}{\partial y}\right|_{y_i} = \frac{u_i - u_{i-1}}{\Delta y} + \mathcal{O}(\Delta y). \tag{3.12}$$

Second Order Central Difference Method

Expanding $u(y_i + \Delta y)$ and $u(y_i - \Delta y)$ in a Taylor series we obtain

$$u_{i+1} = u_i + \Delta y \left.\frac{\partial u}{\partial y}\right|_{y_i} + \frac{\Delta y}{2!}\left.\frac{\partial^2 u}{\partial y^2}\right|_{y_i} + \frac{(\Delta y)^3}{3!}\left.\frac{\partial^3 u}{\partial y^3}\right|_{y_i} + ... \tag{3.13}$$

and

$$u_{i-1} = u_i - \Delta y \left.\frac{\partial u}{\partial y}\right|_{y_i} + \frac{\Delta y}{2!}\left.\frac{\partial^2 u}{\partial y^2}\right|_{y_i} - \frac{(\Delta y)^3}{3!}\left.\frac{\partial^3 u}{\partial y^3}\right|_{y_i} + ... \tag{3.14}$$

Subtracting Eq. (3.14) from Eq. (3.13) we obtain

$$u_{i+1} - u_{i-1} = 2\Delta y \left.\frac{\partial u}{\partial y}\right|_{y_i} + \frac{2(\Delta y)^3}{3!}\left.\frac{\partial^3 u}{\partial y^3}\right|_{y_i} + ... \tag{3.15}$$

Rearranging and solving

$$\left.\frac{\partial u}{\partial y}\right|_{y_i} = \frac{u_{i+1} - u_{i-1}}{2\Delta y} - \frac{(\Delta y)^2}{3!}\left.\frac{\partial^3}{\partial y^3}\right|_{y_i} + ... \tag{3.16}$$

Using the big $\mathcal{O}$ notation Eq. (3.16) becomes

$$\left.\frac{\partial u}{\partial y}\right|_{y_i} = \frac{u_{i+1} - u_{i-1}}{2\Delta y} - \mathcal{O}(\Delta y^2). \tag{3.17}$$

$$u_{i+1} + u_{i-1} = 2u_i + (\Delta y)^2 \left.\frac{\partial^2 u}{\partial y^2}\right|_{y_i} + \frac{2(\Delta y)^4}{4!}\left.\frac{\partial^4}{\partial y^4}\right|_{y_i} + ... \tag{3.18}$$

Solving for $\frac{\partial^2 u}{\partial y^2}$ at y_i

$$\left.\frac{\partial^2 u}{\partial y^2}\right|_{y_i} = \frac{u_{i+1} - 2u_i + u_{i+1}}{\Delta y^2} + \frac{(\Delta y)^2}{4!}\left.\frac{\partial^4}{\partial y^4}\right|_{y_i} + ... \tag{3.19}$$

Using the big $\mathcal{O}$ notation.

$$\left.\frac{\partial^2 u}{\partial y^2}\right|_{y_i} = \frac{u_{i+1} - 2u_{i+1} + u_{i-1}}{\Delta y^2} + \mathcal{O}(\Delta y^2). \tag{3.20}$$

Manipulating Eqs. (3.13) and (3.14) yields higher order finite difference approximations for $\frac{\partial u}{\partial y}$ and $\frac{\partial^2 y}{\partial y^2}$.

3.5 Schemes for the Momentum Equation

The finite difference approximations developed in the preceding sections are now assembled into a discrete approximation of Eq. (3.1). This approach involves both the time and spatial derivatives to be replaced by finite differences. The replacement requires specifications of both the time and spatial locations of the u values in the finite difference formulas.

3.5.1 Forward Time, Centered Space

Approximate the time derivate in Eq. (3.1) with a *forward difference* approximation

$$\left.\frac{\partial u}{\partial t}\right|_{y_i,t_m} = \frac{u_i^{m+1} - u_i^m}{\Delta t} + \mathcal{O}(\Delta t), \tag{3.21}$$

and the spatial derivative by a *central difference* approximation

$$\left.\frac{\partial^2 u}{\partial y^2}\right|_{y_i,t_m} = \frac{u_{i-1}^m - 2u_i^m + u_{i+1}^m}{\Delta y^2} + \mathcal{O}(\Delta y^2). \tag{3.22}$$

Substitute Eq. (3.21) into the left hand side of Eq. (3.1); substitute Eq. (3.22) into the right hand side of Eq. (3.1); and collect the terms to obtain

$$\rho\frac{u_i^{m+1} - u_i^m}{\Delta t} = \nu\frac{u_{i-1}^m - 2u_i^m + u_{i+1}^m}{\Delta y^2} + \mathcal{O}(\Delta t) + \mathcal{O}(\Delta y^2). \tag{3.23}$$

The two error terms, temporal error and spatial error are not of the same order. We can explicitly solve for u_i^{m+1} in terms of the other values of u. Drop the truncation error terms, cross multiply by Δt, rearrange Eq. (3.23) and solve for u_i^{m+1} to obtain

$$u_i^{m+1} = u_i^m + \frac{\nu\Delta t}{\rho\Delta y^2}(u_{i-1}^m - 2u_i^m + u_{i+1}^m). \tag{3.24}$$

Eq. (3.24) can be improved slightly in computational efficiency by rearrangement and grouping like terms, to obtain

$$u_i^{m+1} = ru_{i+1}^m + (1-2r)u_i^m + ru_{i-1}^m \tag{3.25}$$

where

$$r = \frac{\nu\Delta t}{\rho\Delta y^2}.$$

Using this recurrence relation and knowing the values at the boundaries, one can obtain the approximate values at t_{m+1}, if we know the values at t_m. The computational molecule stencil for the explicit method can be found in Figure (3.6).

The solution of the momentum equation Eq. (3.1) subject to the initial and boundary conditions in Eq. (3.2) is bounded. The FTCS can produce unstable solutions that oscillate and grow if Δt is too large. Stable solutions with FTCS scheme are only obtained if [34]

$$r = \alpha \frac{\Delta t}{\Delta y^2} \leq \frac{1}{2} \quad \text{where } \alpha = \frac{\nu}{\rho}.$$

We note that Eq. (3.24) gives rise to an $(N-1)$ x $(N-1)$ matrix for the unknown interior approximate solution values where we write the approximation solution at time step m in a column vector as U^m. The matrix equation that moves the approximation forward in time can be expressed as a matrix multiplication

$$U^{m+1} = AU^m, \quad m = 1, 2, 3, ...N,$$

where the tridiagonal matrix A has the form

$$A_{m,n} = \begin{pmatrix} 1 & 0 & 0 & 0 & 0 & 0 \\ r & (1-2r) & r & 0 & 0 & 0 \\ 0 & r & (1-2r) & r & 0 & 0 \\ 0 & 0 & \ddots & \ddots & \ddots & 0 \\ 0 & 0 & 0 & r & (1-2r) & r \\ 0 & 0 & 0 & 0 & 0 & 1 \end{pmatrix}.$$

U^{m+1} is obtained iteratively from U^m by a simple matrix multiplication. U^{m+1} is the vector of u values at time step $m+1$. The first and last rows of A are adjusted so that the boundary values of u do not change when the matrix-vector product is computed.

3.5.2 Backward Time, Centered Space

In the derivation of Eq. (3.24), the forward difference was used to approximate the time derivative on the left hand side of Eq. (3.1). The forward difference approximation has a major drawback of instability in situations where the time step is chosen of the same order as the spatial mesh/grid size. Choose the backward difference approximation to obtain a more stable method,

$$\left.\frac{\partial u}{\partial t}\right|_{y_i,t_m} = \frac{u_i^m - u_i^{m-1}}{\Delta t} + \mathcal{O}(\Delta t). \tag{3.26}$$

Substitute Eq. (3.26) into the left hand side of Eq. (3.1); substitute Eq. (3.22) into the right hand side of Eq. (3.1) and collect terms, then Eq. (3.1) simplifies to

$$\frac{u_i^m - u_i^{m-1}}{\Delta t} = \alpha\frac{u_{i-1}^m - 2u_i^m + u_{i+1}^m}{\Delta y^2} + \mathcal{O}(\Delta t) + \mathcal{O}(\Delta y^2), \tag{3.27}$$

where

$$\alpha = \frac{\nu}{\rho}.$$

The truncation error of Eq. (3.27) is of the same order of magnitude as that of Eq. (3.23). Looking at Eqs. (3.27) and (3.23) we see that both equations have the parameters u_{i-1}^m, u_i^m; however Eq. (3.27), unlike Eq. (3.23), cannot be rearranged to obtain a simple algebraic formula for computing u_i^m in terms of its right neighbor u_{i+1}^m and left neighbor u_{i-1}^m. The backward difference method is an *implicit* method, while the forward difference method is *explicit*. The computational molecule stencil for the implicit method can be found in Figure (3.6). Thus, Eq. (3.27) is one equation in a system of unknowns for the values of u at the internal nodes of the spatial mesh ($i = 1, 2, 3, 4, 5, ..., N-1$)

at time level t_m.

Dropping the error terms in Eq. (3.27) and rearranging the resulting equation to obtain

$$-\frac{\alpha}{\Delta y^2}u_{i-1}^m + \left(\frac{1}{\Delta t} + \frac{2\alpha}{\Delta y^2}\right)u_i^m - \frac{\alpha}{\Delta y^2}u_{i+1}^m = \frac{1}{\Delta t}u_i^{m-1}. \tag{3.28}$$

The system of equations can be represented in matrix form. If we define the coefficients of the interior nodes as

$$\begin{aligned} a_i &= \frac{-\alpha}{\Delta y^2}, \qquad i = 2, 3, ..., N-1 \\ b_i &= \frac{1}{\Delta t} + \frac{2\alpha}{\Delta y^2}, \\ c_i &= \frac{-\alpha}{\Delta y^2}, \\ d_i &= \frac{1}{\Delta t}u_i^{m-1}, \end{aligned} \tag{3.29}$$

the matrix reduces to,

$$\begin{bmatrix} b_1 & c_1 & 0 & 0 & 0 & 0 \\ a_2 & b_2 & c_2 & 0 & 0 & 0 \\ 0 & 0 & \ddots & \ddots & \ddots & 0 \\ \vdots & \ddots & \ddots & \ddots & \ddots & \vdots \\ 0 & 0 & 0 & a_{N-1} & b_{N-1} & c_{N-1} \\ 0 & 0 & 0 & 0 & a_N & b_N \end{bmatrix} \begin{bmatrix} u_1 \\ u_2 \\ u_3 \\ \vdots \\ u_{N-1} \\ u_N \end{bmatrix} = \begin{bmatrix} d_1 \\ d_2 \\ d_3 \\ \vdots \\ d_{N-1} \\ d_N \end{bmatrix}.$$

The Dirichlet boundary conditions on the interval $[0, L]$ take the form:

$$\begin{aligned} b_1 &= 1, \qquad c_1 = 0, \qquad d_1 = u_0 \\ a_N &= 0, \qquad b_N = 0, \qquad d_N = u_L \end{aligned} \tag{3.30}$$

3.5.3 Crank-Nicolson Method

The momentum equation is approximated as follows. At t_{m-1} use the forward difference approximation of u_t and the central difference of u_{yy}. At t_m use the backward difference approximation of u_t and the central difference approximation of u_{yy}. Adding these two approximations we obtain

$$\frac{u_i^m - u_i^{m-1}}{\Delta t} = \frac{\alpha}{2}\left[\frac{u_{i-1}^m - 2u_i^m + u_{i+1}^m}{\Delta y^2} + \frac{u_{i-1}^{m-1} - 2u_i^{m-1} + u_{i+1}^{m-1}}{\Delta y^2}\right]. \tag{3.31}$$

This is known as the Crank-Nicolson method [32, 33, 35] or the Crank-Nicolson stencil. The computational molecule stencil for the Crank-Nicolson method can be found in Figure (3.6). [Thus we in effect have the central difference at time $t_{m-\frac{1}{2}}$ and a second-order central difference for the space derivative at position y_i].

Rearrange the recurrence relationship, such that the values of u at time step m appear on the left hand side and those at time step $m-1$ are on the right hand side.

$$\begin{aligned} -\frac{\alpha}{2\Delta y^2}u_{i-1}^m + \left(\frac{1}{\Delta t} - \frac{\alpha}{\Delta y^2}\right)u_i^m - \frac{\alpha}{2\Delta y^2}u_{i+1}^m = \\ \frac{\alpha}{2\Delta y^2}u_{i-1}^{m-1} + \left(\frac{1}{\Delta t} + \frac{\alpha}{\Delta y^2}\right)u_i^{m-1} + \frac{\alpha}{2\Delta y^2}u_{i+1}^{m-1}. \end{aligned} \tag{3.32}$$

Now make the substitution,

$$
\begin{aligned}
a_i &= \frac{-\alpha}{2\Delta y^2}, \qquad i = 1, 2, 3, ..., N-1 \\
b_i &= \left(\frac{1}{\Delta t}\right) + \left(\frac{\alpha}{\Delta y^2}\right), \\
c_i &= \frac{-\alpha}{2\Delta y^2}, \\
d_i &= a_i u_{i-1}^{m-1} + \left(\frac{1}{\Delta t} + a_i + c_i\right) u_i^{m-1} + c_i u_{i+1}^{m-1}.
\end{aligned}
\tag{3.33}
$$

Thus the Crank-Nicolson scheme can be represented in a matrix form

$$
i = 1, 2, 3, \cdots, N \begin{bmatrix} a_1 & b_1 & c_1 & 0 & 0 & \dots & 0 \\ 0 & a_2 & b_2 & c_2 & 0 & \dots & 0 \\ 0 & 0 & a_3 & b_3 & c_3 & \dots & 0 \\ 0 & 0 & & \dots\ddots & \ddots & \ddots & 0 \\ 0 & 0 & 0 & \dots & a_{N-1} & b_{N-1} & c_{N-1} \\ 0 & 0 & 0 & \dots & 0 & a_N & b_N \end{bmatrix} \begin{bmatrix} u_1 \\ u_2 \\ u_3 \\ \vdots \\ u_{N-1} \\ u_N \end{bmatrix} = \begin{bmatrix} d_1 \\ d_2 \\ d_3 \\ \vdots \\ d_{N-1} \\ d_N \end{bmatrix},
$$

where $[u_i]$ is a vector of unknown u-values at time level t_m

The scheme is always numerically stable and convergent but usually more numerically intensive as it requires solving a system of equations on each time step. The errors are quadratic over both the time and space step [33]:

$$\Delta u = O(k^2) + O(h^2).$$

The Crank-Nicolson scheme is usually the most accurate scheme for small time steps . The explicit scheme is the least accurate compared to the implicit scheme and can be unstable, but is also the easiest to implement on Matlab and the least numerically intensive. The implicit scheme works the best for large time steps. In section 3.6 we have compared the explicit and implicit method to the exact solution. The plots shows a good comparison between explicit and implicit schemes and the error terms.

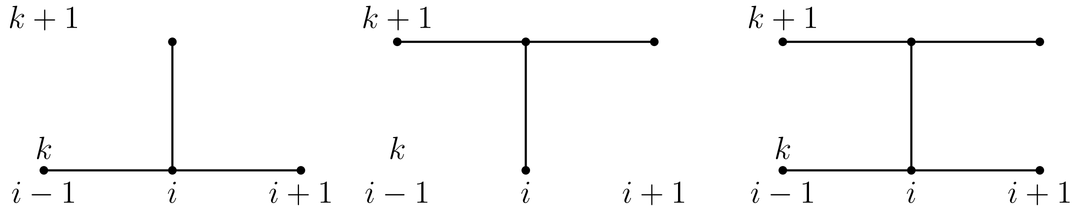

Figure 3.6: Computational stencil.

3.6 Numerical Results and Conclusion

The explicit method (forward time, centered space), the implicit method (backward time, centered space) and the Crank-Nicolson scheme have been developed. The calculations obtained using MATLAB with finer mesh points on each scheme have demonstrated the theoretical predictions of how their truncation errors depend on time step size and mesh point spacing as shown in Figure (3.7) and Figure (3.8). The FTCS and BTCS both have the truncation error of $\mathcal{O}(\Delta t) + \mathcal{O}(\Delta y^2)$ and the Crank-Nicolson has a truncation error of $\mathcal{O}(\Delta t^2) + \mathcal{O}(\Delta y^2)$. The $\mathcal{O}$ is defined to be the rate an which the truncation error approaches zero. Hence both the FTCS and BTCS schemes are first order accurate in time spacing as the truncation error terms are proportional to (Δt) and the Crank-Nicolson scheme has temporal truncation error terms proportional to (Δt^2) which is considerably smaller than the FTCS and BTCS.

Running the analysis in MATLAB, the explicit method gives much better accuracy than the implicit algorithm for small time steps. However the implicit method is good for large time steps. In both the explicit and implicit methods the mesh spacing is proportional to (Δy^2). Hence a better accuracy can be obtained when the interval is divided into a smaller mesh size see Figure (3.8). The Crank- Nicolson method gives a better approximation when compared to FTCS and BTCS. This is shown by Figures (3.9) and (3.10) for the sine and the cosine oscillation. Figures (3.8) and (3.11) show the comparison for the sine oscillation and the cosine oscillation. In the Crank-Nicolson scheme the order of the truncation error is (Δt^2) and (Δy^2), so that it is recommended to choose the time step size that has the same order of magnitude as the mesh spacing, $\Delta t \approx \Delta y$.

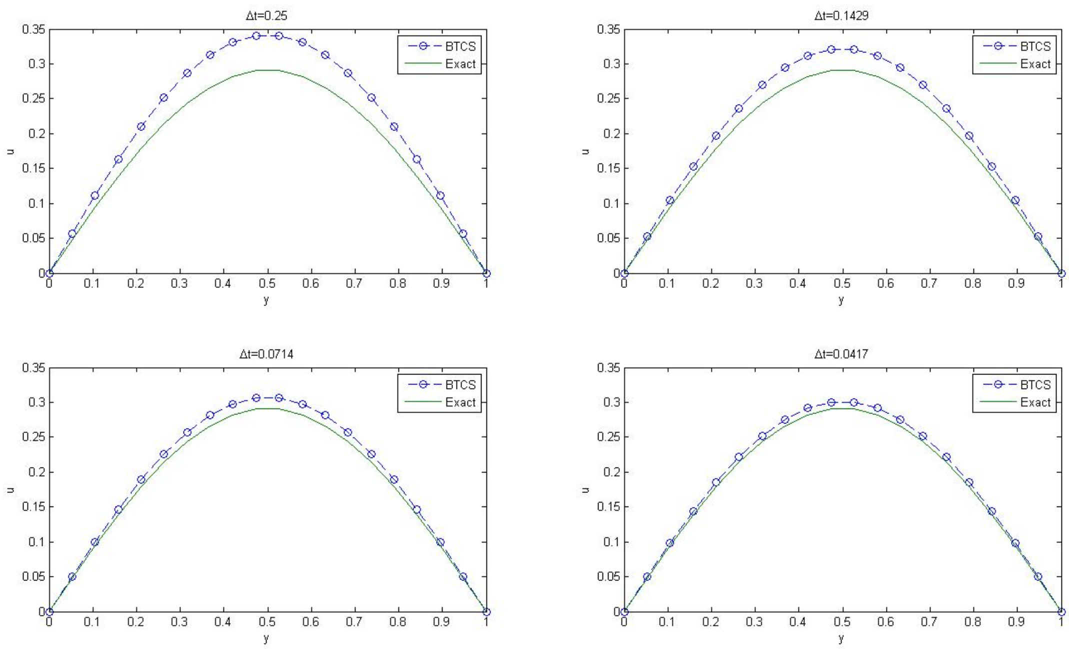

Figure 3.7: BTCS time step compared for the sine oscillation for a fixed $\Delta y = 0.0526$.

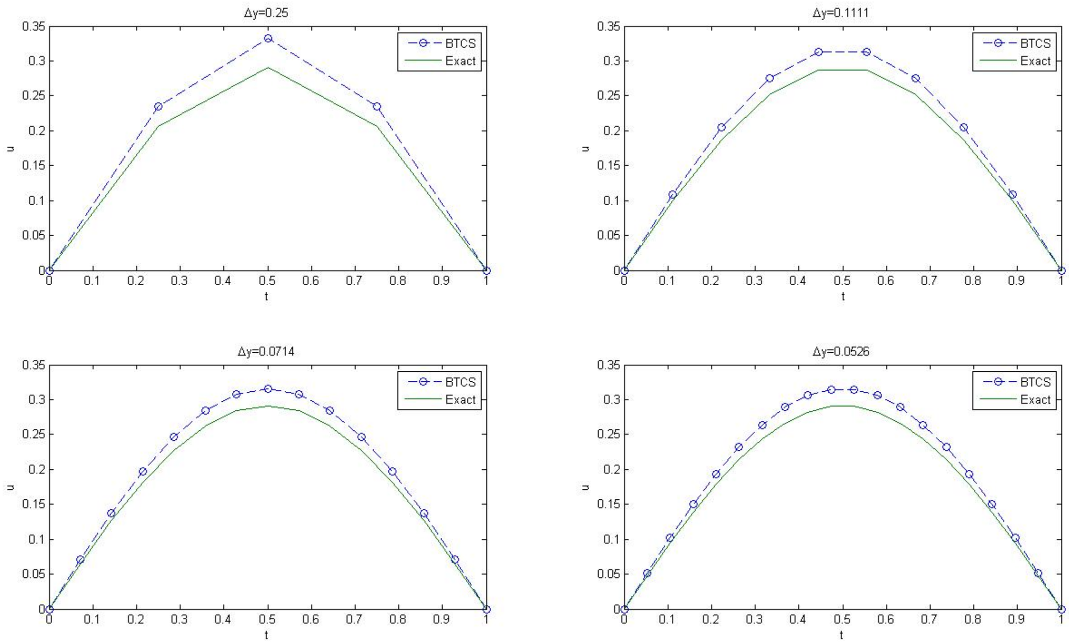

Figure 3.8: BTCS mesh step compared for the sine oscillation for a fixed $\Delta t = 0.1111$.

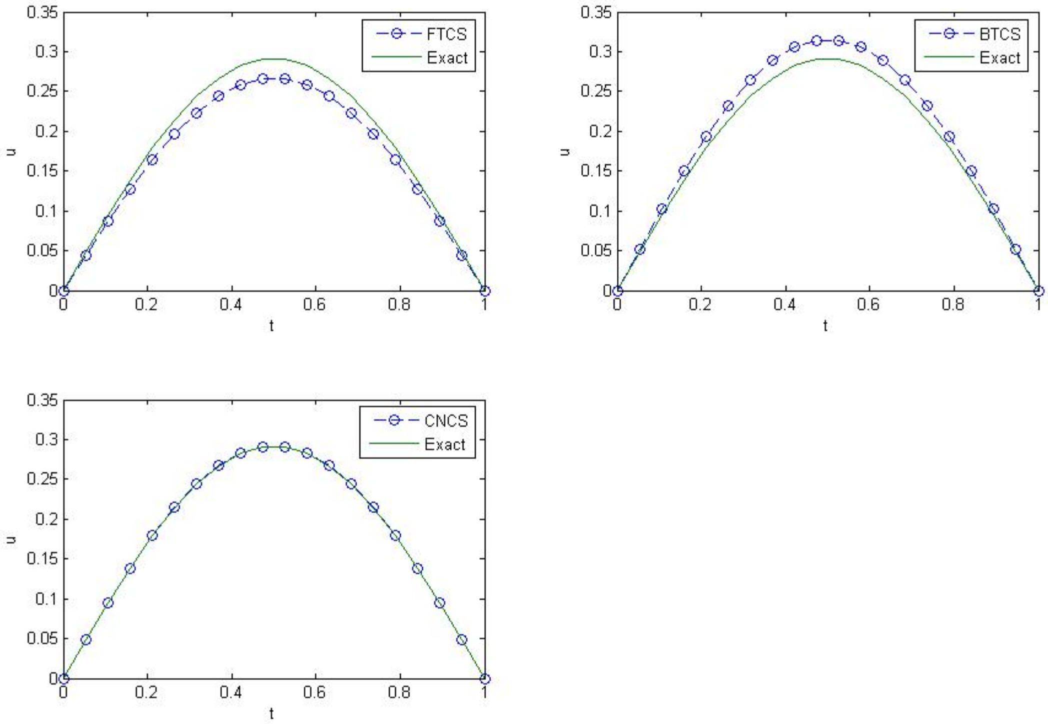

Figure 3.9: FTCS, BTCS and CNCS for the sine oscillation for $\Delta t = 0.1111$ and $\Delta t = 0.0526$.

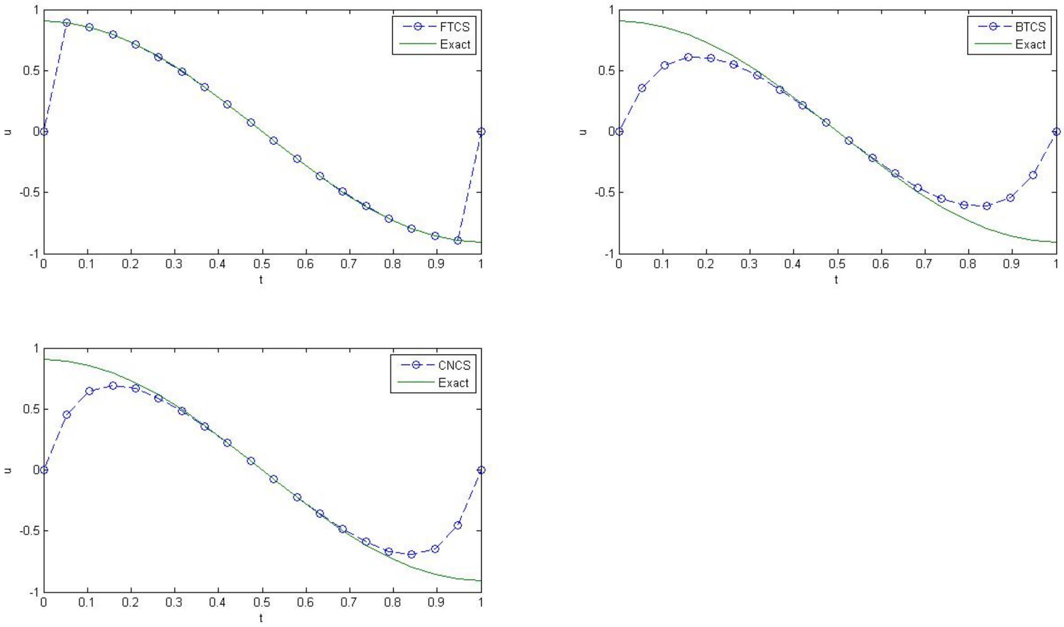

Figure 3.10: FTCS, BTCS and CNCS for the cosine oscillation.

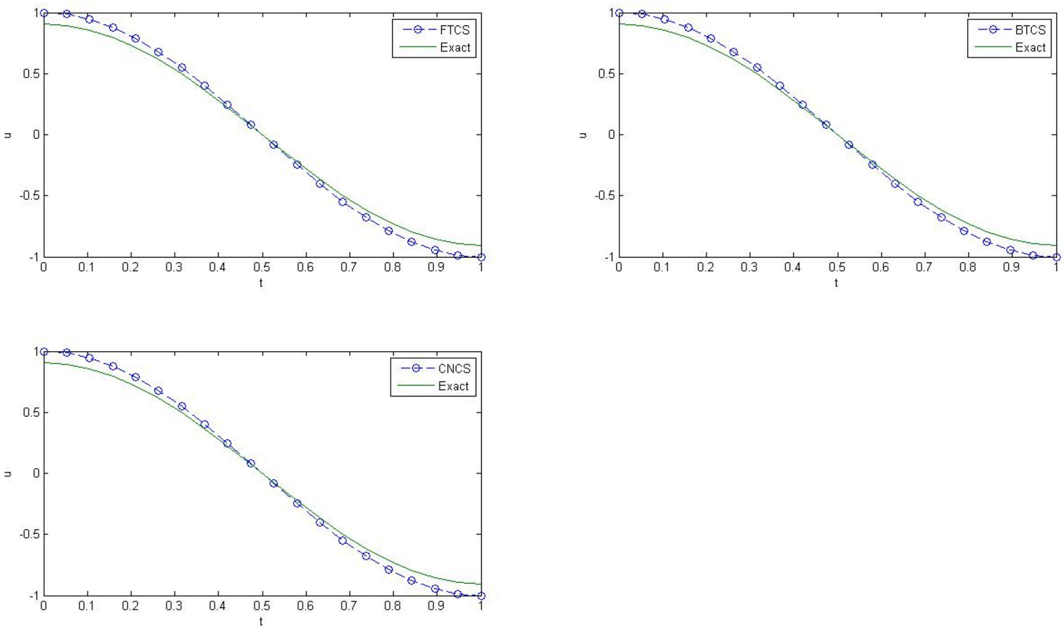

Figure 3.11: FTCS, BTCS and CNCS for the cosine oscillation.

Chapter 4

Homotopy Pertubation Method (HPM)

4.1 Introduction

In this chapter, homotopy pertubation method (HPM) will be applied to the momentum equation for fluid flow. In the literature there are very few exact solutions of the Navier-Stokes equations since the Navier-Stokes equations are highly nonlinear. These solutions are exceptional when the constitutive equations of non-Newtonian fluids are introduced. The homotopy pertubation method was first proposed by He who used it to solve the diffusion equation. Perturbation techniques [36, 37, 38] are applied for obtaining approximate solutions to equations involving a small parameter ε. These techniques are very effective and sometimes the requirements of the small parameter ε is artificially ignored to eliminate the limitations of the traditional pertubation techniques [37]. Hashmi, Khan and Mahmood [39] used the HPM to determine the asymptotic solution for thin film flow of a third grade fluid with partial slip.

Vahidi, Azimzadeh and Didgar [40] used HPM to solve the Riccati equation. Siddiqui, Ahmed and Ghori [41] used HPM to study Couette and Poiseuille flows for non-Newtonian fluids.

The rest of this chapter is organized as follows: Section 4.2 illustrates the idea of the homotopy technique on the momentum equation with boundary conditions; Section 4.3 applies the traditional pertubation technique on the momentum equation with boundary conditions to obtain the solution of the problem. Section 4.4 develops an equation that shows how to calculate the approximate error term compared to the exact solution. The conclusion is given in Section 4.5.

4.2 Homotopy Pertubation Method (HPM)

To illustrate the basic idea of the homotopy pertubation technique on the momentum equation (2.2), we first consider the nonlinear partial differential equation [37].

$$A(u) = f(r), \quad r \in \Omega, \tag{4.1}$$

with boundary conditions:

$$B\left(u, \frac{\partial u}{\partial n}\right) = 0, \quad r \in \Gamma. \tag{4.2}$$

The operator A is a general differential operator, which can be divided into two parts L and N. Therefore Eq. (4.1) can be rewritten as follows

$$L(u) + N(u) = f(r), \quad r \in \Omega, \tag{4.3}$$

where B is a boundary operator, L is a linear operator, N is a nonlinear operator, Ω is a bounded domain in R^d, Γ is the boundary of the domain Ω and $f(r)$ is a known analytic function.

He [37] constructed a homotopy

$$v(r, p) : \Omega \times [0, 1] \to \mathbb{R} \tag{4.4}$$

which satisfies

$$\mathcal{H}(v, p) = (1-p)[L(v)-L(u_0)]+p[L(v)+N(u)-f(r)] = 0, \quad p \in [0, 1], \quad r \in \Omega \tag{4.5}$$

or

$$\mathcal{H}(v, p) = L(v) - L(u_0) + p(L(u_0) + p[N(v) - f(r)] = 0, \quad p \in [0, 1], \quad r \in \Omega \tag{4.6}$$

where $p \in \Omega$ is an embedding parameter, u_0 is an initial approximation to the solution u which satisfies the boundary conditions (4.5) and (4.6) of Eq. (4.3). Obviously when $p = 0$ and $p = 1$, Eqs. (4.5) and (4.6) reduce to Eqs. (4.7) and (4.8):

$$\mathcal{H}(v, 0) = L(v) - N(u_0) = 0, \tag{4.7}$$

and

$$\mathcal{H}(v,1) = L(v) + N(u_0) - f(r) = 0. \tag{4.8}$$

According to the HPM [42], the use of the embedding parameter p as a "small parameter" and a basic assumption is that the solution of Eq. (4.1) can be written as a power series in p.

$$\begin{aligned} v &= \sum_{i=0}^{\infty} v_i p^i \\ &= v_0 + p^1 v_1 + p^2 v_2 + p^3 v_3 + p^4 v_4 + ... \end{aligned} \tag{4.9}$$

Setting $p = 1$, results in the approximate solutions of Eq. (4.9)

$$v = v_0 + v_1 + v_2 + v_3 + v_4 + ... \tag{4.10}$$

The series Eq. (4.10) is convergent [37].

By substituting Eq. (4.9) into Eq. (4.6) we have

$$L\left(\sum_{i=0}^{\infty} v_i p^i\right) - L(u_0) = -pL(u_0) + p\left(\left[-N\left(\sum_{i=0}^{\infty} v_i p^i\right) + f(r)\right]\right). \tag{4.11}$$

Comparing the coefficients of the terms with identical powers of p, leads to a solution:

$$\begin{aligned} &p^0 : L(v) = L(u_0) \\ &p^1 : L(u_0) = f(r) - N(v) \\ &\vdots \end{aligned} \tag{4.12}$$

with condition $v_i(r,0) = 0$ for $i = 0, 1, 2, ...$

4.3 The HPM applied to the momentum equation

The HPM will be considered on

$$\frac{\partial u}{\partial t} = v\frac{\partial^2 u}{\partial y^2}; \quad 0 \leq y \leq L \tag{4.13}$$

with boundary condition for the cosine oscillation

$$u(0,t) = U\cos(\omega t) \text{ for all } t > 0,$$

and initial condition

$$u(y,0) = 0 \text{ for all } y > 0.$$

The other boundary and initial conditions for the sine oscillation are

$$u(0,t) = U\sin(\omega t) \text{ for all } t > 0,$$
$$u(y,0) = 0 \text{ for all } y \geq 0,$$
$$u(y,t) \to 0 \text{ as } y \to \infty.$$

We construct the following homotopy:

$$\frac{\partial v}{\partial t} - \frac{\partial u_0}{\partial t} = p\left(\frac{\partial u_0}{\partial t} + \rho\left(\frac{\partial^2 v}{\partial y^2}\right)\right). \tag{4.14}$$

Suppose the solution of Eq. (4.13) is of a series form

$$
\begin{aligned}
v &= \sum_{i=0}^{\infty} v_i p^i \qquad (4.15)\\
&= v_0 + p^1 v_1 + p^2 v_2 + p^3 v_3 + p^4 v_4 + ...
\end{aligned}
$$

Substituting Eq.(4.15) into the homotopy perturbation of momentum equation Eq.(4.14), and comparing coefficients of the terms with identical powers of p , leads to:

$$
\begin{aligned}
p^0 &: (v_0)_t - (u_0)_t = 0\\
p^1 &: (v_1)_t = (u_0)_t + \rho(v_0)_{yy}\\
p^2 &: (v_2)_t = \rho(v_1)_{yy}\\
p^3 &: (v_3)_t = \rho(v_2)_{yy}\\
&\vdots
\end{aligned}
$$

with condition

$$
v_i(y,0) = 0, \quad i = 1, 2, 3, ...
$$

We can easily obtain the components of series Eq. (4.15) as

$$
\begin{aligned}
(v_0)_t &= -U\omega\sin(\omega t) \\
(v_1)_t &= -U\omega\sin(\omega t) \\
(v_2)_t &= 0 \\
(v_3)_t &= 0 \\
&\vdots
\end{aligned}
$$

Thus, we have the solution given by

$$u(y,t) = u_0 + u_1 + u_2 + u_3 + ...$$

This solution is the same solution given by Eq. (4.9) which is

$$u = \sum_{i=0}^{\infty} v_k = v_0 + v_1 + v_2 + v_3 + ...$$

Hence, we have

$$u(y,t) = U\cos(\omega t) - 2U\sin(\omega t).$$

With similar computation, for the sine wave oscillation we obtain

$$
\begin{aligned}
(v_0)_t &= U\omega\cos(\omega t) \\
(v_1)_t &= U\omega\cos(\omega t) \\
(v_2)_t &= 0 \\
(v_3)_t &= 0 \\
&\vdots
\end{aligned}
\tag{4.16}
$$

and by repeating this computational series we obtain, $(v_4)_t = (v_5)_t = \cdots = 0 = (v_n)_t$.

Therefore, the approximate solution can be obtained as

$$u = \sum_{i=0}^{\infty} v_k = v_0 + v_1 + v_2 + v_3 + ...$$

and hence, we have

$$u(y,t) = U\sin(\omega t) - 2U\cos(\omega t).$$

4.4 Numerical Approximation Error Terms

For the numerical computation Ghoreishi and Ismail [43] defined the expression

$$\Psi_m(y,t) = \sum_{k=0}^{m-1} u_k(y,t)$$

to denote the m-term approximation to $u(y,t)$.

Let the absolute error be given by $E_m(y,t)$,

$$E_m(y,t) = |u(y,t) - \Psi_m(y,t)|.$$

The absolute error is the difference between the exact solution and the m-term approximate solution $\Psi_m(y,t)$.

4.5 Numerical Results and Conclusion

In this chapter, we have shown the application of He's HPM on solving the momentum equation. The HPM reduces a complex problem domain into a simple problem examination. The homotopy method depends on the choice of initial condition. The method generates a convergent series solution. Thus having a good guess for the initial condition, a few iterations are enough to give a good approximate solution. The homotopy method can be used to solve various other nonlinear problems without any difficulty. The method simplifies the problem domain into an easy one and the accomplished results are correct on the whole solution domain. The method does not use computation discretized methods for solution of partial differential equations. The results reveal that He's HPM is very effective and simple to apply

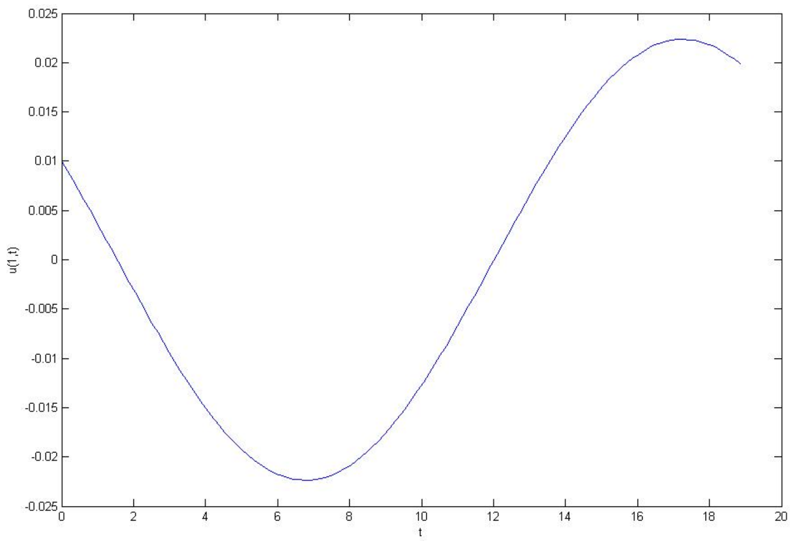

Figure 4.1: Velocity profile field $u(y,t)$ for flow induced by a cosine oscillation at $y = 1$ $U = 0.01$, $\mu = 0.3$ and time t, $t \,\epsilon\, [0, 6\pi]$ with $\Delta t = \frac{\pi}{20}$

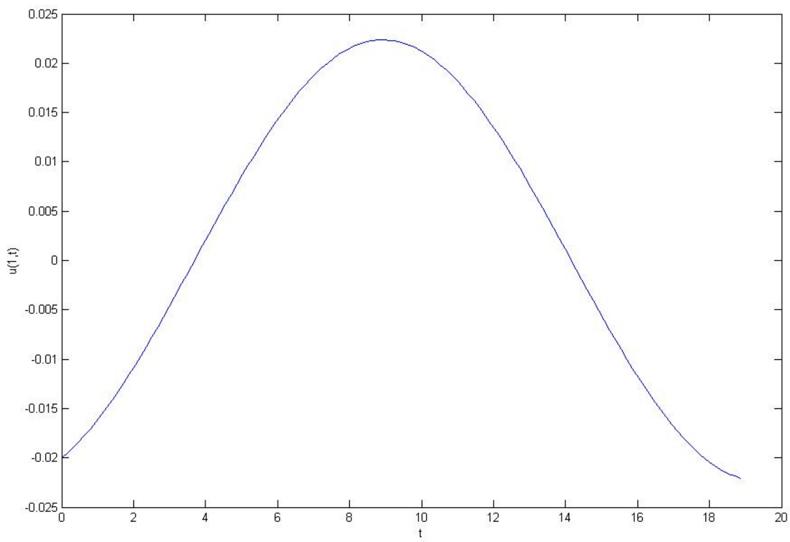

Figure 4.2: Velocity profile field $u(y, t)$ for flow induced by a sine oscillation at $y = 1$ $U = 0.01$, $\mu = 0.3$ and time t, $t \in [0, 6\pi]$ with $\Delta t = \frac{\pi}{20}$

Chapter 5

Solving the Momentum Equation using Differential Transformation Method

5.1 Introduction

In this chapter, the differential transform method (DTM) will be applied to the momentum equation for fluid flow. The DTM is a numerical method based on Taylor series expansions. We first examine the application of DTM on one dimensional problems and then we examine the application of DTM on two dimensional problems. Some special cases of the momentum equation subject to different initial and boundary conditions given by sine oscillations and cosine oscillations are illustrated. Numerical results obtained by DTM are compared with pdepe MATLAB solution. The results are very accurate.

5.2 Basic of Differential Transformation Method

The DTM is frequently presented as a (relatively) new method for solving differential equations [44, 45, 46]. This method is based on Taylor series expansion, though different from the traditional Taylor series expansion. DTM has systematically been used to solve differential equations.

5.2.1 One-dimensional Differential Transform

Definition 1. The one-dimensional differential transform

A k-th order differential transform of a function $c(x)$ is defined as follows:

$$C(k) = \frac{1}{k!}\left[\frac{d^k}{dx^k}c(x)\right]_{x=x_0} \tag{5.1}$$

where k belongs to the set of non-negative integers, denoted as the k-domain.

Definition 2. The function $c(x)$ is expressed as a differential transform $C(x)$. The differential inverse transform of $C(k)$ is defined as follows:

$$c(k) = \sum_{k=0}^{\infty} C(k)(x - x_0)^k. \tag{5.2}$$

Combining Eqs. (5.1) and (5.2) we obtain

$$c(x) = \sum_{k=0}^{\infty} \frac{(x - x_0)}{k!}\left\{\frac{d^k}{dx^k}c(x)\right\}\Bigg|_{x=0} \tag{5.3}$$

which is actually the Taylor series expansion for $c(x)$ when $x = x_0$.

5.2.2 Two-dimensional Differential Transform

Considering a function of two variables $u(x, y)$ analytic in the domain K and let $(x, y) = (x_0, y_0)$ be the initial condition in this domain. The function $u(x, y)$ is then represented by a power series located at (x_0, y_0). The function $u(x, y)$ has a differential transform of the form

$$U(k,h) = \frac{1}{k!h!}\left[\frac{\partial^{k+h}}{\partial x^k \partial y^h} u(x,y)\right]_{(x_0,y_0)} \tag{5.4}$$

where $u(x, y)$ is the original function and $U(k, h)$ is the transformed function. The transform is a T-function and the lower case and upper case letters represent the original and transformed functions respectively. The inverse differential transform of $U(k, h)$ is defined as:

$$u(x,y) = \sum_{k=0}^{\infty}\sum_{h=0}^{\infty} U(k,h)(x-x_0)^k(y-y_0)^h. \tag{5.5}$$

Combining Eqs. (5.4) and (5.5) we can conclude:

$$u(x,y) = \sum_{k=0}^{\infty}\sum_{h=0}^{\infty} \frac{1}{k!}\frac{1}{h!}\left\{\frac{\partial^{k+h}}{\partial x^k \partial y^h} u(k,h)\right\}\Bigg|_{(x_0,y_0)} (x-x_0)^k(y-y_0)^h. \tag{5.6}$$

Taking Eq. (5.4) at the point $(x_0, y_0) \equiv (0, 0)$ results in Eq. (5.6) to be written in a finite series form as:

$$u(x,y) = \begin{cases} U(0,0)x^0y^0 + U(0,1)x^0y^1 + U(0,2)x^0y^2 + \cdots + U(0,N)x^0y^N + \\ U(1,0)x^1y^0 + U(1,1)x^1y^1 + U(1,2)x^1y^2 + \cdots + U(1,N)x^1y^N + \\ U(2,0)x^2y^0 + U(2,1)x^2y^1 + U(2,2)x^2y^2 + \cdots + U(2,N)x^2y^N + \\ U(3,0)x^3y^0 + U(3,1)x^3y^1 + U(3,2)x^3y^2 + \cdots + U(3,N)x^3y^N + \\ \vdots \\ U(M,0)x^M + U(M,1)x^My + U(M,2)x^My^2 + \cdots + U(M,N)x^My^N \end{cases}$$

which can be written as

$$u(x,y) = \sum_{k=0}^{M} \left(U(k,0)x^k + U(k,1)x^ky + U(k,2)x^ky^2 + + \cdots + U(k,N)x^ky^N \right), \tag{5.7}$$

$$= \sum_{k=0}^{M}\sum_{h=0}^{N} U(k,h)x^ky^h. \tag{5.8}$$

The fundamental theorem proofs of the two-dimensional transform are found in Appendix B.

5.3 Differential Transform Method for the Momentum Equation

The application of the DTM will be discussed here to illustrate how to use the two-dimensional differential transform to solve the momentum equation.

Consider a non-Newtonian fluid where the x coordinates is parallel to the infinitely extended flat plate and the fluid occupies the space $y > 0$, with the

y axis in the vertical direction. The plate is initially at rest. At a time $t = 0^+$, the plate is disturbed from rest and subjected to a velocity $u_\omega = U_0 \cos \omega t$ in it's own plane, resulting in induced flow. The governing equation is given by

$$\rho \frac{\partial u}{\partial t} = \frac{\partial}{\partial y}\left(\mu \frac{\partial u}{\partial y}\right), \tag{5.9}$$

where u, t and μ are the velocity in the y- direction, time and the dynamic viscosity of the fluid. For the momentum equation we consider the initial condition given by,

$$u(y, 0) = \cos y \tag{5.10}$$

and the boundary conditions

$$\begin{aligned} u(0,t) &= U_0 \cos(\ \omega t) \quad \text{for } t > 0 \\ u(\infty, t) &= 0, \end{aligned} \tag{5.11}$$

where ω is the frequency of the oscillation and U_0 is the representative velocity. Another set of boundary conditions may be given by

$$\begin{aligned} u(0,t) &= U_0 \sin(\ \omega t) \quad \text{for } t > 0 \\ u(\infty, t) &= 0. \end{aligned} \tag{5.12}$$

Now consider the governing momentum equation Eq. (5.9), with initial condition (5.10) and boundary condition (5.11). We now show how to apply the DTM to solve Eqs. (5.9)-(5.12)

After taking the differential transform of both sides of Eq. (5.9), it reduces to the following form

$$\rho U(k, h+1)) = \frac{1}{(h+1)}\mu\left[(k+1)(k+2)U(k+2,h)\right] \tag{5.13}$$

Case 1: $u(y,0) = \cos y$

The related initial condition should also be transformed as follows

$$\begin{aligned} &U(k,0) = \frac{1}{k!}\cos(\frac{k\pi}{2}) \quad k = 0,1,2,... \\ &U(0,0) = 1. \end{aligned} \tag{5.14}$$

From the boundary condition (5.11), we can write

$$\begin{aligned} &U(k,h) = U_0\frac{\omega^h}{h!}\cos(\frac{h\pi}{2}) \quad k = 0,1,2,..., \quad h = 0,1,2,..., \\ &U(\infty,h) = 0, \quad h = 0,1,2,..., \end{aligned} \tag{5.15}$$

After taking the differential transform of both sides in Eq. (5.9), for $k = 0, 1, 2, 3\cdots$, we obtain the following

$$\rho(k+1)U_{k+1}(y) = \mu\frac{\partial^2}{\partial y^2}U_k(y). \tag{5.16}$$

By taking the differential transform of the initial and boundary conditions (5.14) and (5.15) respectively, their reduced DTM version will be:

$$
\begin{aligned}
U_0(y) &= \cos y, \\
U_t(y) &= U_0 \cos \omega t, \\
U_t(\infty) &= 0 \qquad (5.17)
\end{aligned}
$$

where $U_i(y)$ is the reduced differential transform of $u(y,t)$.

After expanding the reduced DTM recurrence equations with initial condition (5.14) with the initial value $U_0(y) = \cos y$, for $k = 0, 1, 2, 3, \cdots, N$ the terms of $U_k(y)$, are as follows;

$$
\begin{aligned}
U_1(y) &= -\frac{\mu}{\rho}\cos y, \\
U_2(y) &= \frac{1}{2}\left(\frac{\mu}{\rho}\right)^2 \cos y, \\
U_3(y) &= -\frac{1}{6}\left(\frac{\mu}{\rho}\right)^3 \cos y, \\
U_4(y) &= \frac{1}{24}\left(\frac{\mu}{\rho}\right)^4 \cos y, \\
U_5(y) &= -\frac{1}{120}\left(\frac{\mu}{\rho}\right)^5 \cos y, \\
&\vdots \\
U_N(y) &= \frac{1}{N+1}\left(\frac{\mu}{\rho}\right)\frac{\partial^2}{\partial y^2}U_{N-1}(y) \\
&= \frac{1}{N!}\left(\frac{\mu}{\rho}\right)^N \cos y. \qquad (5.18)
\end{aligned}
$$

Therefore, the approximate solution of Eq. (5.9) in series form is

$$
\begin{aligned}
U(y,t) &= U_0(y) + U_1(y)t + U_2(y)t^2 + U_3(y)t^3 + U_4(y)t^4 + \cdots + U_N(y)t^N \\
&= \cos y \left\{1 - \left(\frac{\mu}{\rho}\right)t + \frac{1}{2!}\left(\frac{\mu}{\rho}\right)^2 t^2 - \frac{1}{3!}\left(\frac{\mu}{\rho}\right)^3 t^3 + \cdots + \frac{1}{N!}\left(\frac{\mu}{\rho}\right)^N t^N\right\}.
\end{aligned}
$$

(5.19)

The approximate solution of Eq. (5.19) in closed form is:

$$U(y,t) = e^{-(\frac{\mu}{\rho})t}\text{cos}y. \tag{5.20}$$

Case 2: $u(y,0) = \text{sin}y$

The related initial condition should also be transformed as follows

$$\begin{aligned} U(k,0) &= \frac{1}{k!}\text{sin}(\frac{k\pi}{2}) \quad k = 0,1,2,... \\ U(0,0) &= 1. \end{aligned} \tag{5.21}$$

From the boundary condition can write

$$\begin{aligned} U(k,h) &= U_0\frac{\omega^h}{h!}\text{sin}(\frac{h\pi}{2}) \quad k = 0,1,2,..., \quad h = 0,1,2,..., \\ U(\infty,h) &= 0, \quad h = 0,1,2,..., \end{aligned} \tag{5.22}$$

After taking the differential transform of both sides in Eq. (5.22), for $k = 0,1,2,3\cdots$, we obtain the following

$$\rho(k+1)U_{k+1}(y) = \mu\frac{\partial^2}{\partial y^2}U_k(y). \tag{5.23}$$

Similarly by taking the differential transform of the initial and boundary conditions (5.12) respectively, their reduced DTM version will be:

$$\begin{aligned} U_0(y) &= \text{sin}y, \\ U_t(y) &= U_0 \sin \omega t, \\ U_t(\infty) &= 0 \end{aligned} \tag{5.24}$$

where $U_i(y)$ is the reduced differential transform of $u(y,t)$.

Similarly $U_0(y) = \sin y$, for $k = 0, 1, 2, 3, 4, \cdots, N$ the terms of $U_k(y)$ are

$$
\begin{aligned}
U_1(y) &= -\frac{\mu}{\rho}\sin y,\\
U_2(y) &= \frac{1}{2}\left(\frac{\mu}{\rho}\right)^2 \sin y,\\
U_3(y) &= -\frac{1}{6}\left(\frac{\mu}{\rho}\right)^3 \sin y,\\
U_4(y) &= \frac{1}{24}\left(\frac{\mu}{\rho}\right)^4 \sin y,\\
U_5(y) &= -\frac{1}{120}\left(\frac{\mu}{\rho}\right)^5 \sin y,\\
&\vdots\\
U_N(y) &= \frac{1}{N+1}\left(\frac{\mu}{\rho}\right)\frac{\partial^2}{\partial y^2}U_{N-1}(y)\\
&= \frac{1}{N!}\left(\frac{\mu}{\rho}\right)^N \sin y.
\end{aligned}
\tag{5.25}
$$

Therefore, the approximate solution of equation Eq. (5.9) in series form is

$$
\begin{aligned}
U(y,t) &= U_0(y) + U_1(y)t + U_2(y)t^2 + U_3(y)t^3 + U_4(y)t^4 + \cdots + U_N(y)t^N\\
&= \sin y\left\{1 - \left(\frac{\mu}{\rho}\right)t + \frac{1}{2!}\left(\frac{\mu}{\rho}\right)^2 t^2 - \frac{1}{3!}\left(\frac{\mu}{\rho}\right)^3 t^3 + \cdots + \frac{1}{N!}\left(\frac{\mu}{\rho}\right)^N t^N\right\}.
\end{aligned}
\tag{5.26}
$$

The approximation solution of Eq. (5.26) in closed form is:

$$
U(y,t) = e^{-\left(\frac{\mu}{\rho}\right)t}\sin y. \tag{5.27}
$$

5.4 Numerical Results and Conclusion

The DTM which depends on Taylor series expansion has been studied. The approximate solution of the momentum equation has been obtained in the form of a polynomial series solution based on an iterative procedure. The DTM is capable of reducing the challenge arising in calculation of Adomian polynomials. The method can easily be applied for solving linear and nonlinear partial differential equations. The results obtained compared with exact solutions acknowledge that the DTM is very effective and easy to apply. Tables 5.1 and 5.2 show a comparison of DTM solution Eq. (5.19) for the cosine wave and Eq. (5.26) for the sine wave oscillation compared to the exact solution, for $N = 1$ and $N = 3$. Tables 5.1 - 5.6 show a decrease in error as we increase the approximate solution from $N = 1$ to $N = 3$ for $u(y,t)$, where $t = 0.0075$ $\mu = 0.01$, $\rho = 0.05$ and $y \ \varepsilon \ [0, 0.5]$ with a step size of 0.1. Figures 5.1 and 5.5 show a three dimensional surface plot and a two dimensional comparison of DTM and pdepe MATLAB solution. Figures 5.2 and 5.6 compare DTM solution to pdepe MATLAB for different times; the plot shows that as time $t \to \infty$ the amplitude of the cosine and the sine waves decreases and the flows turn to a steady-state. The plots in Figures 5.3 and 5.7 show the behaviour of DTM compared to pdepe MATLAB solution. In both solutions the approximation time has a direct effect. Figures 5.4 and 5.8 show that the term $\frac{\mu}{\rho}$ plays an important rule on the DTM solution when compared with the pdepe MATLAB solution. When $\frac{\mu}{\rho}$ is small the DTM solution has a bigger error when compared to the pdepe MATLAB solution. In our investigation for both the cosine and sine wave the term $\frac{\mu}{\rho} = 1$ resulted in lesser error. Careful consideration needs to be taken on the choice of the term $\frac{\mu}{\rho}$. The computational results are motivated by the work of Malek Abazari

[47] when determining the solution of reaction diffusion problems by DTM.

time (t)	method	y						
		0	0.1653	0.3307	0.4960	0.6614	0.8267	0.9921
0	pdepe MATLAB	0	0.1646	0.3247	0.4759	0.6142	0.7357	0.8372
	DTM	0	0.1646	0.3247	0.4759	0.6142	0.7357	0.8372
0.1111	pdepe MATLAB	0	0.1474	0.2908	0.4263	0.5502	0.6590	0.7499
	DTM	0	0.1473	0.2906	0.4259	0.5496	0.6584	0.7491
0.2222	pdepe MATLAB	0	0.1320	0.2603	0.3816	0.4924	0.5899	0.6712
	DTM	0	0.1318	0.2600	0.3811	0.4918	0.5891	0.6704
0.3333	pdepe MATLAB	0	0.1181	0.2330	0.3415	0.4407	0.5279	0.6007
	DTM	0	0.1179	0.2327	0.3410	0.4401	0.5272	0.5999
0.4444	pdepe MATLAB	0	0.1057	0.2085	0.3056	0.3944	0.4724	0.5375
	DTM	0	0.1055	0.2082	0.3052	0.3938	0.4717	0.5368
0.5556	pdepe MATLAB	0	0.0946	0.1866	0.2735	0.3530	0.4228	0.4811
	DTM	0	0.0944	0.1863	0.2731	0.3524	0.4221	0.4803
0.6667	pdepe MATLAB	0	0.0847	0.1670	0.2448	0.3159	0.3784	0.4306
	DTM	0	0.0845	0.1667	0.2444	0.3153	0.3777	0.4298
0.7778	pdepe MATLAB	0	0.0758	0.1495	0.2191	0.2828	0.3387	0.3854
	DTM	0	0.0756	0.1492	0.2187	0.2822	0.3380	0.3846
0.8889	pdepe MATLAB	0	0.0678	0.1338	0.1961	0.2531	0.3032	0.3450
	DTM	0	0.0677	0.1335	0.1957	0.2525	0.3025	0.3442
1.0000	pdepe MATLAB	0	0.0607	0.1198	0.1756	0.2265	0.2714	0.3088
	DTM	0	0.0606	0.1195	0.1751	0.2260	0.2707	0.3080

Table 5.1: The approximate solutions for the sine oscillation obtained by the DTM and pdepe MATLAB where $y \epsilon [0, 0.9921]$, $t \epsilon [0, 1]$.

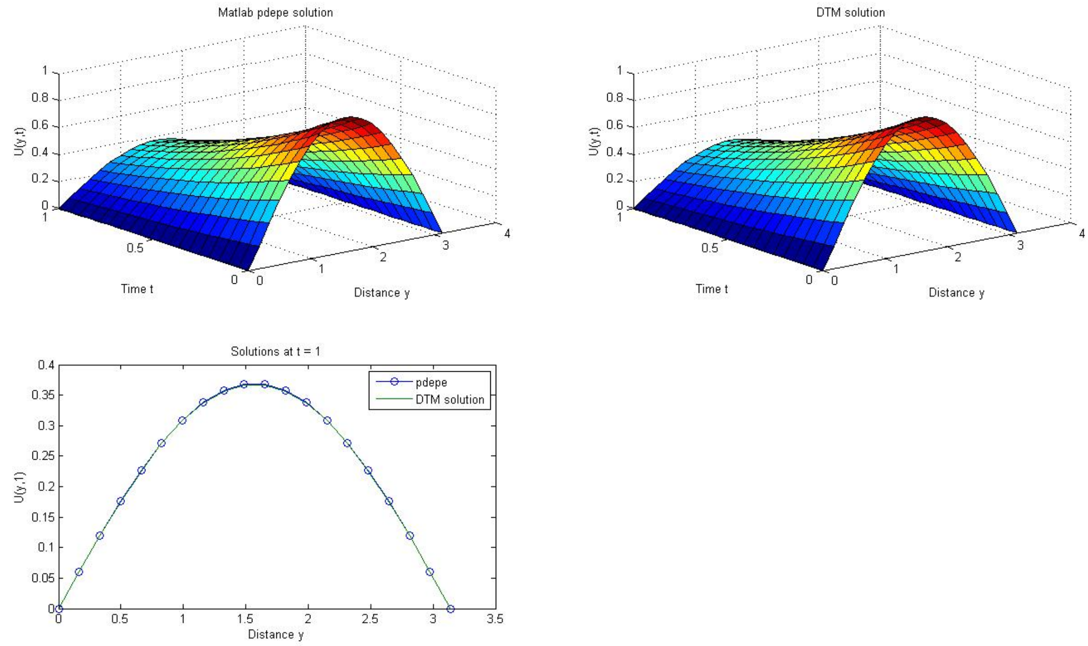

Figure 5.1: Comparison of pdepe MATLAB with DTM solution, on intervals $0 \leq y \leq \pi$ with $\Delta y = \frac{\pi}{20}$ and $0 \leq t \leq 1$ with $\Delta t = 0.1$ for sine oscillation where $\frac{\mu}{\rho} = 1$.

time (t)	method	y						
		1.1574	1.3228	1.4881	1.6535	1.8188	1.9842	2.1495
0	pdepe MATLAB	0.9158	0.9694	0.9966	0.9966	0.9694	0.9158	0.8372
	DTM	0.9158	0.9694	0.9966	0.9966	0.9694	0.9158	0.8372
0.1111	pdepe MATLAB	0.8203	0.8683	0.8927	0.8927	0.8683	0.8203	0.7499
	DTM	0.8195	0.8675	0.8918	0.8918	0.8675	0.8195	0.7491
0.2222	pdepe MATLAB	0.7342	0.7772	0.7990	0.7990	0.7772	0.7342	0.6712
	DTM	0.7333	0.7762	0.7980	0.7980	0.7762	0.7333	0.6704
0.3333	pdepe MATLAB	0.6571	0.6955	0.7150	0.7150	0.6955	0.6571	0.6007
	DTM	0.6562	0.6946	0.7141	0.7141	0.6946	0.6562	0.5999
0.4444	pdepe MATLAB	0.5880	0.6224	0.6399	0.6399	0.6224	0.5880	0.5375
	DTM	0.5872	0.6216	0.6390	0.6390	0.6216	0.5872	0.5368
0.5556	pdepe MATLAB	0.5262	0.5571	0.5727	0.5727	0.5571	0.5262	0.4811
	DTM	0.5254	0.5562	0.5718	0.5718	0.5562	0.5254	0.4803
0.6667	pdepe MATLAB	0.4710	0.4986	0.5126	0.5126	0.4986	0.4710	0.4306
	DTM	0.4702	0.4977	0.5117	0.5117	0.4977	0.4702	0.4298
0.7778	pdepe MATLAB	0.4216	0.4463	0.4588	0.4588	0.4463	0.4216	0.3854
	DTM	0.4207	0.4454	0.4579	0.4579	0.4454	0.4207	0.3846
0.8889	pdepe MATLAB	0.3774	0.3995	0.4107	0.4107	0.3995	0.3774	0.3450
	DTM	0.3765	0.3985	0.4097	0.4097	0.3985	0.3765	0.3442
1.0000	pdepe MATLAB	0.3378	0.3576	0.3676	0.3676	0.3576	0.3378	0.3088
	DTM	0.3369	0.3566	0.3666	0.3666	0.3566	0.3369	0.3080

Table 5.2: The approximate solutions for the sine oscillation obtained by the DTM and pdepe MATLAB where $y \, \epsilon \, [1.1574, 2.1495]$, $t \, \epsilon \, [0, 1]$.

time (t)	method	y					
		2.3149	2.4802	2.6456	2.8109	2.9762	3.1416
0	pdepe MATLAB	0.7357	0.6142	0.4759	0.3247	0.1646	0.0000
	DTM	0.7357	0.6142	0.4759	0.3247	0.1646	0.0000
0.1111	pdepe MATLAB	0.6590	0.5502	0.4263	0.2908	0.1474	0.0000
	DTM	0.6584	0.5496	0.4259	0.2906	0.1473	0.0000
0.2222	pdepe MATLAB	0.5899	0.4924	0.3816	0.2603	0.1320	0
	DTM	0.5891	0.4918	0.3811	0.2600	0.1318	0.0000
0.3333	pdepe MATLAB	0.5279	0.4407	0.3415	0.2330	0.1181	0
	DTM	0.5272	0.4401	0.3410	0.2327	0.1179	0.0000
0.4444	pdepe MATLAB	0.4724	0.3944	0.3056	0.2085	0.1057	0
	DTM	0.4717	0.3938	0.3052	0.2082	0.1055	0.0000
0.5556	pdepe MATLAB	0.4228	0.3530	0.2735	0.1866	0.0946	0
	DTM	0.4221	0.3524	0.2731	0.1863	0.0944	0.0000
0.6667	pdepe MATLAB	0.3784	0.3159	0.2448	0.1670	0.0847	0
	DTM	0.3777	0.3153	0.2444	0.1667	0.0845	0.0000
0.7778	pdepe MATLAB	0.3387	0.2828	0.2191	0.1495	0.0758	0
	DTM	0.3380	0.2822	0.2187	0.1492	0.0756	0.0000
0.8889	pdepe MATLAB	0.3032	0.2531	0.1961	0.1338	0.0678	0
	DTM	0.3025	0.2525	0.1957	0.1335	0.0677	0.0000
1.0000	pdepe MATLAB	0.2714	0.2265	0.1756	0.1198	0.0607	0
	DTM	0.2707	0.2260	0.1751	0.1195	0.0606	0.0000

Table 5.3: The approximate solutions for the sine oscillation obtained by the DTM and pdepe MATLAB where $y \in [2.3149, \pi]$, $t \in [0, 1]$.

time (t)	method	y						
		0	0.2632	0.5263	0.7895	1.0526	1.3158	1.5789
0	pdepe MATLAB	0	0.9656	0.8647	0.7042	0.4953	0.2523	-0.0082
	DTM	1.0000	0.9656	0.8647	0.7042	0.4953	0.2523	-0.0082
0.0333	pdepe MATLAB	0	0.6217	0.7725	0.6719	0.4781	0.2439	-0.0079
	DTM	0.9640	0.9308	0.8335	0.6789	0.4775	0.2432	-0.0079
0.0667	pdepe MATLAB	0	0.4547	0.6529	0.6174	0.4547	0.2345	-0.0079
	DTM	0.9293	0.8973	0.8035	0.6544	0.4603	0.2344	-0.0076
0.1000	pdepe MATLAB	0	0.3567	0.5507	0.5538	0.4235	0.2221	-0.0087
	DTM	0.8958	0.8650	0.7746	0.6309	0.4437	0.2260	-0.0073
0.1333	pdepe MATLAB	0	0.2913	0.4681	0.4909	0.3874	0.2062	-0.0112
	DTM	0.8636	0.8339	0.7467	0.6082	0.4277	0.2178	-0.0070
0.1667	pdepe MATLAB	0	0.2436	0.4011	0.4328	0.3496	0.1875	-0.0156
	DTM	0.8325	0.8038	0.7198	0.5863	0.4123	0.2100	-0.0068
0.2000	pdepe MATLAB	0	0.2069	0.3459	0.3804	0.3120	0.1670	-0.0217
	DTM	0.8187	0.7905	0.7079	0.5766	0.4055	0.2065	-0.0067
0.2333	pdepe MATLAB	0	0.1775	0.2997	0.3336	0.2760	0.1457	-0.0293
	DTM	0.7919	0.7646	0.6847	0.5577	0.3922	0.1998	-0.0065
0.2667	pdepe MATLAB	0	0.1532	0.2604	0.2920	0.2421	0.1243	-0.0379
	DTM	0.7659	0.7396	0.6623	0.5394	0.3794	0.1932	-0.0062
0.3000	pdepe MATLAB	0	0.1328	0.2266	0.2550	0.2106	0.1032	-0.0472
	DTM	0.7408	0.7153	0.6406	0.5217	0.3669	0.1869	-0.0060

Table 5.4: The approximate solutions for the cosine oscillation obtained by the DTM and pdepe MATLAB where $y \, \epsilon \, [0, 1.5789]$, $t \, \epsilon \, [0, 0.3]$.

time (t)	method	y						
		1.8421	2.1053	2.3684	2.6316	2.8947	3.1579	3.4211
0	pdepe MATLAB	-0.2680	-0.5094	-0.7157	-0.8727	-0.9697	-0.9999	-0.9612
	DTM	-0.0082	-0.2680	-0.5094	-0.7157	-0.8727	-0.9697	-0.9999
0.0333	pdepe MATLAB	-0.2593	-0.4928	-0.6924	-0.8443	-0.9381	-0.9673	-0.9299
	DTM	-0.2592	-0.4927	-0.6922	-0.8441	-0.9379	-0.9671	-0.9297
0.0667	pdepe MATLAB	-0.2508	-0.4767	-0.6698	-0.8168	-0.9075	-0.9358	-0.8996
	DTM	-0.2507	-0.4765	-0.6695	-0.8165	-0.9071	-0.9354	-0.8992
0.1000	pdepe MATLAB	-0.2429	-0.4612	-0.6480	-0.7901	-0.8779	-0.9053	-0.8706
	DTM	-0.2425	-0.4609	-0.6476	-0.7897	-0.8774	-0.9047	-0.8697
0.1333	pdepe MATLAB	-0.2357	-0.4464	-0.6269	-0.7644	-0.8494	-0.8760	-0.8430
	DTM	-0.2345	-0.4458	-0.6264	-0.7638	-0.8486	-0.8751	-0.8412
0.1667	pdepe MATLAB	-0.2296	-0.4323	-0.6066	-0.7395	-0.8218	-0.8479	-0.8169
	DTM	-0.2269	-0.4312	-0.6058	-0.7388	-0.820	-0.8464	-0.8136
0.2000	pdepe MATLAB	-0.2248	-0.4191	-0.5871	-0.7156	-0.7953	-0.8210	-0.7921
	DTM	-0.2194	-0.4170	-0.5860	-0.7145	-0.7939	-0.8186	-0.7870
0.2333	pdepe MATLAB	-0.2212	-0.4069	-0.5686	-0.6926	-0.7698	-0.7953	-0.7687
	DTM	-0.2122	-0.4034	-0.5668	-0.6911	-0.7679	-0.7918	-0.7612
0.2667	pdepe MATLAB	-0.2188	-0.3958	-0.5510	-0.6706	-0.7455	-0.7708	-0.7463
	DTM	-0.2053	-0.3902	-0.5482	-0.6685	-0.7427	-0.7658	-0.7362
0.3000	pdepe MATLAB	-0.2174	-0.3858	-0.5344	-0.6496	-0.7221	-0.7474	-0.7250
	DTM	-0.1985	-0.3774	-0.5302	-0.6465	-0.7184	-0.7407	-0.7121

Table 5.5: The approximate solutions for the cosine oscillation obtained by the DTM and pdepe MATLAB where $y \,\epsilon\, [1.8421, 3.4211]$, $t \,\epsilon\, [0, 0.3]$.

time (t)	method	y					
		3.6842	3.9474	4.2105	4.4737	4.7368	5.0000
0	pdepe MATLAB	-0.8564	-0.6926	-0.4811	-0.2364	0.0245	0
	DTM	-0.8564	-0.6926	-0.4811	-0.2364	0.0245	0.2837
0.0333	pdepe MATLAB	-0.8285	-0.6703	-0.4680	-0.2469	-0.0650	0
	DTM	-0.8283	-0.6698	-0.4653	-0.2287	0.0236	0.2744
0.0667	pdepe MATLAB	-0.8019	-0.6507	-0.4620	-0.2656	-0.1045	0
	DTM	-0.8011	-0.6479	-0.4500	-0.2212	0.0229	0.2654
0.1000	pdepe MATLAB	-0.7771	-0.6341	-0.4593	-0.2799	-0.1247	0
	DTM	-0.7749	-0.6266	-0.4353	-0.2139	0.0221	0.2567
0.1333	pdepe MATLAB	-0.7542	-0.6197	-0.4570	-0.2891	-0.1358	0
	DTM	-0.7495	-0.6061	-0.4210	-0.2069	0.0214	0.2483
0.1667	pdepe MATLAB	-0.7330	-0.6067	-0.4541	-0.2944	-0.1423	0
	DTM	-0.7249	-0.5862	-0.4072	-0.2001	0.0207	0.2401
0.2000	pdepe MATLAB	-0.7132	-0.5943	-0.4502	-0.2967	-0.1458	0
	DTM	-0.7011	-0.5670	-0.3939	-0.1936	0.0200	0.2322
0.2333	pdepe MATLAB	-0.6945	-0.5823	-0.4452	-0.2970	-0.1475	0
	DTM	-0.6781	-0.5484	-0.3809	-0.1872	0.0194	0.2246
0.2667	pdepe MATLAB	-0.6766	-0.5704	-0.4394	-0.2957	-0.1479	0
	DTM	-0.6559	-0.5304	-0.3685	-0.1811	0.0187	0.2173
0.3000	pdepe MATLAB	-0.6593	-0.5585	-0.4329	-0.2932	-0.1474	0
	DTM	-0.6344	-0.5131	-0.3564	-0.1752	0.0181	0.2101

Table 5.6: The approximate solutions for the cosine oscillation obtained by the DTM and pdepe MATLAB where $y \epsilon [3.6842, 5]$, $t \epsilon [0, 0.3]$.

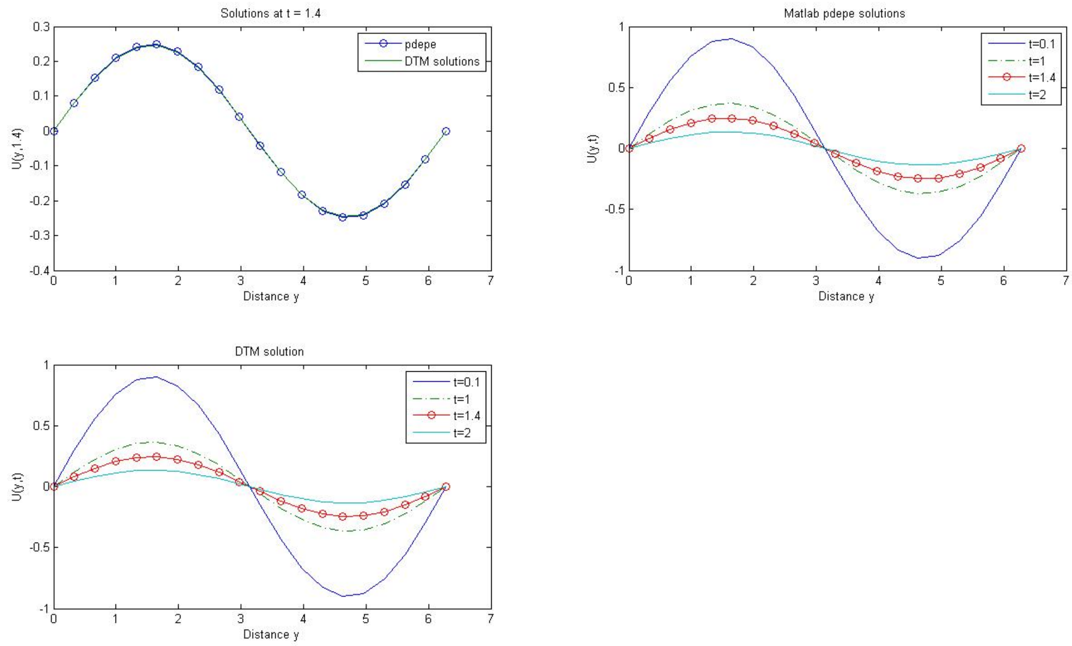

Figure 5.2: Comparison of pdepe MATLAB solutions and DTM solution at different time, $t = 0.1, 1, 1.4, 2$ on the interval $0 \leq y \leq 2\pi$ with $\Delta y = \frac{\pi}{10}$ and $\Delta t = 0.05$ for sine oscillation where $\frac{\mu}{\rho} = 1$.

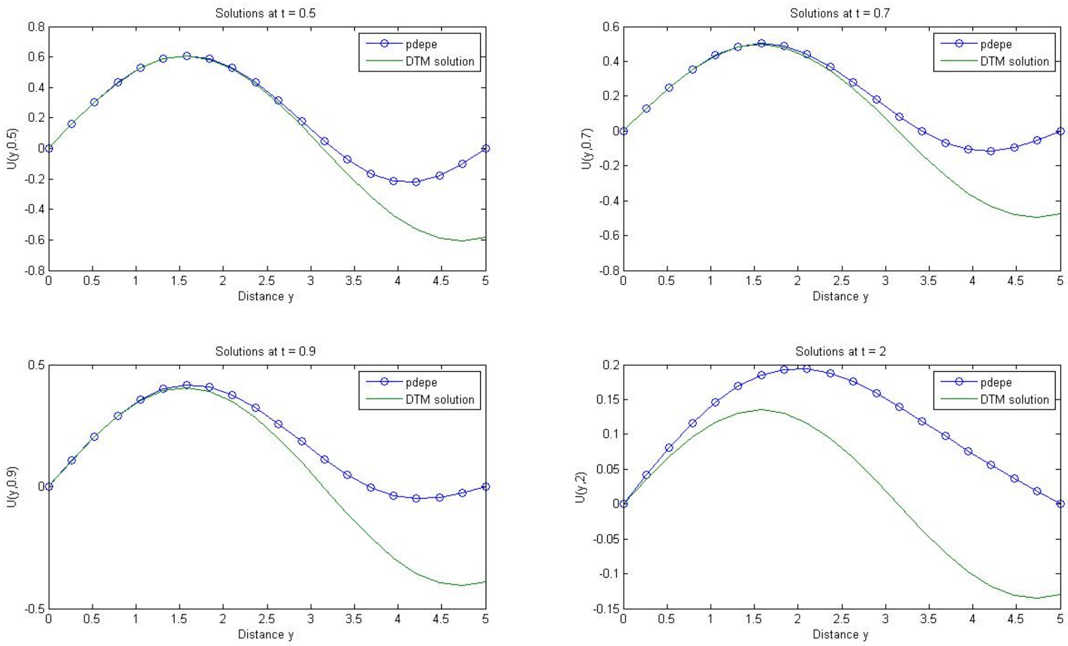

Figure 5.3: Comparison of pdepe MATLAB solution with DTM solution at different time, $t = 0.5, 0.7, 0.9, 2$ on the interval where $0 \leq y \leq 5$ with $\Delta y = \frac{\pi}{10}$ for sine oscillation where $\frac{\mu}{\rho} = 1$.

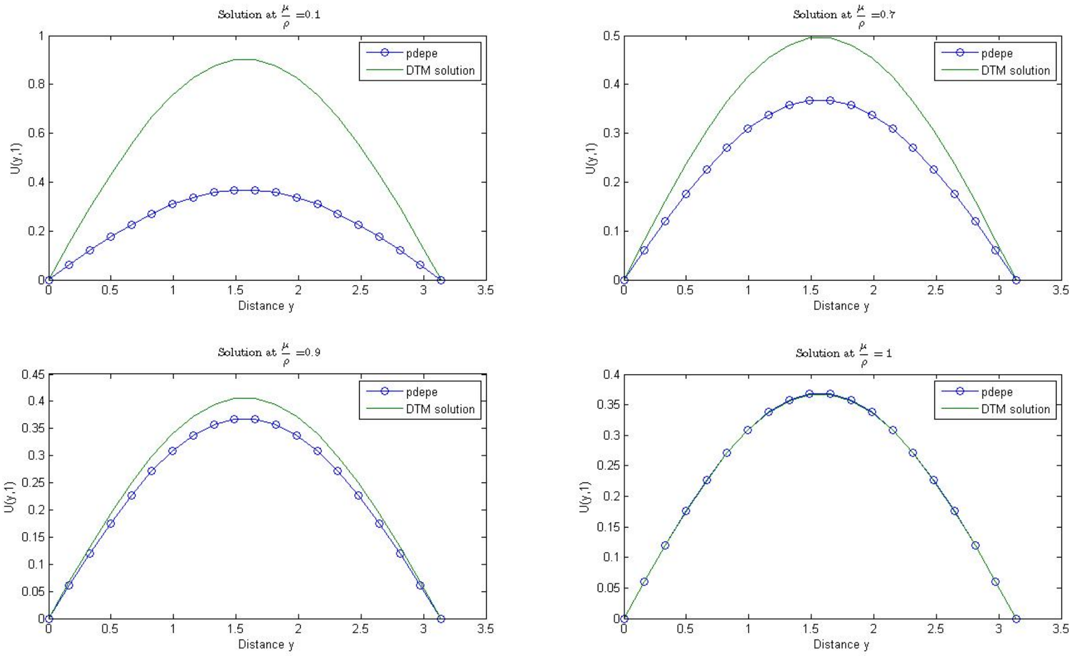

Figure 5.4: Comparison of pdepe MATLAB solution with DTM solution at different $\frac{\mu}{\rho} = 0.1, 0.7, 0.9, 1$ on the interval $0 \leq y \leq \pi$ where $\Delta y = \frac{\pi}{10}$ and $\Delta t = 0.05$ for sine oscillation.

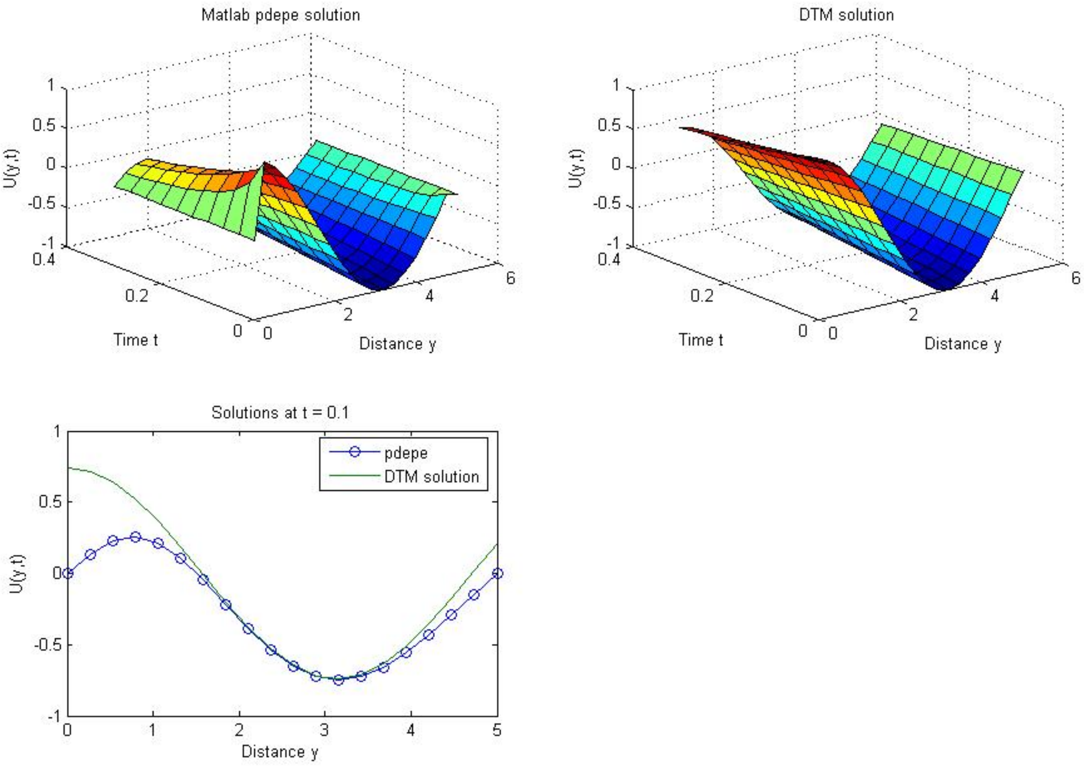

Figure 5.5: Comparison of pdepe MATLAB with DTM solution, on intervals $0 \leq y \leq 5$ with $\Delta y = 0.5$ and $0 \leq t \leq 0.3$ with $\Delta t = 0.015$ for cosine oscillation where $\frac{\mu}{\rho} = 1$.

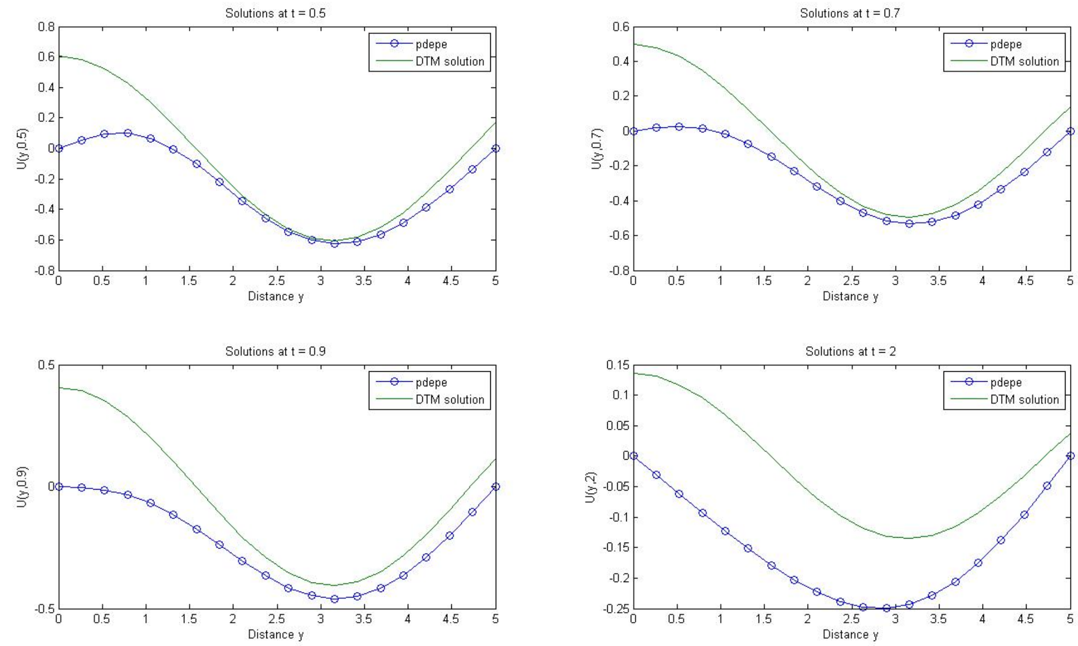

Figure 5.6: Comparison of pdepe MATLAB solution with DTM solution at different time, $t = 0.5, 0.7, 0.9, 2$ on the interval where $0 \leq y \leq 5$ with $\Delta y = 0.5$ for cosine oscillation where $\frac{\mu}{\rho} = 1$.

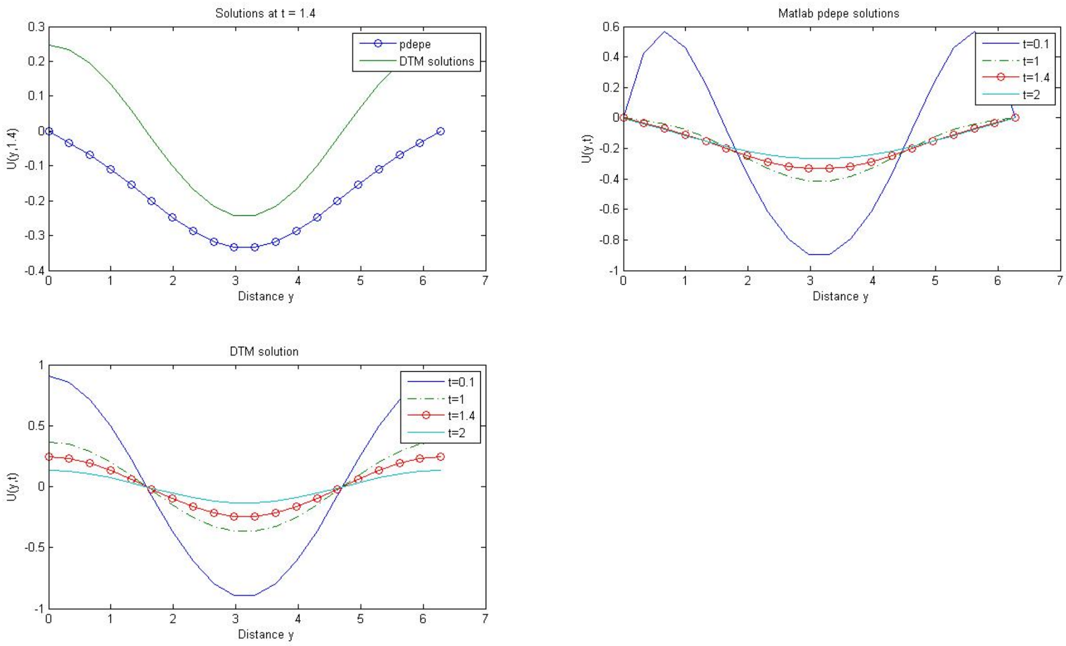

Figure 5.7: Comparison of pdepe MATLAB solutions and DTM solution at different time, $t = 0.1, 1, 1.4, 2$ on the interval $0 \leq y \leq 2\pi$ with $\Delta y = 0.5$ and $\Delta t = 0.05$ for cosine oscillation where $\frac{\mu}{\rho} = 1$.

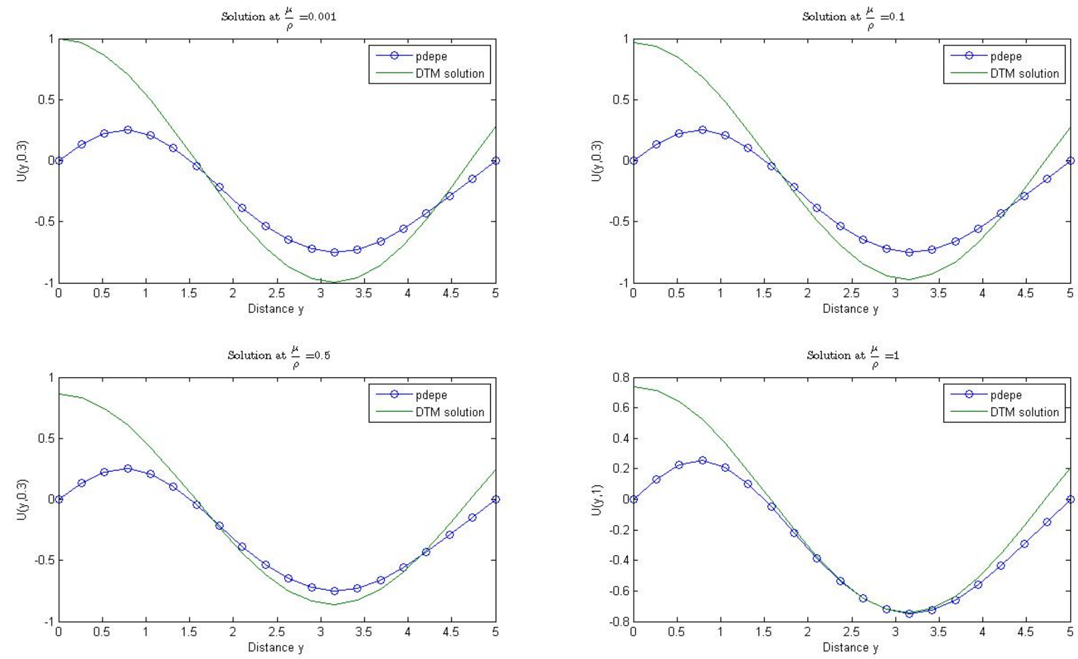

Figure 5.8: Comparison of pdepe MATLAB solution with DTM solution at different $\frac{\mu}{\rho} = 0.001, 0.1, 0.5, 1$ on the interval $0 \leq y \leq 5$ where $\Delta y = 0.5$ and $\Delta t = 0.03$ for cosine oscillation.

Chapter 6

An Approximate Solution of Momentum Equation using Adomain Decomposition

6.1 Introduction

In this chapter, the Adomian decomposition method (ADM) will be applied to the momentum equation for fluid flow. ADM is a semi-analytical method for solving ordinary and partial nonlinear differential equations. The ADM was first realized and developed by Adomian. A wide class of fluid dynamics problems that appear in areas such as engineering, physics, applied maths and the other science disciplines are modeled mathematically by partial differential equations as linear and nonlinear differential equations, fractional differential equations, stochastic differential equations etc [48, 49, 50]. Some of these problems are solved by the ADM. Mohamed [51] used ADM to solve equation governing the unsteady flow of a polytropic gas. Wazwaz [52] used DTM for the treatment of the Bratu-type equations.

The rest of the chapter is organized in this form, Section 6.2 formulates the problem space, Section 6.3 gives an illustration Adomain decomposition method of solution, where the solution space lies on a decomposed series form. In section 6.4 the Adomians' special polynomials are derived. Section 6.5 gives conclusions and outlines Adomain numerical results.

6.2 Formulation of the Problem

We consider the problem as defined in Section 3.3 The governing equation in one dimension has the following form:

$$\rho \frac{\partial u}{\partial t} = \frac{\partial}{\partial y}\left(\nu \frac{\partial u}{\partial y}\right) \quad y > 0 \tag{6.1}$$

where the first term is a linear term and the second term is the highest order term. u, t and ν are the velocity in the x direction, time and the dynamic viscosity of the fluid.

Eq. (6.1) can be written as

$$\frac{\partial u}{\partial t} = \frac{1}{\rho}\nu' \frac{\partial u}{\partial y} + \frac{\nu}{\rho}\left(\frac{\partial^2 u}{\partial y^2}\right). \tag{6.2}$$

Introducing the new operators L_t, B and L_y, the new operators take the form

$$L_t u = \frac{\partial u}{\partial t} \quad L_y u = \frac{\partial^2 u}{\partial y^2} \quad Bu = \nu' \frac{\partial u}{\partial y}. \tag{6.3}$$

Using Eq. (6.3) in Eq. (6.1), Eq. (6.1) takes the form

$$Ru = \frac{1}{\rho}Bu + \frac{\nu}{\rho}Lu \tag{6.4}$$

where $L = L_y u$ is the highest order term, Bu represents the nonlinear term and $Ru = L_t u$ is the rate of diffusion in time.

We solve Eq. (6.4) subjected to the initial condition

$$u(y, 0) = 0 \tag{6.5}$$

and the boundary conditions are defined as a sine oscillation

$$\begin{aligned} u(0, t) &= U_0 \sin \omega t \qquad \text{for } t > 0 \\ \text{and} \quad u(\infty, t) &= 0. \end{aligned} \tag{6.6}$$

6.3 Method of Solution

Solving Eq. (6.2) for $L_t u$ and $L_y u$ separately, we obtain

$$\begin{aligned} L_t u &= \frac{1}{\rho}Bu + \frac{\nu}{\rho}L_y u \\ L_y u &= \frac{\rho}{\nu}L_t u - \frac{1}{\nu}Bu. \end{aligned} \tag{6.7}$$

The inverse operator L_t^{-1} and L_y^{-1} of $L_t u$ and $L_y u$ is given by

$$\begin{aligned} L_t^{-1} &= \int (.)\, dt \ , \quad \text{and} \\ L_y^{-1} &= \int\int (.)\, dy\, dy. \end{aligned} \tag{6.8}$$

Applying the inverse operator L_t^{-1} and L_y^{-1} to both sides of Eq. (6.2) respectively, we obtain

$$
\begin{aligned}
u(y,t) &= u_{t_0} + L_t^{-1}\left(\frac{1}{\rho}Bu + \frac{\nu}{\rho}L_y u\right) \\
u(y,t) &= u_{y_0} + L_y^{-1}\left(\frac{\rho}{\nu}L_t u - \frac{1}{\nu}Bu\right).
\end{aligned} \tag{6.9}
$$

The required solution is a decomposition of the unknown function $u(y,t)$ as a sum of components defined in a series form, is known as the ADM [53].

$$
u(y,t) = \sum_{n=0}^{\infty} u_n(y,t) \tag{6.10}
$$

or

$$
u(y,t) = u_0(y,t) + u_n(y,t) \quad n \geq 1, \tag{6.11}
$$

and the terms $u_1, u_2, u_3, u_4, u_5, \ldots$ are calculated recursively

$$
\begin{aligned}
u_0 &= u(y,0) \\
u_1 &= L_t^{-1}\left[(A_0)\right], \\
u_2 &= L_t^{-1}\left[(A_1)\right], \\
u_3 &= L_t^{-1}\left[(A_2)\right], \\
u_4 &= L_t^{-1}\left[(A_3)\right], \\
&\vdots \\
u_{n+1} &= L_t^{-1}\left[(A_n)\right]
\end{aligned} \tag{6.12}
$$

where A_n are the Adomian polynomials for the nonlinear operator

In Eq . (6.9) u_{t_0} and u_{y_0} are solutions of the following equations

$$\begin{aligned} &\frac{\partial u}{\partial t} = 0 \quad \text{and} \\ &\frac{\partial^2 u}{\partial^2 y} = 0. \end{aligned} \tag{6.13}$$

Equations $(6.9)_1$ and $(6.9)_2$ are solved subject to the initial conditions and boundary conditions and we obtain

$$\begin{aligned} u_{t_0} &= U_0 \sin \omega t \quad \text{and} \\ u_{y_0} &= 0. \end{aligned} \tag{6.14}$$

Combining Eqs. $(6.9)_1$ and $(6.9)_2$ and dividing by 2, we obtain

$$\begin{aligned} u(y,t) &= \frac{1}{2}\left[(u_{t_0} + u_{y_0}) + L_t^{-1}\left(\frac{1}{\rho}Bu + \frac{\nu}{\rho}L_y u\right) + L_y^{-1}\left(\frac{\rho}{\nu}L_t u - \frac{1}{\nu}Bu\right)\right], \\ &= \Phi_0 \sin \omega t + \frac{1}{2}\left[L_t^{-1}\left(\frac{1}{\rho}Bu + \frac{\nu}{\rho}L_y u\right) + L_y^{-1}\left(\frac{\rho}{\nu}L_t u - \frac{1}{\nu}Bu\right)\right], \end{aligned} \tag{6.15}$$

where we define Φ_0 and u_0 as

$$\begin{aligned} &\Phi_0 = \frac{U_0}{2} \quad \text{and} \;\; U_0 = 2e^{-y\sqrt{(\frac{\omega}{2\nu})}} \\ &u_0 = \Phi_0 \sin \omega t. \end{aligned} \tag{6.16}$$

The parametric form of Eq. (6.15) is

$$\begin{aligned} u &= u_0(y,t) + \gamma\frac{1}{2}\left[L_t^{-1}\left(\frac{1}{\rho}Bu + \frac{\nu}{\rho}L_y u\right) + L_y^{-1}\left(\frac{\rho}{\nu}L_t u - \frac{1}{\nu}Bu\right)\right] \\ &= u_0(y,t) + \gamma\frac{1}{2}\left[L_t^{-1}\left(\frac{1}{\rho}\right)\left(u'\frac{\partial u}{\partial x} + \nu\frac{\partial^2 u}{\partial y^2}\right) + L_y^{-1}\left(\frac{1}{\nu}\right)\left(\rho\frac{\partial u}{\partial t} - u'\frac{\partial u}{\partial x}\right)\right]. \end{aligned} \tag{6.17}$$

The decomposed parameterized form for u is

$$u = \sum_{n=0}^{\infty} \gamma^n u_n, \tag{6.18}$$

and the decomposed parameterized form for Bu

$$Bu = u'\frac{\partial u}{\partial x} = \sum_{n=0}^{\infty} \gamma^n A_n. \tag{6.19}$$

The parameter γ is used for grouping the terms. Thus terms of $\gamma^0, \gamma^1, \gamma^2, \cdots$ and A_n are the Adomian's special polynomials [44, 54, 55, 56], still to be calculated. Substitution of Eqs. (6.17) and (6.18) into Eq. (6.15) results in

$$\begin{aligned} \sum_{n=0}^{\infty} \gamma^n u_n = u_0(y,t) + \gamma\frac{1}{2}\Bigg[L_t^{-1}\left(\frac{1}{\rho}\right)\left(\sum_{n=0}^{\infty}\gamma^n A_n + \nu\frac{\partial^2\left(\sum\limits_{n=0}^{\infty}\gamma^n u_n\right)}{\partial y^2}\right) + \\ L_y^{-1}\left(\frac{1}{\nu}\right)\left(\rho\frac{\partial\left(\sum\limits_{n=0}^{\infty}\gamma^n u_n\right)}{\partial t} - \sum_{n=0}^{\infty}\gamma^n A_n\right)\Bigg]. \end{aligned} \tag{6.20}$$

When comparing like terms we obtain

$$
\begin{aligned}
u_0 &= \Phi_0 \sin \omega t \\
u_1 &= \gamma \frac{1}{2}\left[L_t^{-1}\left(\frac{1}{\rho}\right)\left(A_0 + \nu \frac{\partial^2 u_0}{\partial y^2}\right) + L_y^{-1}\left(\frac{1}{\nu}\right)\left(\rho \frac{\partial u_0}{\partial t} - A_0\right)\right] \\
u_2 &= \gamma \frac{1}{2}\left[L_t^{-1}\left(\frac{1}{\rho}\right)\left(A_1 + \nu \frac{\partial^2 u_1}{\partial y^2}\right) + L_y^{-1}\left(\frac{1}{\nu}\right)\left(\rho \frac{\partial u_1}{\partial t} - A_1\right)\right] \\
u_3 &= \gamma \frac{1}{2}\left[L_t^{-1}\left(\frac{1}{\rho}\right)\left(A_2 + \nu \frac{\partial^2 u_2}{\partial y^2}\right) + L_y^{-1}\left(\frac{1}{\nu}\right)\left(\rho \frac{\partial u_2}{\partial t} - A_2\right)\right] \\
u_4 &= \gamma \frac{1}{2}\left[L_t^{-1}\left(\frac{1}{\rho}\right)\left(A_3 + \nu \frac{\partial^2 u_3}{\partial y^2}\right) + L_y^{-1}\left(\frac{1}{\nu}\right)\left(\rho \frac{\partial u_3}{\partial t} - A_3\right)\right] \\
u_5 &= \gamma \frac{1}{2}\left[L_t^{-1}\left(\frac{1}{\rho}\right)\left(A_4 + \nu \frac{\partial^2 u_4}{\partial y^2}\right) + L_y^{-1}\left(\frac{1}{\nu}\right)\left(\rho \frac{\partial u_4}{\partial t} - A_4\right)\right] \\
&\vdots \quad \cdots \quad \cdots \quad \cdots \quad \cdots \quad \cdots \quad \cdots \quad \cdots \quad \cdots \quad \cdots \quad \cdots \quad \cdots \\
&\vdots \quad \cdots \quad \cdots \quad \cdots \quad \cdots \quad \cdots \quad \cdots \quad \cdots \quad \cdots \quad \cdots \quad \cdots \quad \cdots \\
u_{n+1} &= \gamma \frac{1}{2}\left[L_t^{-1}\left(\frac{1}{\rho}\right)\left(A_n + \nu \frac{\partial^2 u_n}{\partial y^2}\right) + L_y^{-1}\left(\frac{1}{\nu}\right)\left(\rho \frac{\partial u_n}{\partial t} - A_n\right)\right]. \qquad (6.21)
\end{aligned}
$$

6.4 Derivation of Adomian's Special Polynomials

$$
Bu = u' \frac{\partial u}{\partial y} = (u'_0 + u'_1 \gamma + u'_2 \gamma^2 + \cdots)\left(\frac{\partial u_0}{\partial y} + \frac{\partial u_1}{\partial y} + \frac{\partial u_2}{\partial y} + \cdots\right). \qquad (6.22)
$$

By grouping like terms with respect to the power of γ Eq . (6.22) reduces to

$$
\begin{aligned}
Bu =& u'_0 \frac{\partial u_0}{\partial y} + u'_1 \gamma \left(u'_0 \frac{\partial u_1}{\partial y} + u'_1 \frac{\partial u_0}{\partial y}\right) + \gamma^2 \left(u'_0 \frac{\partial u_2}{\partial y} + u'_1 \frac{\partial u_1}{\partial y} + u'_2 \frac{\partial u_0}{\partial y}\right) \\
&+ \gamma^3 \left(u'_0 \frac{\partial u_3}{\partial y} + u'_1 \frac{\partial u_2}{\partial y} + u'_2 \frac{\partial u_1}{\partial y} + u'_3 \frac{\partial u_0}{\partial y}\right) \\
&+ \gamma^4 \left(u'_0 \frac{\partial u_4}{\partial y} + u'_1 \frac{\partial u_3}{\partial y} + u'_2 \frac{\partial u_2}{\partial y} + u'_3 \frac{\partial u_1}{\partial y} + u'_4 \frac{\partial u_0}{\partial y}\right) + \cdots \qquad (6.23)
\end{aligned}
$$

From Eq. (6.23) Adomian polynomials can be derived as follows

$$\begin{aligned}
A_0 &= u_0' \frac{\partial u_0}{\partial y}, \\
A_1 &= u_0' \frac{\partial u_1}{\partial y} + u_1' \frac{\partial u_0}{\partial y}, \\
A_2 &= u_0' \frac{\partial u_2}{\partial y} + u_1' \frac{\partial u_1}{\partial y} + u_2' \frac{\partial u_0}{\partial y}, \\
A_3 &= u_0' \frac{\partial u_3}{\partial y} + u_1' \frac{\partial u_2}{\partial y} + u_2' \frac{\partial u_1}{\partial y} + u_3' \frac{\partial u_0}{\partial y}, \\
A_4 &= u_0' \frac{\partial u_4}{\partial y} + u_1' \frac{\partial u_3}{\partial y} + u_2' \frac{\partial u_2}{\partial y} + u_3' \frac{\partial u_1}{\partial y} + u_4' \frac{\partial u_0}{\partial y}, \\
&\vdots \quad \cdots \quad \cdots \quad \cdots \quad \cdots \quad \cdots \quad \cdots \quad \cdots \quad \cdots \quad \cdots \quad \cdots \\
&\vdots
\end{aligned} \tag{6.24}$$

and so on. The rest of the polynomials can be constructed in a similar manner. Hence, by using Eq. $(6.21)_1$ the polynomials A_0 have the following form:

$$A_0 = \nu_0' \frac{\partial u_0}{\partial y} = \nu_0' \left[\Phi_0' \sin \omega t + \Phi_0 \ (\sin \omega t)'\right]. \tag{6.25}$$

Using Eq. (6.9) taking the case where $n = 1$, we suggest an approximate solution $u(y, t)$ for only two terms,

$$u(y, t) = u_0 + u_1. \tag{6.26}$$

Taking A_0 from Eq. (6.24) and u_0 from Eq. (6.21) and substitute into the expression of u_1 in Eq. (6.11) we have,

$$u = u_0 + u_1. \tag{6.27}$$

The general principle is known to enhance the approximation; more components in the decomposition series form are possible to be determined. In view of Eq. (6.26), the solution $u(y,t)$ is obtained in a series form hence

$$u(y,t) = u_0 + \gamma\frac{1}{2}\left[L_t^{-1}\left(\frac{1}{\rho}\right)\left(A_0 + \nu\frac{\partial^2 u_0}{\partial y^2}\right) + L_y^{-1}\left(\frac{1}{\nu}\right)\left(\rho\frac{\partial u_0}{\partial t} - A_0\right)\right] \tag{6.28}$$

where

$$A_0 + \nu\frac{\partial^2 u_0}{\partial y^2} = \frac{2\nu}{\omega}\sin(\omega t)\left(e^{y^2\frac{\omega}{2\nu}}\sin(\omega t) + \nu e^{-y\sqrt{(\frac{\omega}{2\nu})}}\right) \tag{6.29}$$

and

$$\rho\frac{\partial u_0}{\partial y} - A_0 = \sin(\omega t)\left[\rho\sqrt{(\frac{\omega}{2\nu}})e^{-y\sqrt{(\frac{\omega}{2\nu})}} - \frac{2\nu}{\omega}e^{y^2\frac{\omega}{2\nu}}\sin(\omega t)\right]. \tag{6.30}$$

Equivalently $u(y,t)$ is

$$\begin{aligned} u(y,t) =& e^{-y\sqrt{(\frac{\omega}{2\nu})}}\sin(\omega t) + \frac{1}{\rho}\left(t + \mathrm{A}\right)\frac{2\nu}{\omega}\sin(\omega t)\left[e^{y^2\frac{\omega}{2\nu}}\sin(\omega t) + \nu e^{-y\sqrt{(\frac{\omega}{2\nu})}}\right] + \\ & \frac{1}{\nu}\left(\frac{y^2}{2} + \mathrm{B}\right)\sin(\omega t)\left[\rho\sqrt{(\frac{\omega}{2\nu}})e^{-y\sqrt{(\frac{\omega}{2\nu})}} - \frac{2\nu}{\omega}e^{y^2\frac{\omega}{2\nu}}\sin(\omega t)\right] \end{aligned} \tag{6.31}$$

where A and B are constants which we equate to zero. If $\rho \to \infty$ and $\nu \to \infty$, we obtain

$$u(y,t) = e^{-y\sqrt{(\frac{\omega}{2\nu})}}\sin(\omega t). \tag{6.32}$$

Similarly, if the boundary conditions are defined as a cosine oscillation

$$\begin{aligned} u(0,t) &= U_0 \cos \omega t \quad \text{ for } t > 0 \\ u(\infty,t) &= 0, \end{aligned} \tag{6.33}$$

then

$$u(y,t) = e^{-y\sqrt{(\frac{\omega}{2\nu})}}\cos(\omega t). \tag{6.34}$$

6.5 Numerical Results and Conclusion

In this chapter, the ADM was applied to obtain an approximate analytical solution to the momentum equation. The ADM focuses on avoiding simplifications and restrictions which change the nonlinear problem to a mathematically tractable one, whose solution differs with the physical solution. The approximate solution is expressed in a series form with easily computable components of the decomposition series. The ADM is an efficient and powerful technique for determining approximate solutions of the momentum equation. This method has been used directly avoiding linearisation or any assumptions. It can be seen in Figure 6.1 that the velocity is an increasing function of time for both the sine wave oscillation and the cosine wave oscillation. It is clear from Figure 6.1 that for large time the velocity profile is swiftest to reach a steady-state solution and for small time it is the slowest.

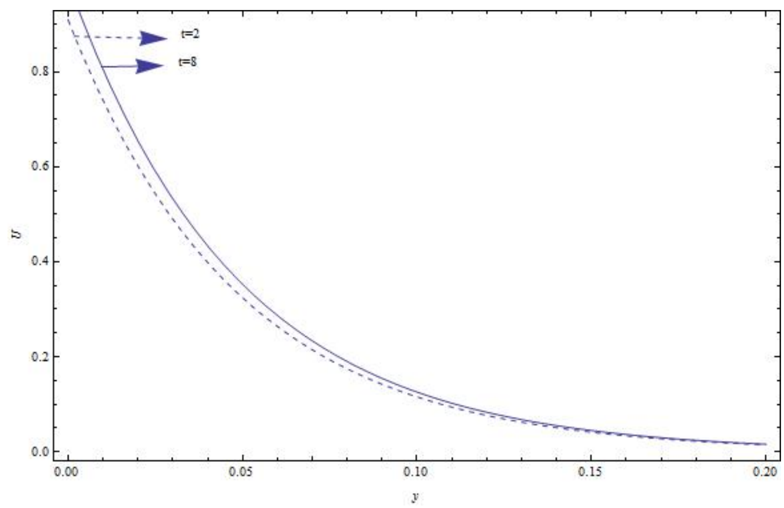

Figure 6.1: Velocity profile field $u(y,t)$ for flow induced by a sine oscillation , for various values of time; $t = 2, t = 8$, $\omega = 1$, $y \epsilon [0, 0.2]$ and $\nu = 0.00746$.

Chapter 7

Summary

In Chapter 1 we discussed background knowledge of fluid dynamics in which mathematical modeling of fluids were briefly reviewed. The rheological properties of Maxwell fluids, Oldroyd-B fluids and Johnson-Segalman fluids are generally specified by their so called constitutive equations in three dimensional form. Equations of motion that describe the behaviour of a physical system in terms of its motion as a function of time were outlined with the Navier-Stokes equations and power law fluid being introduced. Finally, some integral transforms, namely Laplace and the convolution integral were introduced.

In Chapter 2 we investigated the effect of a power law fluid occupying the domain $y > 0$. An infinitely extended flat plate located at $y = 0$ was suddenly accelerated from rest. The fluid was disturbed at time $t = 0^+$ and the flat plate began to oscillate in its plane with angular velocity Ω. The velocity disturbance induced in the fluid at $t > 0$ and shear stress distributions were determined through the use of Laplace transforms. The wall was subjected to both sine and cosine oscillations. The governing equations were non-dimensionalized and mass-balance quantity s was introduced. The solution obtained was presented as a sum of steady-state and transient solutions. The effect of the dimensionless parameter such as power index n, on the flow was analyzed. It was observed that for large time the fluid flow decayed and the magnitude of oscillation was a minimum as $t \to \infty$. The time was indirectly proportional to the frequency of the velocity.

In Chapter 3 we introduced and developed the explicit method (forward time, centered space), the implicit method (backward time, centered space) and the Crank-Nicolson scheme for the momentum equation. The calculations obtained using MATLAB with finer mesh points on each scheme demonstrated the theoretical predictions of how their truncation errors depend on time step size and mesh point spacing. The FTCS and BTCS both have truncation error $\mathcal{O}(\Delta t) + \mathcal{O}(\Delta y^2)$ and the Crank-Nicolson has truncation error $\mathcal{O}(\Delta t^2) + \mathcal{O}(\Delta y^2)$. We observed that the explicit method gave much better accuracy than the implicit algorithm for small time steps. However the implicit method was good for large time steps. In both the explicit and implicit methods the mesh spacing was proportional to (Δy^2). Hence a better accuracy was obtained when the interval was divided into a smaller mesh size. The Crank- Nicolson method gave a better approximation when compared to FTCS and BTCS. In the Crank-Nicolson scheme it is recommended to choose the time step size that has the same order of magnitude as the mesh spacing, $\Delta t \approx \Delta y$.

In Chapter 4 we discussed the application of He's homotopy pertubation method (HPM) for solving the momentum equation. The HPM reduces a complex problem domain into a simple problem examination. The homotopy method depends on the choice of initial condition. The method generates a convergent series solution. By having a good guess for the initial condition, a few iterations are enough to give a good approximate solution. HPM method does not use computation discretized methods for solution of partial differential equations and this makes HPM to be one of the efficient methods in determining approximate solutions for differential equation problems.

In Chapter 5 the DTM which depends on Taylor series expansion was studied. The approximate solution of the momentum equation was obtained in the form of a polynomial series solution based on an iterative procedure. The DTM results obtained for cosine wave and sine wave oscillations were compared with the exact solution. Tables 5.1 - 5.6 showed a decrease in error as we increased the approximate solution from $N = 1$ to $N = 3$ for $u(y, t)$, where $t = 0.0075$ $\mu = 0.01$, $\rho = 0.05$ and $y \ \varepsilon \ [0, 0.5]$ with a step size of 0.1. The obtained results compared with exact solutions acknowledge that the DTM was very effective and easy to apply. The plot shows that as time $t \to \infty$ the amplitude of the cosine and the sine waves decreases and the flows turn to a steady-state.

In Chapter 6 we applied ADM to obtain an approximate analytical solution of the momentum equation. The approximate solution was expressed in a series form with easily computable components of the decomposition series. The ADM is an efficient and powerful technique for determining approximate solutions of the momentum equation. Using the ADM the velocity profile for large time was swiftest to reach a stead-state solution and for small time it was the slowest for both the cosine wave and the sine wave oscillations.

Bibliography

[1] Corina Fetecau, D. Vieru, and C. Fetecau. A note on the second problem of Stokes' for Newtonian fluids. *International Journal of Non-Linear Mechanics*, 43(5):451–457, 2008.

[2] T. Hayat, R. J. Moitsheki, and S. Abelman. Stokes' first problem for sisko fluid over a porous wall. *Applied Mathematics and Computation*, 217(2):622–628, 2010.

[3] L. Ali and K. Vafai. An investigation of Stokes' second problem for non-Newtonian fluids. *International Journal of Computation and Methodology*, 47(10):988–980, 2005.

[4] V. K. Sin and I. K. Wong. Numerical study of Stokes' second flow problem. In *Computational and Information Sciences (ICCIS), 2010 International Conference*, 242-245, 2010.

[5] M. Devakar and T. K. V. Iyengar. Stokes' problems for an incompressible couple stress fluid. *Nonlinear Analysis: Modelling and Control*, 1(2):181–190, 2008.

[6] C. Fetecau and Corina Fetecau. Starting solutions for some unsteady unidirectional flows of a second grade fluid. *International Journal of Engineering Science*, 43:781–789, 2005.

[7] S. Asghar, S. Nadeem, K. Hanif, and T. Hayat. Analytical solution of Stokes' second problem for second-grade fluids. *Mathematical Problems in Engineering*, 1-8, 2006.

[8] C. Fetecau and Corina Fetecau. Constitutive relations for Rivlin-Ericksen fluids based on generalized rational approximation. *Arch. Rational Mech. Anal.*, 146:73–93, 2005.

[9] Corina Fetecau, M. Jamil, C. Fetecau, and I. Siddique. A note on the second problem of Stokes' for Maxwell fluids. *International Journal of Non-Linear Mechanics.*, 44(10):1085–1090, 2009.

[10] C. Fetecau, T. Hayat, M. Khan, and C. Fetecau. Unsteady flow of an Oldroyd-B fluid induced by the impulsive motion of a plate between two side walls perpendicular to the plate. *Acta Mechanica*, 198:21–23, 2008.

[11] M. W. Johnson Jr. and D. Segalman. A model for viscoelastic fluid behavior which allows non-affine deformation. *Journal of Non-Newtonian Fluid Mechanics*, 2(3):255–270, 1977.

[12] T. Hayat, S. Asghar, and A. M. Siddiqui. Stokes' second problem for a Johnson-Segalman fluid. *Applied Mathematics and Computation*, 148(3):697–706, 2004.

[13] I. J. Rao and K. R. Rajagopal. Some simple flows of a Johnson-Segalman fluid. *Acta Mechanica*, 132:209–219, 1999.

[14] R. G. Lerner and G. L. Trigg. *Encyclopaedia of Physics*. VHC Publishers, second edition, 1991.

[15] L. N. Hand and J. D. Finch. *Analytical Mechanics*. Cambridge University Press, first edition, 1998.

[16] P. J. Nahin. Behind the Laplace transform. *IEEE SPECTRUM*, 28(3):60, 1991.

[17] J. R. A. Pearson and P. M. J. Tardy. Models for flow of non-Newtonian and complex fluids through porous media. *Journal of Non-Newtonian Fluid Mechanics*, 102(2):447–473, 2002.

[18] G. W. Scott. Blair, J. C. Hening, and A. Wagstaff. The flow of cream through narrow glass tubes. *J. Phys. Chem.*, 43(7):853–864, 1938.

[19] P. Neofytou and D. Drikakis. non-Newtonian flow instability in a channel with a sudden expansion. *Journal of Non-Newtonian Fluid Mechanics*, 111(23):127–150, 2003.

[20] W. Akhtar, Corina Fetecau, V. Tigoiu, and Constantin Fetecau. Flow of a Maxwell fluid between two side walls induced by a constantly accelerating plate. *Zeitschrift fur Angewandte Mathematik und Physik*, 60(3):498–510, 2009.

[21] N. Aksel, M. Scholle, and C. Fetecau. Starting solutions for some unsteady unidirectional flows of Oldroyd-B fluids. *Zeitschrift fur Angewandte Mathematik und Physik ZAMP*, 57:815–831, 2006.

[22] S. Asghar, M. Khan, and T. Hayat. Magnetohydrodynamic transient flows of a non-Newtonian fluid. *International Journal of Non-Linear Mechanics*, 40(5):589–601, 2005.

[23] K. R. Rajagopal. A note on unsteady unidirectional flows of a non-Newtonian fluid. *International Journal of Non-Linear Mechanics*, 17(56):369–373, 1982.

[24] C. Fetecau and Corina Fetecau. Starting solutions for some unsteady unidirectional flows of a second grade fluid. *International Journal of Engineering Science*, 43(10):781–789, 2005.

[25] K. R. Rajagopal. *On boundary conditions for fluids of the differential type, in: A Seuerira (Ed.), Navier-Stokes Equations and Related Problems.* Plenum Press, New York, 1995.

[26] P. P. G. Dyke. *An introduction to Laplace transforms and Fourier series first course in numerical analysis.* Springer, London; New York, second edition, 2001.

[27] M. E. Erdogan. A note on an unsteady flow of a viscous fluid due to an oscillating plane wall. *International Journal of Non-Linear Mechanics*, 5:1–6, 2000.

[28] K. Hu and K. Zhu. The exact solution of Stokes' second problem including start-up process with fractional element. *Acta Mechanica Sinica*, 25(5):577–582, 2009.

[29] M. Khan, A. Anjum, and C. Fetecau. On exact solutions of Stokes' second problem for a burgers' fluid, I the case $\gamma < \lambda^2/4$. *Zeitschrift fur Angewandte Mathematik und Physik*, 61(4):697–720, 2009.

[30] M. Nazar, Corina Fetecau, and D. Vieru. New exact solutions corresponding to the second problem of Stokes' for second grade fluids. *Nonlinear Analysis-Real World Applications*, 11:584–591, 2010.

[31] M. Nazar, C. Fetecau, and D. Vieru. A note on the second problem of Stokes' for Maxwell fluids. *International Journal of Non-Linear Mechanics*, 44:1085–1090, 2009.

[32] J. Crank. *The Mathematics of Diffusion*. Oxford University Press,New York, p. 143, second edition, 1975.

[33] R. L. Burden and J. D. Faires. *Numerical Analysis*. Thomson Brooks/Cole, a part of The Thomson Corporation, USA, eighth edition, 2005.

[34] A. Ralston. *A first course in numerical analysis*. McGraw- Hill, Tokyo, second edition, 1978.

[35] V. S. Arpaci. *Conducting Heat Transfer*. Addison-Wesley Publishing Company, Reading, Massachusetts, second edition, 1967.

[36] A. M. Siddiqui, R. Mahmood, and Q. K. Ghori. Homotopy perturbation method for thin film flow of a third grade fluid down an inclined plane. *Chaos, Solitons and Fractals*, 35(1):140–147, 2008.

[37] J. H. He. Homotopy perturbation technique. *Computer Methods in Applied Mechanics and Engineering*, 178(3-4):257–262, 1999.

[38] H. A. Zedan and E. El Adrous. The application of the homotopy perturbation method and the homotopy analysis method to the generalized Zakharov equations. *Abstract and Applied Analysis*, vol. 2012, Article ID 561252, 19 pages, 2012. doi:10.1155/2012/561252.

[39] M. S. Hashmi, N. Khan, and T. Mahmood. Optimal homotopy asymptotic solution for thin film flow of a third grade fluid with partial slip. *World Applied Sciences Journal*, 21(12):1782–1788, 2013.

[40] A. R. Vahidi, Z. Azimzadeh, and M. Didgar. An efficient method for solving Riccati equation using homotopy perturbation method. *Indian Journal of Physics*, 87(5):447–454, 2013.

[41] A. M. Siddiqui, M. Ahmed, and Q. K. Ghori. Couette and Poiseuille flows for non-Newtonian fluids. *International Journal of Nonlinear Sciences and Numerical Simulation*, 7(1):15–26, 2011.

[42] J. H. He. An approximate solution technique not depending on small parameters: A special example. *Comput. Methods Appl. Mech. Eng*, 30(3):371–380, 1995.

[43] M. Ghoreishi and A. I. B. Ismail. An approximate solution technique not depending on small parameters: A special example. *Applied Mathematics Sciences*, 5(3):113–123, 1995.

[44] G. E. Pukhov. Computational structure for solving differential equations by Taylor transformations. *Cybernetics*, 14(3):383–390, 1978.

[45] C. Bervillier. Status of the differential transformation method. *Applied Mathematics and Computation*, 218(20):10158–10170, 2012.

[46] G. E. Pukhov. Differential transforms and circuit theory. *The Institute of Simularion Problems in Energetics, Academy of Sciences of the Ukrainian SSR, Kiev, U.S.S.R.*, 10(3):265–276, 1982.

[47] M. Abazari. Solutions of the reaction diffusion problems by a reduced form of differential transform method. *Australian Journal of Basic and Applied Sciences*, 5(12):403–413, 2011.

[48] H. Jafari and V. Daftardar-Gejji. Revised Adomian decomposition method for solving a system of nonlinear equations. *Applied Mathematics and Computation*, 175(1):1–7, 2006.

[49] E. M. Abulwafa, M. A. Abdou, and A. A. Mahmoud. The solution of nonlinear coagulation problem with mass loss. *Chaos, Solitons and Fractals*, 29(2):313–330, 2006.

[50] T. M. Atanackovic and B. Stankovic. On a system of differential equations with fractional derivatives arising in rod theory. *Chaos, Solitons and Fractals*, 37(4):1241–1250, 2004.

[51] M. A. Mohamed. Adomian decomposition method for a reliable treatment of the Bratu-type equations. *Applications and Applied Mathematics: An International Journal ISSN: 1932-9466 (AAM)*, 4(1):52–61, 2009.

[52] A. M. Wazwaz. Adomian decomposition method for a reliable treatment of the Bratu-type equations. *Applied Mathematics and Computation*, 166(3):652–663, 2005.

[53] G. Adomian. A review of the decomposition method in applied mathematics. *Journal of Mathematical Analysis and Applications*, 135(2):501–544, 1988.

[54] K. Haldar. Application of Adomian's approximation to blood flow through arteries in the presence of a magnetic field. *Journal of Applied Mathematics and Computing*, 12(1-2):267–279, 2003.

[55] M. Inc and N. Bildik. Non-pertubative solution of the Ginzburg-Landau equation. *Mathematical and Computational Applications*, 5(2):113–117, 2000.

[56] C. M. Amaloukas. Application of the decomposition method to the Kortweg-de Vries equation. *The Conference of Applied Different Geometry- Differential Geometry and Lie Algebras*, 135(2):79–87, 2002.

Appendix A

A1

The inverse Laplace transform of a compound function $F(w(q))$, is defined as

$$\mathfrak{L}^{-1}\left\{F(w(q))\right\} = \int_0^\infty f(u)g(u,t)du,$$

where

$$f(t) = \mathfrak{L}^{-1}\left\{F(q)\right\}$$

and

$$g(u,t) = \mathfrak{L}^{-1}\left\{e^{-}uw(q)\right\}.$$

A2

$$\mathfrak{L}^{-1}\left\{e^{-a\sqrt{q}}\right\} = \frac{a}{2t\sqrt{\pi t}}\exp\left(\frac{-a^2}{4t}\right); \quad Re\ (a^2) > 0.$$

A3

$$(\zeta * f)(t) = (f * \zeta)(t) = f(t) \quad \text{for each continuous function} \quad f(.).$$

Appendix B

Theorem 1.

Proof. By Definition 1 we have

$$U(k,h)=\frac{1}{k!h!}\left[\frac{\partial^{k+h}}{\partial x^k\partial y^h}w(x,y)\right]_{x=0,y=0},$$

$$V(k,h)=\frac{1}{k!h!}\left[\frac{\partial^{k+h}}{\partial x^k\partial y^h}v(x,y)\right]_{x=0,y=0},$$

$$W(k,h)=\frac{1}{k!h!}\left[\frac{\partial^{k+h}}{\partial x^k\partial y^h}\left[u(x,y)+v(x,y)\right]\right]_{x=0,y=0},$$

using$U(k,h), V(k,h)$ and and $W(k,h)$, we have

$$W(k,h)=U(k,h)\pm V(k,h).$$

Theorem 2.

Proof. By Definition 1 we have

$$U(k,h)=\frac{1}{k!h!}\left[\frac{\partial^{k+h}}{\partial x^k\partial y^h}u(x,y)\right]_{x=0,y=0},$$

$$W(k,h)=\frac{1}{k!h!}\left[\frac{\partial^{k+h}}{\partial x^k\partial y^h}\left[\lambda u(x,y)\right]\right]_{x=0,y=0},$$

using $U(k,h)$ and $W(k,h)$ we have

$$W(k,h)=\lambda U(k,h).$$

Theorem 3.

Proof. By Definition 1 we have

$$\begin{aligned} W(k,h) &= \frac{1}{k!h!}\left[\frac{\partial^{k+h}}{\partial x^k \partial y^h}\left[\frac{\partial u(x,y)}{\partial x}\right]\right]_{x=0,y=0}, \\ &= \frac{k+1}{(k+1)\,h!}\left[\frac{\partial^{k+h+1}}{\partial x^{k+1}\partial y^h}u(x,y)\right]_{x=0,y=0}, \end{aligned}$$

then

$$W(k,h) = (k+1)U(k+1,h).$$

Theorem 4.

Proof. By Definition 1 we have

$$\begin{aligned} W(k,h) &= \frac{1}{k!h!}\left[\frac{\partial^{k+h}}{\partial x^k \partial y^h}\left[\frac{\partial u(x,y)}{\partial x}\right]\right]_{x=0,y=0}, \\ &= \frac{h+1}{k!\,(h+1)!}\left[\frac{\partial^{k+h+1}}{\partial x^{k}\partial y^{h+1}}u(x,y)\right]_{x=0,y=0}, \end{aligned}$$

then

$$W(k,h) = (h+1)U(k,h+1).$$

Theorem 5.

Proof. By Definition 1 we have

$$\begin{aligned} W(k,h) &= \frac{1}{k!h!}\left[\frac{\partial^{k+h}}{\partial x^k \partial y^h}\left[\frac{\partial^{r+s} u(x,y)}{\partial x^k \partial y^s}\right]\right]_{x=0,y=0}, \\ &= \frac{(k+1)(k+2)\dots(k+r)(h+1)(h+2)\dots(h+s)}{(k+r)!(h+s)!} \\ &= \frac{k+1}{(k+1)\,h!}\left[\frac{\partial^{k+h+1}}{\partial x^{k+1}\partial y^h}u(x,y)\right]_{x=0,y=0}, \end{aligned}$$

then

$$W(k,h) = (k+1)(k+2)(k+3)\dots(h+2)(h+3)\dots(h+s)U(k+r,h+s).$$

Theorem 6.

Proof. By Definition 1 we have

$$\begin{aligned}
W(1,0) &= \frac{1}{2!0!}\frac{\partial}{\partial x}\left[u(x,y)v(x,y)\right]_{x=0,y=0} \\
&= \left[\frac{\partial u(x,y)}{\partial x}v(x,y) + u(x,y)\frac{\partial v(x,y)}{\partial x}\right]_{x=0,y=0} \\
&= U(1,0)V(0,0) + U(0,0)V(0,0),
\end{aligned}$$

$$\begin{aligned}
W(2,0) &= \frac{1}{2!0!}\frac{\partial^2}{\partial x^2}\left[u(x,y)v(x,y)\right]_{x=0,y=0} \\
&= U(2,0)V(0,0) + U(1,0)V(1,0) + U(0,0)V(2,0), \\
W(0,1) &= U(0,1)V(0,0) + U(0,0)V(0,1), \\
W(1,1) &= U(1,1)V(0,0) + U(1,0)V(0,1) + U(0,1)V(1,0) + U(0,0)V(1,1), \\
W(1,2) &= U(1,2)V(0,0) + U(1,1)V(0,1) + U(1,0)V(0,2) + U(1,0)V(0,2) \\
&\quad + U(1,2)V(0,0) + U(0,2)V(1,0) + U(0,1)V(1,1) + U(0,0)V(1,2), \\
&\vdots \\
W(k,h) &= \sum_{r=0}^{k}\sum_{s=0}^{h} U(r,h-s)V(k-r,s).
\end{aligned}$$

Theorem 7.

Proof. Due to

$$\left[\frac{\partial w(x,y)^{k+h}}{\partial x^k \partial y^h}\right]_{x=0,y=0} = \begin{cases} k!h!, & k=m, \text{ and } h=n, \\ 0, & k \neq m \text{ or } h \neq n \end{cases}$$

we have

$$W(k,h) = \left[\frac{1}{k!h!}\frac{\partial w(x,y)^{k+h}}{\partial x^k \partial y^h}\right]_{x=0,y=0}$$
$$= \delta(k-m, h-n)$$
$$= \delta(k-m)\delta(h-n)$$

where

$$\delta(k-m) = \begin{cases} 1, & k = m, \\ 0. & k \neq m, \end{cases}$$
$$\delta(h-n) = \begin{cases} 1, & h = n, \\ 0. & h \neq n. \end{cases}$$